

**STAKING, SOIL SAMPLING, PROSPECTING AND AIRBORNE GEOPHYSICS REPORT – SEAGULL TIN  
PROJECT**

NTS: 105B 03, 04

Watson Lake Mining District, Yukon Territory, Canada

60°9' N 131° 27' W

Author

**Tomasz Kalkowski, B.Sc.**, GIT

**Franz Dziuba, B.Sc.**, P.Geoph.

**Jim Robinson, B.Sc.**, P.Geo.

CLAIMS:

DO 1-4 [YD106431 – YD106434]

DO 5-20 [YE31802 – YE31817]

ECCLES 1-16 [YE31848 – YE31833]

LAUGHTER 1-4 [YD106423-YD106426]

MUSIC 1-4 [YD106419-YD106422]

TUNA 1-4 [YD106415-YD106418]

BEANS 1-36 [YD106379-YD106414]

SNIPS 1-24 [YE32355-YE32378]

CON 1-4 [YD106427-YD106430]

CORN 1-4 [YD106435-YD106438]

FIRE 1-4 [YD106439-YD106442]

MILK 1-4 [YD106447-YD106450]

PEAS 1-4 [YD106443-YD106446]

GOODS 1-4 [YD106451-YD106454]

WORK PERFORMED:

October 7-22, 2014

January 21, 2015

Prepared for:

**UCORE RARE METALS INC.**

Prepared by:



**AURORA GEOSCIENCES**

**TECHNICAL REPORT  
SOIL SAMPLING, PROSPECTING AND AIRBORNE GEOPHYSICS REPORT – SEAGULL TIN PROJECT**

Effective Date: January 21, 2015

Prepared for:  
**Ucore Rare Metals Inc.**  
**210 Waterfront Drive, Suite 106**  
**Bedford, Nova Scotia, Canada**  
**B4A 0H3**

Prepared by:  
**Aurora Geosciences Ltd.**  
34A Laberge Road, Whitehorse, YT Y1A 5Y9  
Phone: 867.668.7672 Fax: 867.393.3577  
[www.aurorageosciences.com](http://www.aurorageosciences.com)

**Author**  
**Tomasz Kalkowski, B.Sc., GIT**  
**Franz Dziuba, B.Sc., P.Geoph.**  
**Jim Robinson, B.Sc., P.Geo**

## TABLE OF CONTENTS

1	EXECUTIVE SUMMARY .....	1
2	INTRODUCTION .....	3
3	LOCATION & ACCESS .....	3
4	PROPERTY DESCRIPTION .....	5
5	CLIMATE & TOPOGRAPHY .....	8
6	EXPLORATION HISTORY .....	8
7	DEPOSIT MODEL .....	10
8	REGIONAL GEOLOGY .....	11
8.1	Tectonic setting .....	11
8.2	Stratigraphy .....	11
8.3	Structure .....	12
9	WORK PROGRAM .....	14
9.1	Airborne Magnetic and Radiometric Survey .....	14
9.1.1	Survey Specifications .....	14
9.1.2	Data Preparation .....	14
9.1.3	Inverse Modelling .....	14
9.2	Geochemical Soil Sediment Survey .....	14
9.2.1	Personnel & equipment .....	14
9.2.2	Soil sediment sample specifications .....	15
9.3	Prospecting .....	16
9.3.1	Personnel & equipment .....	16
9.3.2	Rock sample specifications .....	16
10	SAMPLE COLLECTION, SECURITY, PREPARATION & ANALYSIS .....	17
10.1	Soil Sediment Samples .....	17
10.2	Rock Samples .....	17
11	RESULTS .....	18
11.1	Geochemical and Prospecting Surveys .....	18
11.1.1	Statistics .....	18
11.1.2	Geochemical anomalies of interest .....	18
11.2	Geophysical Surveys .....	22

11.2.1	Corn and Do Claims .....	22
11.2.2	Goods, Eccles and Milk Claims .....	26
11.2.3	Fired and Milk Claims .....	29
11.2.4	Con Claims.....	32
11.2.5	Beans and Music Claims .....	35
11.2.6	Beans and Music Claims.....	38
11.2.7	Peas Claims .....	41
11.2.8	Snip and Tuna Claims .....	44
12	INTERPRETATION AND CONCLUSIONS.....	47
13	RECOMMENDATIONS .....	49
14	REFERENCES .....	50

## LIST OF FIGURES

FIGURE 1.	SEAGULL TIN PROPERTY LOCATION MAP .....	3
FIGURE 2.	2014 CLAIM MAP FOR THE SOUTHEAST PORTION OF THE PROJECT AREA .....	5
FIGURE 3.	2014 CLAIM MAP FOR THE NORTHWEST PORTION OF THE PROJECT AREA.....	6
FIGURE 4.	REGIONAL GEOLOGY MAP .....	12
FIGURE 5.	2014 DO CLAIMS SOIL AND ROCK SAMPLE TIN ASSAY RESULTS .....	<b>ERROR! BOOKMARK NOT DEFINED.</b> 19
FIGURE 6.	2014 SNIPS CLAIMS SOIL SAMPLE TIN ASSAY RESULTS.....	20
FIGURE 7.	TOTAL MAGNETIC INTENSITY MAP .....	21
FIGURE 8.	RESIDUAL MAGNETIC INTENSITY ON THE CORN AND DO CLAIMS .....	<b>ERROR! BOOKMARK NOT DEFINED.</b> 23
FIGURE 9.	MAGNETIC VECTOR INVERSION SUSCEPTIBILITY MODEL FOR THE CORN AND DO CLAIMS .....	24
FIGURE 10.	RESIDUAL MAGNETIC INTENSITY ON THE GOODS, ECCLES AND MILK CLAIMS .....	<b>ERROR! BOOKMARK NOT DEFINED.</b> 26
FIGURE 11.	MAGNETIC VECTOR INVERSION SUSCEPTIBILITY MODEL FOR THE GOODS, ECCLES AND MILK CLAIMS .....	27
FIGURE 12.	RESIDUAL MAGNETIC INTENSITY ON THE FIRED AND MILK CLAIMS .....	<b>ERROR! BOOKMARK NOT DEFINED.</b> 29
FIGURE 13.	MAGNETIC VECTOR INVERSION SUSCEPTIBILITY MODEL FOR THE FIRED AND MILK CLAIMS .....	30
FIGURE 14.	RESIDUAL MAGNETIC INTENSITY ON THE CON CLAIMS .....	<b>ERROR! BOOKMARK NOT DEFINED.</b> 32
FIGURE 15.	MAGNETIC VECTOR INVERSION SUSCEPTIBILITY MODEL FOR THE CON CLAIMS .....	33
FIGURE 16.	RESIDUAL MAGNETIC INTENSITY ON THE BEANS AND MUSIC CLAIMS .....	<b>ERROR! BOOKMARK NOT DEFINED.</b> 35
FIGURE 17.	MAGNETIC VECTOR INVERSION SUSCEPTIBILITY MODEL FOR THE BEANS AND MUSIC CLAIMS.....	36
FIGURE 18.	RESIDUAL MAGNETIC INTENSITY ON THE LAUGHTER CLAIMS .....	<b>ERROR! BOOKMARK NOT DEFINED.</b> 38
FIGURE 19.	MAGNETIC VECTOR INVERSION SUSCEPTIBILITY MODEL FOR THE LAUGHTER CLAIMS .....	39
FIGURE 20.	RESIDUAL MAGNETIC INTENSITY ON THE PEAS CLAIMS .....	<b>ERROR! BOOKMARK NOT DEFINED.</b> 41
FIGURE 21.	MAGNETIC VECTOR INVERSION SUSCEPTIBILITY MODEL FOR THE PEAS CLAIMS .....	42
FIGURE 22.	RESIDUAL MAGNETIC INTENSITY ON THE SNIPS AND TUNA CLAIMS .....	<b>ERROR! BOOKMARK NOT DEFINED.</b> 44
FIGURE 23.	MAGNETIC VECTOR INVERSION SUSCEPTIBILITY MODEL FOR THE SNIPS AND TUNA CLAIMS .....	45

## LIST OF TABLES

TABLE 1. CLAIM DATA .....	4
TABLE 2. SHOWINGS .....	8
TABLE 3. REGIONAL STRATIGRAPHY IN THE PROJECT AREA .....	10
TABLE 4. DEFORMATIONAL HISTORY IN THE PROJECT AREA .....	11
TABLE 5. SUMMARY STATISTICS, SNIPS PROPERTY – SOIL SEDIMENT SAMPLE ANALYSIS .....	<b>ERROR! BOOKMARK NOT DEFINED.</b> 17
TABLE 6. SUMMARY STATISTICS, DO PROPERTY – SOIL SEDIMENT SAMPLE ANALYSIS .....	17

## LIST OF APPENDICES

APPENDIX I .....	STATEMENT OF QUALIFICATIONS
APPENDIX II .....	PROJECT LOG
APPENDIX III .....	STATEMENT OF EXPENDITURES
APPENDIX IV .....	PRECISION GEOSURVEYS AIRBORNE MAGNETIC AND RADIOMETRIC SURVEY REPORT
APPENDIX V .....	<b>ERROR! BOOKMARK NOT DEFINED.</b> ROCK AND SOIL SAMPLE DESCRIPTIONS
APPENDIX VI .....	ASSAY CERTIFICATES

## 1 EXECUTIVE SUMMARY

In September of 2014, Aurora Geosciences Ltd. was retained by Ucore Rare Metals Inc. to conduct a sampling, prospecting and airborne geophysics program to locate new bedrock tin targets and delineate identified mineralization within the current claims. This report describes a helicopter-borne magnetic and radiometric survey flown by Precision GeoSurveys and a soil sampling and prospecting program conducted at the Seagull Tin Project in the southern Yukon Territory between the September 7<sup>th</sup> and September 22<sup>nd</sup>, 2014.

The Seagull Tin Project is centred at 60°9' N 131° 27' W 20 km north of Swift River. The Property is accessible by helicopter and consists of 132 Quartz Claims recorded in the Watson Lake Mining District. The claim blocks cover tin and tin-tungsten mineralization documented in the Yukon Minfile. It was staked in 2011 by Panarc Resources Ltd., and is subject to an option to purchase by Ucore Rare Metals Inc.

The Project area is primarily underlain by Cretaceous Seagull Batholith granite intruding Carboniferous metavolcanics, clastics and carbonates. The Seagull Batholith is a highly evolved S-type granite, particularly enriched in Sn, B and F.

Between 2011 and 2013, Panarc Resources Ltd conducted a number of successive exploration programs on the property, including mapping, prospecting, soil and stream sampling and shallow drilling. Grab samples from the Con, Do, Milk and Eccles Claims produced economic tin grades of up to 2.5% tin. A tin-in-soil anomaly was also located on the Do Claims covering 500m along slope and below exposed bedrock mineralization. A regional aerochemical sampling program conducted in 2012 identified a strong coincident tin-tungsten anomaly in what is now the Snips Claim Block. Prior to this, the property had been mainly staked and explored by Du Pont Exploration in the 1980's.

The geochemical results of the 2014 program have identified the source of the geochemical anomaly on the Snips Claims to be northeast of Tin Creek. Geochemical sampling on the Do Claims identified a 250 metre square area of anomalous area with tin values averaging 553 ppm and that is open towards the north. A total 2421 line kilometres was flown during the course of the airborne geophysical survey at 300 metre line spacing. The lithological contacts between the Seagull Batholith granite and the carbonate, clastic and greisen units on the Con, Do, Eccles, Goods, Milk, Peas and Tuna Claims were identified by gradational contacts between higher and lower magnetic intensity values.

Based on these results, a program consisting of additional geological mapping, prospecting and mapping is recommended throughout the Seagull Project area focusing on the identified geochemical anomaly areas and the contacts between higher and lower magnetic intensity. Additional ground or airborne magnetic surveys along with ground induced polarization is also recommended in order to increase the resolution of current data and further delineate lithological contacts and areas of mineralization.



## 2 INTRODUCTION

This report describes a helicopter-borne magnetic and radiometric survey and a soil sampling and prospecting program conducted at the Seagull Tin Project in the southern Yukon Territory. Aurora Geosciences Ltd. was retained by Ucore Rare Metals Inc. to conduct this program to locate new bedrock tin targets and delineate identified mineralization within the current claims.

All geographic locations in this report are relative to North American Datum 1983. Non-geodetic coordinates are expressed in Universal Transverse Mercator Zone 9N metric coordinates. All measurements are expressed in the metric system unless they are measurements quoted from historic reports expressed in other units of measure. All geophysical data units are in the metric SI system. Angles are expressed relative to true north unless otherwise stated.

## 3 LOCATION & ACCESS

The Seagull Tin Project is centred at 60°9' N 131° 27' W on NTS Map Sheets 105 B3 and B4 in the Watson Lake Mining District. The property location is shown in Figure 1. The Property is 210 km southeast of Whitehorse and 150 km west-northwest of Watson Lake, the closest major communities. The property is accessible by helicopter with the nearest staging point being Swift River (Km 1136 on the Alaska Highway), 20 km south of the property centre and 283 km south of Whitehorse by road. There are old overgrown bulldozer trails to the property from the Alaska Highway near Swift River. The Property is also accessible by float plane to Dorsey Lake from either Whitehorse or Watson Lake.

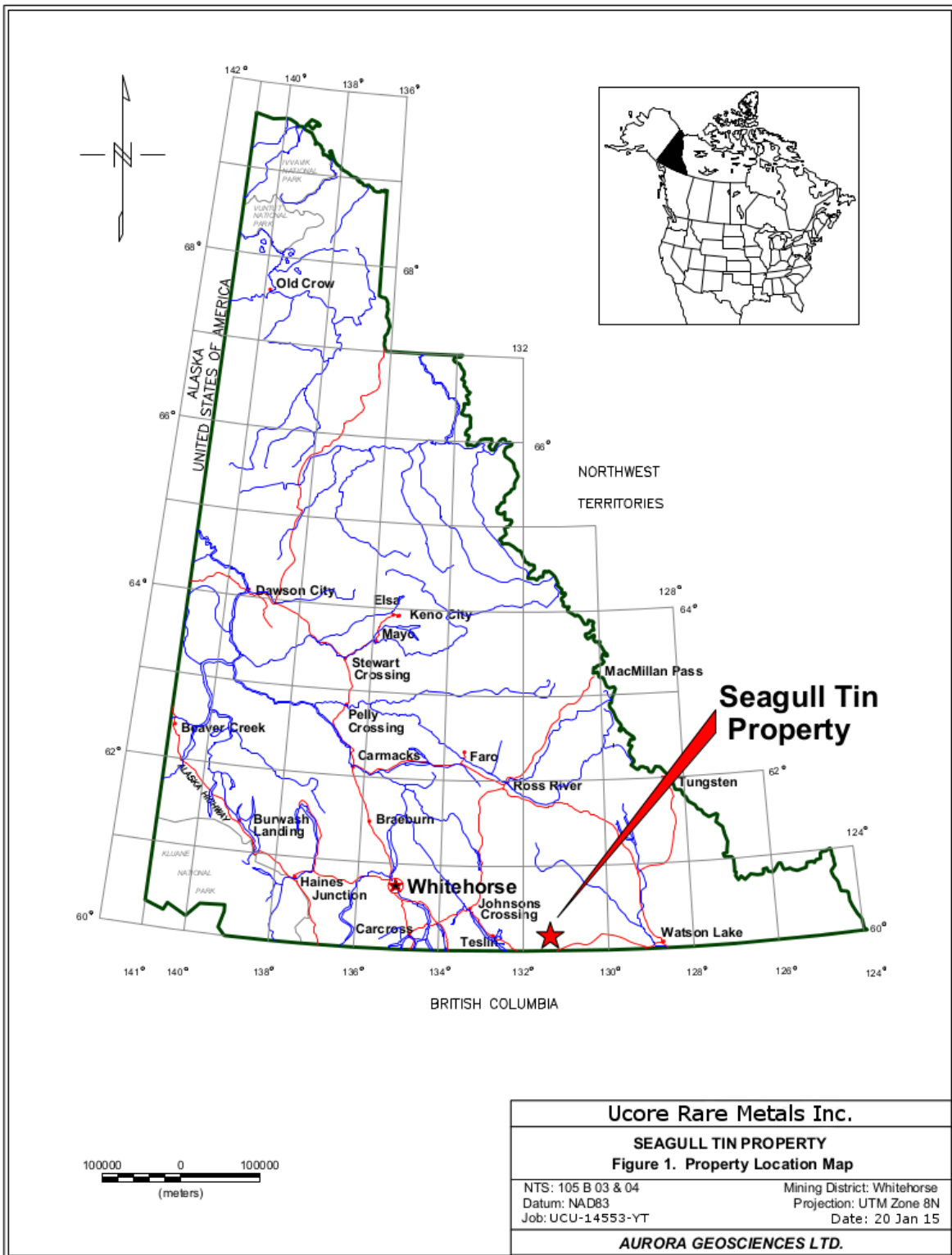


Figure 1. Seagull Tin Property location map.

## 4 PROPERTY DESCRIPTION

The Seagull Tin Project consists of 132 un-surveyed Quartz Claims recorded in the Watson Lake Mining District (Figure 2, 3). Claim information<sup>1</sup> for those claims on which the work was performed is summarized below:

**Table 1. Claim data**

Claim Name	Tag Number	Anniversary Date
DO 1-4	YD106431 – YD106434	April 4, 2017
DO 5-20	YE31802 – YE31817	January 19, 2015
ECCLES 1-16	YE31818 – YE31833	January 19, 2019
LAUGHTER 1-4	YD106423-YD106426	April 4, 2017
MUSIC 1-4	YD106419-YD106422	April 4, 2017
TUNA 1-4	YD106415-YD106418	April 4, 2017
BEANS 1-36	YD106379-YD106414	October 9, 2015
SNIPS 1-24	YE32355-YE32378	October 9, 2015
CON 1-4	YD106427-YD106430	April 4, 2017
CORN 1-4	YD106435-YD106438	April 4, 2017
FIRE 1-4	YD106439-YD106442	April 4, 2017
MILK 1-4	YD106447-YD106450	April 4, 2017
PEAS 1-4	YD106443-YD106446	April 4, 2017
GOODS 1-4	YD106451-YD106454	April 4, 2017

The claims comprising the Property may be retained in good standing by performing assessment work in the amount of \$100 per claim and paying assessment filing fees of \$10 per claim (Yukon). The Seagull Tin Property is under option to purchase by Ucore Rare Metals Ltd.

<sup>1</sup> Claim information as provided by the Watson Lake Mining Recorder ([www.yukonminingrecorder.ca](http://www.yukonminingrecorder.ca)) on January 16, 2015.

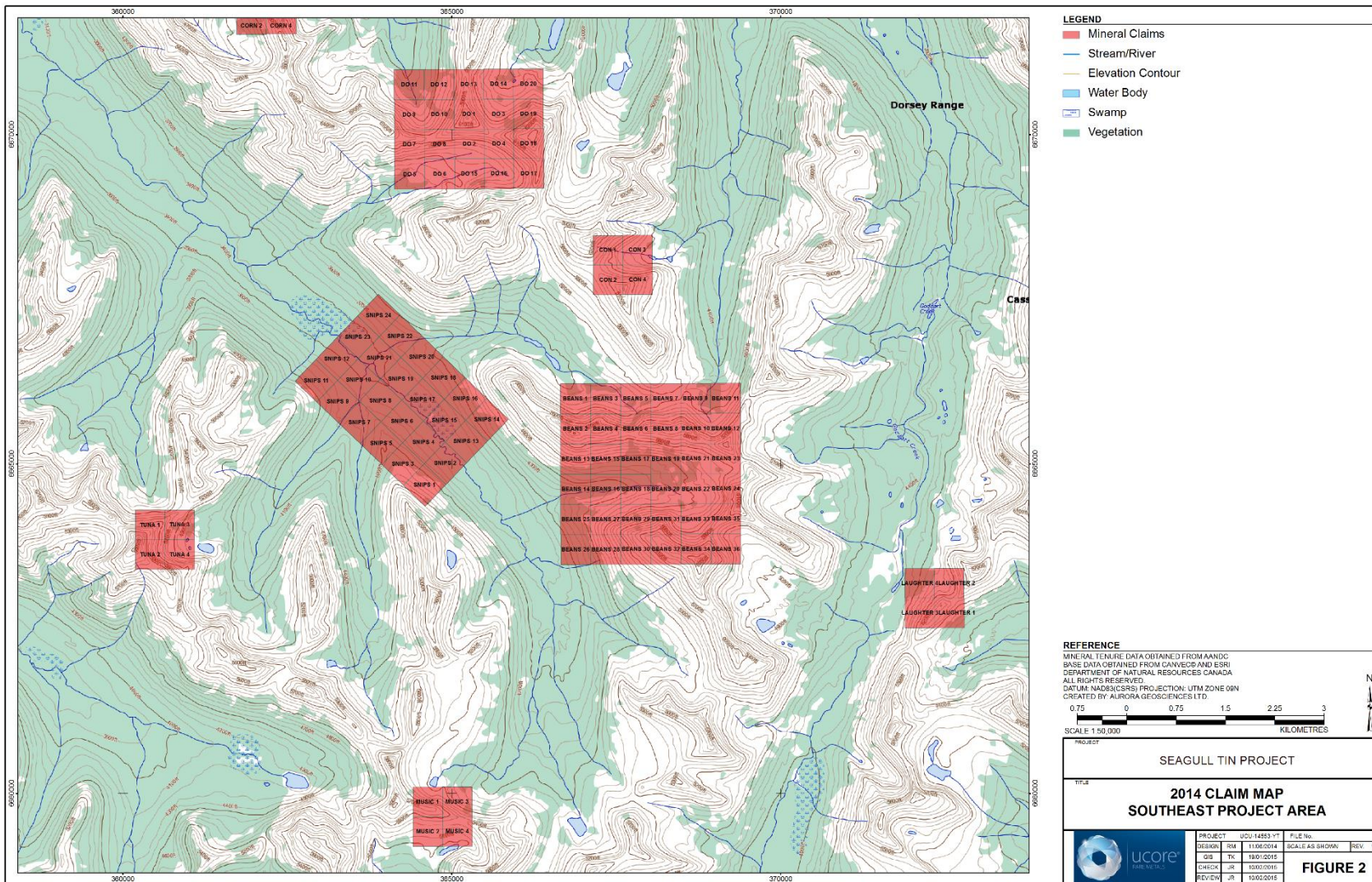


Figure 2. 2014 Claim map for the southeast portion of the project area.

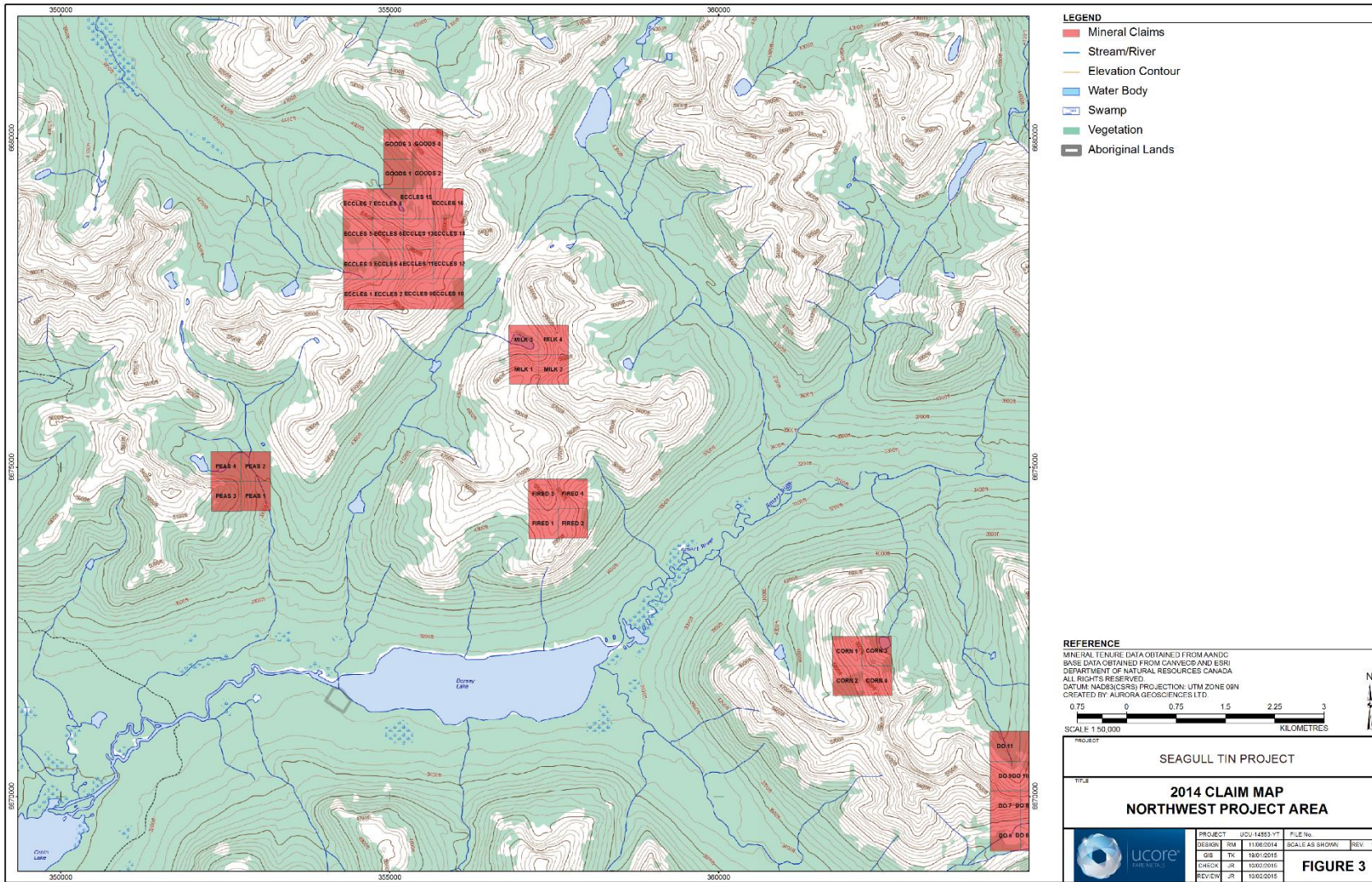


Figure 3. 2014 Claim map for the northwest portion of the project area.

## 5 CLIMATE & TOPOGRAPHY

The Seagull Tin Property is located in the Cassiar Mountains of the Yukon Plateau. Topography in the area consists of rugged peaks with steep north-facing cirques and scoured U-shaped valleys. Elevations in the project area range from 910 to 2070 m (3000 to 6800 feet). Above 5500 feet, the terrain is rugged with steep ridges and impassable rocky slopes. The glacial scour line at between 5000 to 5500 feet is readily visible in some cirque headwalls. At lower elevations, mountains and hills are rounded with convex, steep sided slopes. Boulder talus aprons occur at the base of most of the rocky faces and these are succeeded by grassy slopes with immature brown soils. Below tree line at roughly 4000 feet, more mature soils and dense vegetation predominates.

The project area is drained by south-flowing creeks and rivers, the largest of which is the Smart River. This drains through Dorsey Lake in the north center of the property area. Dorsey Lake is approximately 3 km long and is the largest water body in the project area. Vegetation in the property area ranges from mosses, grass and sedges at elevations above 5000 feet through a zone of willow and sparse spruce and fir down to tree line. Below tree line, alpine fir and black spruce predominate.

The climate in the property area consists of long, cold winters, short wet summers and short spring and fall seasons. At Watson Lake, the closest nearby community, average daily temperatures range from -24° C (January) to +15° C (July) and average annual precipitation consists of 40.4 cm of rain and snow with the majority falling in June and July (Environment Canada, 2014).

## 6 EXPLORATION HISTORY

The Seagull Tin Property is located in the area of the Seagull Batholith; an area that contains numerous tin, lead-zinc and tungsten showings. The Seagull Tin Property covers eleven Yukon Minfile showings, staked and explored for tin and tin-tungsten mineralization between 1978 and 1982. Information for the individual showings is summarized in the table 2. Additionally, regional stream sediment geochemistry published by the Yukon Geological Survey in 2003 in the area of the Seagull Batholith is highly anomalous in tin (Heon, 2003).

Between 2011 and 2013, Panarc Resources Ltd. re-staked the area encompassed by the Seagull Tin Property and completed a number of exploration programs consisting of stream and soil sampling, prospecting and shallow diamond drilling. Economic tin values from bedrock samples were returned from four of the eleven claim blocks investigated thus far: the Do, Goods, Eccles and Con Claims. Grab samples from these claim blocks returned up to 2.459% Sn. Contour soil sampling run on the Do Claims below an area with identified skarn and vein mineralization defined a zone at least 500m long with elevated soil values greater than 200 ppm Sn and peak values to 1300 ppm Sn. Additionally, a regional airborne geochemical program in 2012 investigating 161 km of stream detected a strong coincident tin and tungsten anomaly in the informally named Tin Creek which drains northwest into Dorsey Lake. Lastly, a shallow drilling program was conducted in 2013 on the Eccles Claims utilizing a Boyle Winkie

drill and testing an observed greisen zone on the Property. Four holes with a total completed footage of 48.3m were drilled testing approximately 50m of the eastern end of the greisen zone. The best results from the drill program were 231 ppm Sn over 0.44m from the bottom of the last hole in the program which bottomed into the greisen zone.

**Table 2. Showings**

Minfile Name Number [Current claim block]	Summary
Stoddart 105B 035 [Beans 1-36]	Staked by Rip Van Mining Ltd. in 1969 and re-staked by the Klinkit Joint Venture (DuPont of Canada Exploration Ltd. and Duval Corporation) in 1978. Tin, lead-zinc-silver skarn mineralization reported with a chip sample running 3.9% Zn, 17.1 g/t Ag over 6.7 m with no tin values cited. Two holes were drilled in 1984 for which results are not reported.
Hollister 105B 112 [Tuna 1-4]	Staked by the Klinkit Joint Venture in 1978, the block was explored with geochemical surveys and mapping in 1978-1980 and 1982. Scheelite skarn is reported at the contact between the Seagull Batholith and the overlying limestone.
Slouce 105B 080 [Music 1-4]	Staked by the Klinkit Joint Venture in 1978, the property was explored by mapping, trenching and sampling from 1978 to 1980. Portions were re-staked by McPrez Mining Exploration Ltd. and optioned to Player Petroleum Ltd. in 1981 who explored their claims with mapping, geochemical sampling and trenching. Five skarn zones over a length of 400 m returned up to 1.2% Sn from tourmaline-magnetite-amphibole-chalcopyrite skarn up to 0.5 m wide in limestone near the contact with the Seagull Batholith.
Skin 105B 079 [Laughter 1-4]	The Skin Showing consists of two separate showings staked by the Klinkit Joint Venture in 1978 and explored by mapping and hand trenching in 1979 - 1980. In both cases, mineralization is hosted by quartz-muscovite-arsenopyrite veins within the Seagull Batholith. The western showing returned two samples averaging 0.3% Sn and a sample from the eastern showing returned 0.435% Sn.
Current 105B 073 [Con 1-4]	Staked by the JC Syndicate (Dome Exploration and Cominco Ltd.) In 1977 and explored in 1977-79 with mapping, sampling, geochemical and magnetometer surveys and two drill holes. Malayaite, sphalerite, pyrrhotite, rare galena and fluorite occur in skarned metavolcanics, clastics and limestone near the contact with the Seagull Batholith. Report chip samples returned 6.5% Zn and 0.03% WO <sub>3</sub> over 1.2 m but the drill holes failed to intersect significant mineralization.
Sin 105B 083 [Do 1-16]	Staked by Welcome North Mines Ltd. in 1978 and optioned to the Klinkit Joint Venture, the Sin Showing covers a suspected tin porphyry. Weak greisen zones returned samples from 0.1% Sn to 0.2% Sn from quartz-tourmaline-muscovite-fluorite veins and magnetite-garnet skarn. A large soil anomaly, over 1 km long was outlined by contour surveying below the showings with values ranging from 200 ppm Sn to 0.26% Sn.
Pont 105B 082 [Corn 1-4]	The Pont Showing was staked by the Klinkit Joint Venture in 1978 and explored by mapping and sampling in 1978-79 and 1982. Minor cassiterite in skarn and disseminated within the underlying Seagull Batholith is reported in the Minfile but no assays are included in the assessment report (090470).
Dorsey 105B 111 [Fired 1-4]	The Dorsey Showing was staked as part of the larger DU block in 1978 and explored by mapping and geochemical sampling in 1978 and 1979. The Minfile occurrence covers a tin soil geochemical anomaly with no known bedrock source. Sn in soils from 200 to 575 ppm occurs south of the ridge on which the nominal Minfile location is plotted. On the north side of the ridge, a single soil sample surrounded by a large area of no samples returned 300 ppm Sn.

JC 105B 040 [Peas 1-4]	The JC Showing was staked by Esannee Exploration Ltd. in 1967 who explored by bull dozer trenching. Cypress Exploration Ltd. staked the showing twice, and drilled two short holes. Restaked by the JC Syndicate in 1977, it was subsequently explored by mapping, geochemistry, both ground and airborne mag surveys, and two rounds of drilling. The showing covered by the Peas block is peripheral to the main JC showings and is underlain by skarned limestone and underlying Seagull Batholith granite. Best reported assays were 1.26% Sn over 2.6 m in a 1978 trench but many assays were not reported.
Du 105B 084 [Milk 1-4]	The Du Showing is centered on Eccles Ridge north of Dorsey Lake and was staked by the Klinkit Joint Venture in 1978 and explored by mapping, geochemical sampling and trenching during 1978-1980 and by drilling one hole in 1981. The showing consists primarily of a greisen vein system exposed over a distance of about 60 m from which selected samples to 2% Sn were recovered. The single hole beneath the showing returned 0.14% Sn over 1.0 m.
Duval 105B 081 [Goods 1-4] [Eccles 1-16]	The Duval Showing was staked as part of the larger Du claim block by the Klinkit Joint Venture in 1978 and explored from 1978 to 1981 by geochemical sampling, mapping and one drill hole. Drilling reportedly encountered extensive greisen but only low tin values over narrow widths. The drill results were never filed for assessment.

## 7 DEPOSIT MODEL

Tin deposits occur in four major classes. The claim blocks comprising the Seagull Tin Property includes showings which have been classified in each of these deposit models.

- *Vein-hosted lode deposits.* With type examples at Cornwall (UK), Potosi (Bolivia), Erzgebirge (Czechoslovakia), and Herberton (Australia), this style of mineralization consists of quartz-albite-microcline-cassiterite(-wolframite) veins and pegmatites within localized greisen envelopes in the cupola of granitic intrusions. Grades are in excess of 1% and tonnages are small (<10 MT). The Du Showing (Milk Claims) appears to be a classic greisen vein system.
- *Carbonate hosted deposits.* Type examples include the Renison Bell and Cleveland Deposits in Australia. These are replacement to exoskarn deposits, often structurally controlled, in permissible carbonates proximal to a fertile granitic intrusion. Grades range from 0.7% to 1.0% Sn and tonnages range from 2 to 10 Mt. True skarn deposits are generally smaller and include the JC Deposit, peripheral to the Peas claim groups.
- *Greisen hosted deposits.* Deposits in this class are hosted in extensive greisen alteration envelopes, often adjacent to richer lode deposits. Examples include Mt. Tin near Herberton in Australia. Taylor (1979) estimates these deposits contain from 10 - 80 Mt at about 0.3% Sn. The vein swarms on the Laughter Claims (Skin Showing) appear to fit this deposit type.
- *Porphyry tin deposits.* First recognized by Sillitoe (1975), this style of mineralization includes large (40 - 500 Mt), low grade (0.2 - 0.4% Sn) deposits in hydrothermal breccias within and adjacent to fertile granitic intrusions. Type examples include Llallagua and Chorolque in Bolivia (Sillitoe, *ibid*) and Yinyan in China (Xianghazao et. al. 1996). The Sin Showing (Do Claims) has been classified as a potential tin porphyry.

## 8 REGIONAL GEOLOGY

The regional geology in the property area is summarized by Gordey & Makepeace (1999) from regional mapping by Poole et. al. (1960) and more detailed mapping by Abbot (1981). The geology of the property area is shown in Figure 4.

### 8.1 Tectonic setting

The property lies in the Quesnellia Terrane of the Canadian Cordillera, an allochthonous package of pelagic sediments, carbonates and volcanics, formed in the Early Triassic. The Quesnellia Terrain was subsequently amalgamated with the Stikine, Cache Creek and Slide Mountain Terranes to form the Intermontane Superterrane in the Early Jurassic and completed docking with North America in the Early Cretaceous (Gabrielse and Yorath, 1991).

### 8.2 Stratigraphy

The following formations are mapped in the property area:

**Table 3. Regional stratigraphy in the project area**

<b>Formation (Age)</b>	<b>Description</b>
Overburden (Quaternary - Holocene)	Talus, organic and elluvial soil, boulder till.
<b>mKqC</b> <i>Seagull Batholith</i> [Cretaceous]	Granite, quartz monzonite, granodiorite, locally porphyritic. (117 – 85 Ma)
<b>EjgA</b> [Early Jurassic]	Granodiorite, diorite, monzonite (192 – 185 Ma)
<b>EjgL</b> [Early Jurassic]	Diorite, quartz monzonite (193 – 183 Ma)
<b>TrJ1</b> [Triassic]	Siltstone, sandstone, chloritic meta-tuff, quartzose grit/marble (246 – 204 Ma)
<b>TrJ2</b> [Triassic]	Marble with interbedded chloritic units (246 – 204 Ma)
<b>CK3</b> [Carboniferous]	Shale, argillite, slate and siltstone (353 – 300 Ma)
<b>CK2</b> [Carboniferous]	Limestone, dolostone, chert (353 – 300 Ma)
<b>CK1</b> [Carboniferous]	Mafic volcanic flows, breccias and tuffs (353 – 300 Ma)
<b>DMF1</b> [Late Devonian to Early Carboniferous]	Flows, breccia, tuff (365 – 345 Ma)
<b>DMF3</b> [Late Devonian to Early Carboniferous]	gr-quartzite, qt-mica-schist (365 – 345 Ma)
<b>PDS1</b> [Proterozoic to Devonian]	bt-grnt-schist, quartz meta-grit, minor marble (635 – 375 Ma)

### 8.3 Structure

The structural and intrusive history of the project area is summarized by Abbot (1981) and Gabrielse and Yorath (1991) who describes the following deformational and associated igneous events:

**Table 4. Deformational history in the project area**

Age	Description
Late Cretaceous	Northeast and east-trending normal faulting.
Mid-Late Cretaceous	Intrusion of the Seagull Batholith
Middle Jurassic	Collision of Intermontane Superterrane: transpressional collision (thrust faulting with subsidiary strike slip and normal faulting)
Early Jurassic	Basic to intermediate intrusions; Amalgamation of the Intermontane Superterrane

Templeman-Kluit (1991) summarizes the structural style in the Cassiar Mountains and describes the imbrication of the Dorsey and Slide Mountain Allochthons (Sub-terrane of Quesnellia) over the autochthonous North American basement rocks via northeast directed thrust faulting. In the immediate property area, the stratigraphy appears to be folded into a broad NW-trending synclinal arch or graben with Devonian-Mississippian metavolcanic and metasedimentary rocks flanking a central core of similar Carboniferous rocks.

The Seagull Batholith intrudes the centre of the aforementioned arch forming an elongate, elliptical mass roughly 40 km (NW-SE) by 10 km (NE-SW). Tin-tungsten mineralization in the district appears to be both spatially and genetically related to this intrusion. The Seagull Batholith is a polyphase pluton ranging from aphyric coarse biotite granite through granodiorite to porphyritic quartz-Kspars biotite granite. The intrusion appears to be tilted with apical porphyritic phases more prevalent in the northwest and deeper coarser grained, equigranular intrusive rocks dominant in the southeast. Contacts are generally steeply-dipping on the SW and NE flanks of the intrusion but are flat to gently dipping beneath roof pendants north of Dorsey Lake. Here the valley floors are underlain by Seagull Batholith granite while the surrounding mountains are capped by hornfelsed Carboniferous rocks. Porphyritic phases included rounded quartz and angular potassium feldspar together with local mariolitic ocelli ("bubble texture") in the vicinity of at least one tin showing (Do Claims) (Smith, 1980).

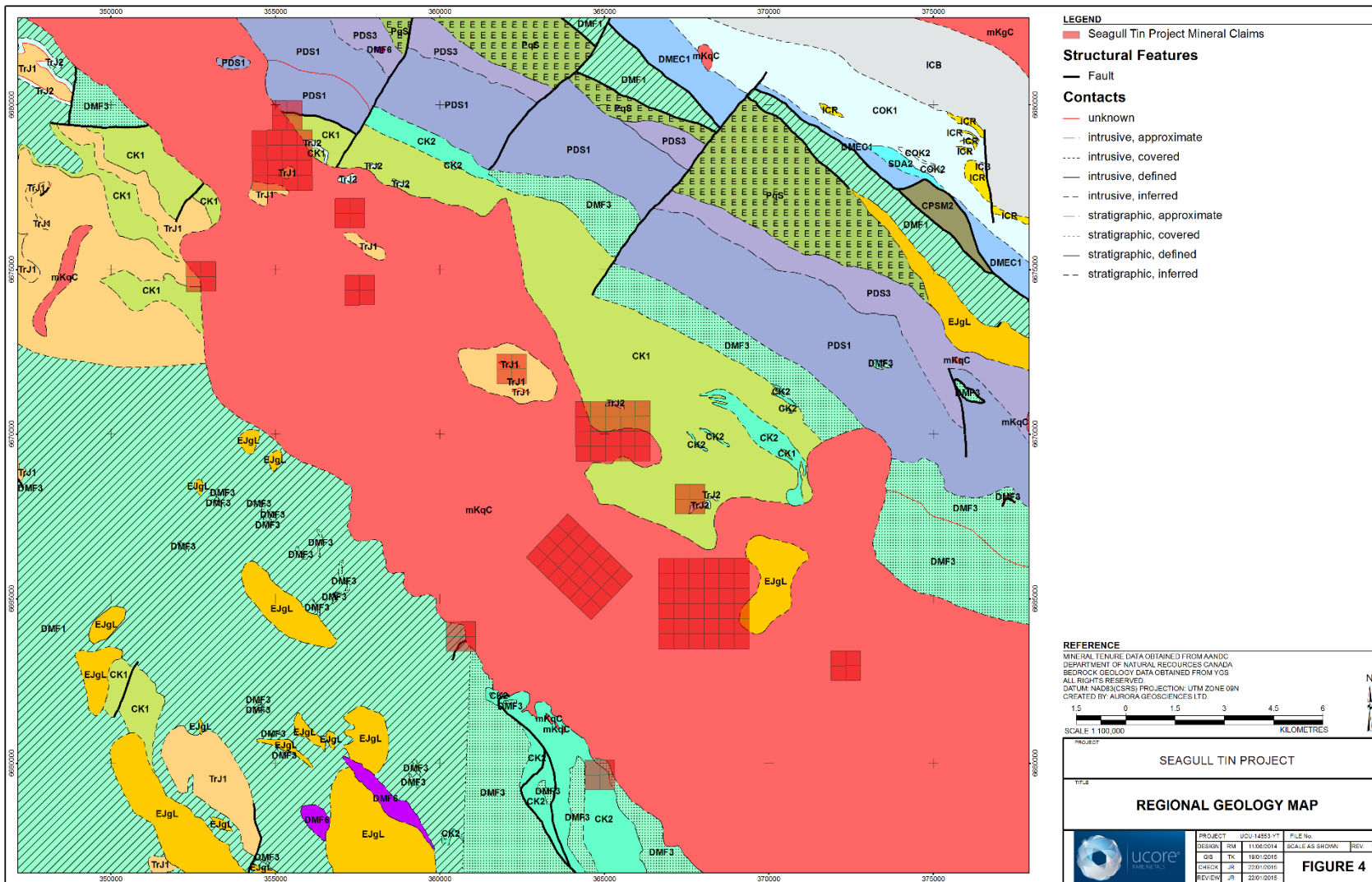


Figure 4. Regional Geology map.

## 9 WORK PROGRAM

This section describes the work program conducted on the Seagull Tin Project in 2014. Appendix II contains a project log and Appendix III contains a summary of expenditures.

### 9.1 Airborne Magnetic and Radiometric Survey

An airborne magnetic and radiometric survey was flown by Precision Geosurveys from October 7<sup>th</sup> to October 22<sup>nd</sup>, 2014. The purpose of this survey was to identify and delineate potential magnetite-bearing skarns and greisen zones surrounding and within the Seagull Batholith.

#### 9.1.1 Survey Specifications

Specifications and procedure for this geophysical survey are described in the Precision GeoSurveys Airborne Geophysical Survey Report in Appendix IV.

#### 9.1.2 Data Preparation

The diurnally corrected magnetic data supplied by Precision GeoSurvey are imported into Geosoft Oasis software. An examination of the survey report along with magnetic field profiles and terrain clearance data indicate that the data is of good quality. No further processing is performed on the data prior to the inversion modelling presented in this report.

#### 9.1.3 Inverse Modelling

Geosoft's VOXI Magnetic Vector inversion software service is used to generate 3D voxel models of magnetic susceptibility from the observed magnetic data. Elevations are assigned to the data according to the values measured by the airborne survey. Prior to the inversion the computed International Geomagnetic Reference Field (IGRF) strength is removed from the data. The earth beneath the grid is discretized by model cell sizes set to 50 metres X 50 metres X 25 metres (deep) over the core survey area to allow the modelling software to recover causative bodies emplaced at similar depths. Coarser padding cells are added adjacent to the core area and at depth to avoid edge effects from exerting any influence on the inversion results. By default, the software filters and de-samples the data to one reading per model cell. A uniform estimate of the error in the total magnetic field data of 10 nT is used in the inversion and the modelling is run un-constrained with only the application of iterative reweighting inversion to improve the geometry of the results.

### 9.2 Geochemical Soil Sediment Survey

A soil sediment geochemical survey was conducted from October 10<sup>th</sup> to October 12<sup>th</sup>, 2014. The purpose of the survey was to locate and constrain any mineralization within the geochemically anomalous areas identified by the airborne stream sediment survey conducted in 2012.

#### 9.2.1 Personnel & equipment

The work program was conducted by the following personnel:

Crew chief:

Phil Jackson

Samplers:

Shane Carlos

The crew was equipped with the following instruments and equipment:

<u>Instruments:</u>	3 – Garmin non-differential GPS receivers
<u>Equipment:</u>	3 – Radios 3 – Digital cameras Iridium satellite phone Compasses Soil augers Mattocks Kraft bags Plastic sample bags Rice bags Flagging Double-sided aluminium butter tags w/ wires Permanent markers Field notebooks Sample tag books

### **9.2.2 Soil sediment sample specifications**

Soil sediment sampling was conducted according to the following specifications:

<u>Mapping Datum:</u>	NAD83 UTM Zone 9N
<u>Location recording:</u>	Non-differential GPS receivers, averaging readings a minimum of 15 times.
<u>Marking:</u>	Soil sample locations were marked with orange and blue flagging and a double-sided aluminum butter tag
<u>Sampling:</u>	Soil samples were collected predominantly from the C horizon, and occasionally the B horizon.
<u>Traverses:</u>	Recorded with non-differential GPS receivers. 50 m spacing between sample locations along traverse lines.
<u>Records:</u>	Information on the location, date, elevation, tag number, station, sample depth, horizon sampled, depth within sampled horizon, sample colour, angled clasts percentage, organics percentage, gravel percentage, sand percentage, silt percentage, clay

percentage, parent material, moisture content, vegetation and topographic position. Between one and two photographs of the sample and location were also taken and are included in the digital archive.

### 9.3 Prospecting

A prospecting survey was conducted on the Do Claims on the October 14<sup>th</sup>, 2014. The purpose of the survey was to check the MinFile showing locations located on Claims, and locate and identify mineralization related to the showing.

#### 9.3.1 Personnel & equipment

The work program was conducted by the following personnel:

<u>Crew chief:</u>	Phil Jackson
<u>Sampler:</u>	Shane Carlos

The crew was equipped with the following instruments and equipment:

<u>Instruments:</u>	3 – Garmin non-differential GPS receivers
<u>Equipment:</u>	3 – Radios 3 – Digital cameras Iridium satellite phone Compasses Soil augers Mattocks Plastic sample bags Rice bags Flagging Double-sided aluminium butter tags w/ wires Permanent markers Field notebooks Sample tag books

#### 9.3.2 Rock sample specifications

Geological prospecting was conducted according to the following specifications:

<u>Mapping Datum:</u>	NAD83 UTM Zone 9N
<u>Location recording:</u>	Non-differential GPS receivers, averaging readings a minimum of 15 times.
<u>Marking:</u>	All sample locations were marked with orange or blue flagging and double-sided aluminum butter tags.

## Records

Information on the location, sampler, sample number, date and description were recorded for each grab sample collected. One or two photographs of the sample and location were also taken and are included in the digital archive.

## **10 SAMPLE COLLECTION, SECURITY, PREPARATION & ANALYSIS**

This section describes principles and procedures used in the collection, security, preparation and chemical analysis of stream sediment samples collected during the program. All samples collected during the program were sealed in rice bags for transportation to the analytical laboratory with security tags. Samples were retained in the custody of Aurora personnel throughout transportation to the laboratory or were conveyed by a commercial carrier with a conveyance and security form attached.

### **10.1 Soil Sediment Samples**

Soil samples were collected predominantly from the C horizon, and on occasion from the B horizon. Samples were collected in Kraft paper bags and filled to the limit to ensure a sufficient weight of sample was collected for analytical processing.

At the laboratory, stream sediment samples were prepared and analyzed as follows (ACME Labs method codes in parenthesis):

1. Samples were dried at 60<sup>o</sup> C (Dry at 60C)
2. A 100 g subsample passing -10 mesh was sieved from the sample (SS10)
3. 100g soil subsample pulverized (PULSL)
4. Refractory and REEs analyzed by fusion and ICP-MS analysis (LF100)
5. Heat treatment of Soils and Sediments (DISP2)

### **10.2 Rock Samples**

Grab samples were collected on the Do Property during the program to determine the range and grade of economic mineralization. The samples were collected along the ridgeline within 500m of the Sin Minfile showing. They comprise of metasedimentary to metavolcanic rocks containing variable iron oxidation and quartz-chlorite veining.

At the laboratory, rock samples were prepared and analyzed as follows (ACME Labs method codes in parenthesis):

1. Crush, split and pulverize 250g rock to 200 mesh (PRP70-250)
2. Total Whole Rock Characterization with AQ200 (LF202)

## 11 RESULTS

### 11.1 Geochemical and Prospecting Surveys

This section describes the results of the geochemical and prospecting surveys performed on the Seagull Tin Property in 2014. A total 102 soil samples and 9 rock samples were collected on the Do and Snips Claims for geochemical analysis.

#### 11.1.1 Statistics

Summary statistics for Sn, W and the rare earth elements are tabulated below:

**Table 5. Summary statistics, Snips Property – Soil sediment sample analyses**

<b>Statistic</b>	<b>Sn</b>	<b>W</b>	<b>LREE</b>	<b>HREE</b>	<b>TREE</b>
No. of observations	46	46	46	46	46
Minimum	4	3.3	60.48	15.97	85.74
Maximum	59	9.4	252.98	96.64	334.28
1st Quartile	7	4.625	136.7225	32.2375	169.205
Median	9	5.3	167.175	38.9	210.065
3rd Quartile	25	6.55	206.7775	52.8275	253.515
Mean	16.91304	5.602174	165.3822	42.62957	208.0117
Standard deviation (n-1)	13.41937	1.503545	48.84285	17.25849	63.47755

**Table 6. Summary statistics, Do Property – Soil sediment sample analyses**

<b>Statistic</b>	<b>Sn</b>	<b>W</b>	<b>LREE</b>	<b>HREE</b>	<b>TREE</b>
No. of observations	58	58	58	58	58
Minimum	15	2	15.93	3.2	19.13
Maximum	1940	26.6	102.13	25.31	127.06
1st Quartile	52.25	5.275	31.035	7.355	37.89
Median	91.5	8.7	44.95	11.53	56.97
3rd Quartile	185.25	10.375	62.5	16.61	78.3675
Mean	227.9828	8.456897	47.19655	12.37741	59.57397
Standard deviation (n-1)	333.6918	4.264897	21.20696	5.979379	26.99313

The data set contains highly anomalous Sn on the Do Property, and weakly anomalous Sn on the Snips Property. Rare earth elements and tungsten assay values are weakly anomalous on the DO Property, and not anomalous on the SNIPS Property.

#### 11.1.2 Geochemical anomalies of interest

Tin data for the Do and Snips Properties has been plotted in dot plot format in Figures 5 and 6, respectively. The bin intervals for soil results were selected on the basis of the summary statistics and from lowest to highest are set at the 1<sup>st</sup> quartile, mean, and the first through 3<sup>rd</sup> standard deviations

above mean. The principal anomaly of interest is a 250 square meter area on the Do Property centered at approximately 365304E 6669831N (Figure 5). Tin values from 15 samples collected within this area averaged 553 ppm and a maximum of 1331 ppm. Additionally, a lone sample collected on the ridgeline approximately 300 meters northwest from the principal anomaly of interest returned 1940 ppm.

There is a weak tin anomaly on the northeast soil line located on the Snips property (Figure 6). Assay values along this line ranged between 17 and 59 ppm tin.

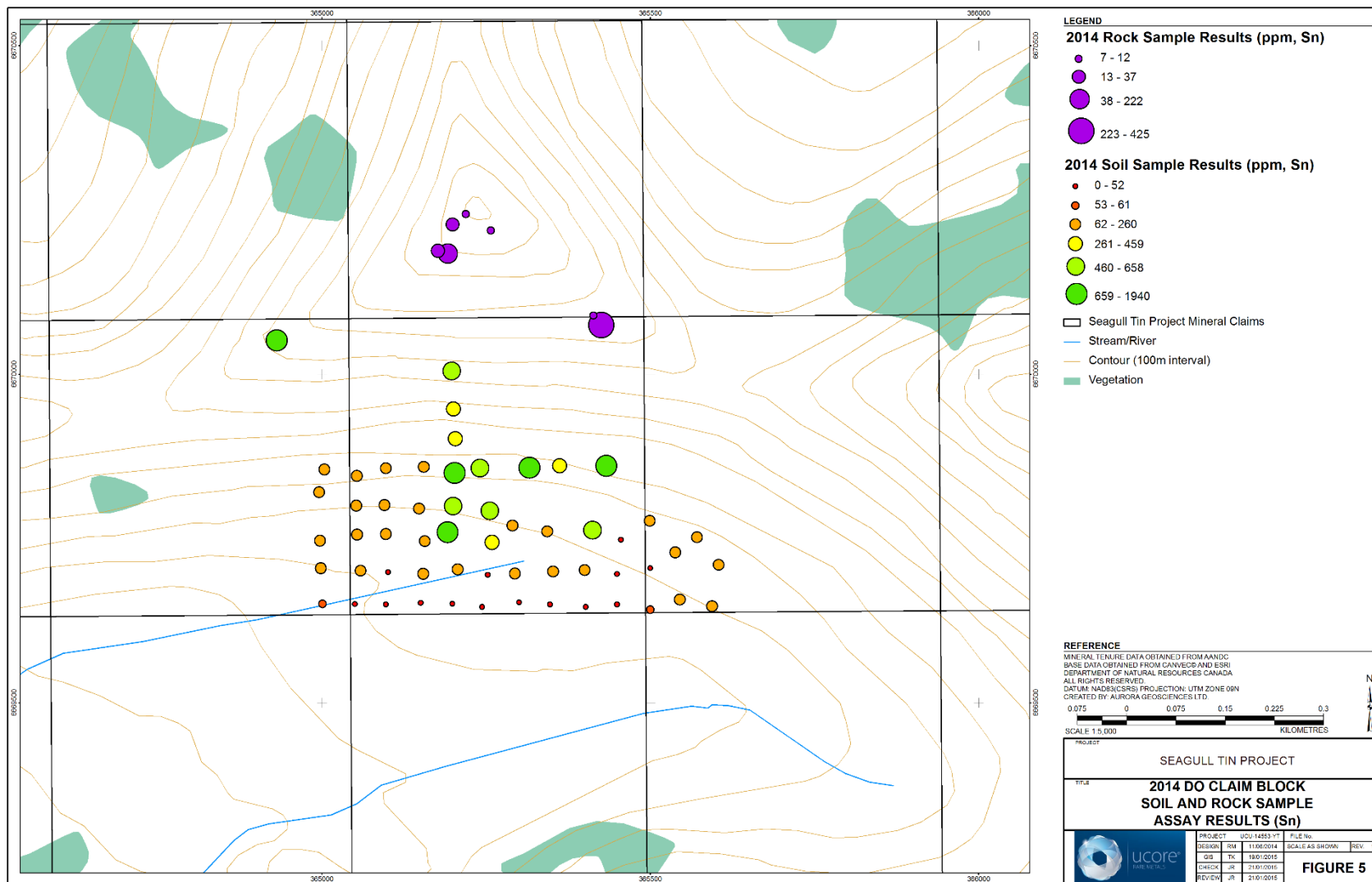


Figure 5. 2014 Do Claims soil and rock sample tin assay results.

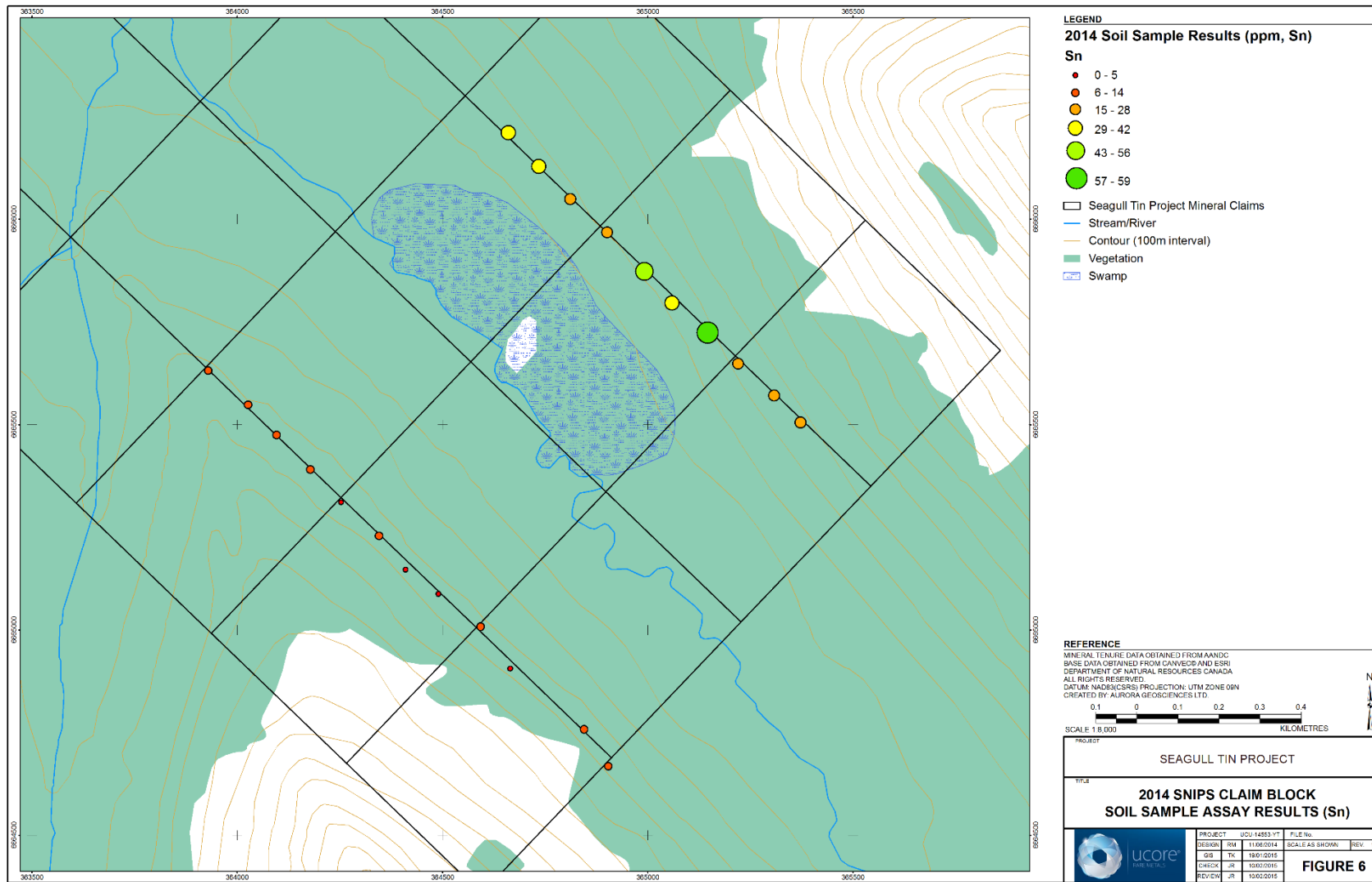


Figure 6. 2014 Snips Claims soil sample tin assay results.

## 11.2 Geophysical Surveys

This section describes the results and processing of the airborne magnetics survey performed on the Seagull Tin Property in 2014. A total 2421 line kilometres was flown at 300 metre line spacing, covering the area within and surrounding the Seagull Tin Claims. The data was processed into eight blocks overlying the claim areas and measuring 7500 metres by 7500 metres (Figure 7).

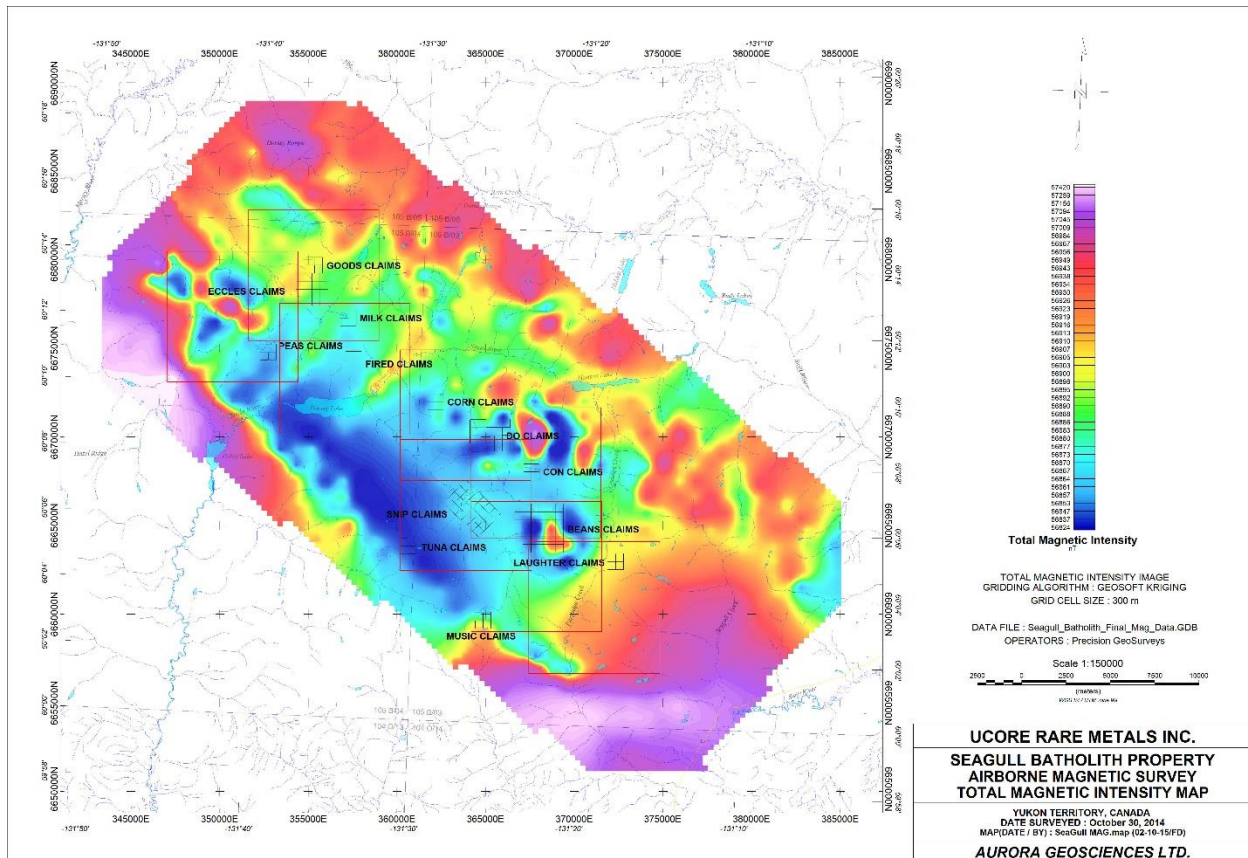


Figure 7. Total Magnetic Intensity Map for the complete airborne survey area. Red squares represent the 7500x7500 metre blocks that have undergone further processing.

### 11.2.1 Corn and Do Claims

A 7500 metre by 7500 metre area of magnetic data from the Seagull batholith aeromagnetic survey dataset encompassing the Pont Showing, Corn Claims and Sin Showing, and Do Claims is examined and inversion modelled (Figures 8 and 9).

Residual magnetic intensity measured over the area range 2178 nT from -1550nT to 627 nT. The highest recorded values form narrow linear magnetic anomalies which strike northwest across the central western portion of the area, immediately north of both the Do and Corn Claim Blocks.

The Corn Claims hosts a continuous though more subdued positive magnetic anomaly which strikes north-northwest through the claims. The anomaly is offset slightly and exhibits lower values near the Pont showing located in the centre of the claim block. The results of the magnetic field inversion

indicate that the observed positive magnetic anomalies are a result of moderately susceptible material forming a zone in the order of 500 metres wide. The zone is semi-continuous through the claim block, extends from near surface to 500 to 750 metres below surface and dips approximately 45 ° to the northeast.

Moderate magnetic highs strike predominantly east-west across the centre of the Do Claims. The highest values are recorded on the western edge of the claims forming a narrow anomaly which gradually becomes broader and loses amplitude to the east before swinging to the north near the centre of the claim block. The eastern portion of the claim block exhibits a broad magnetic high anomaly which diminishes towards the centre of the claim block. Inversion modelling of the magnetic field data indicates that the observed magnetic highs are caused by individual bodies. The westernmost magnetic anomaly is the result of weakly susceptible material located near surface and limited to approximately 200 metres depth extent. The broader eastern magnetic high is the result of deeper body, buried at approximately 100 metres depth and exhibiting high magnetic susceptibility.

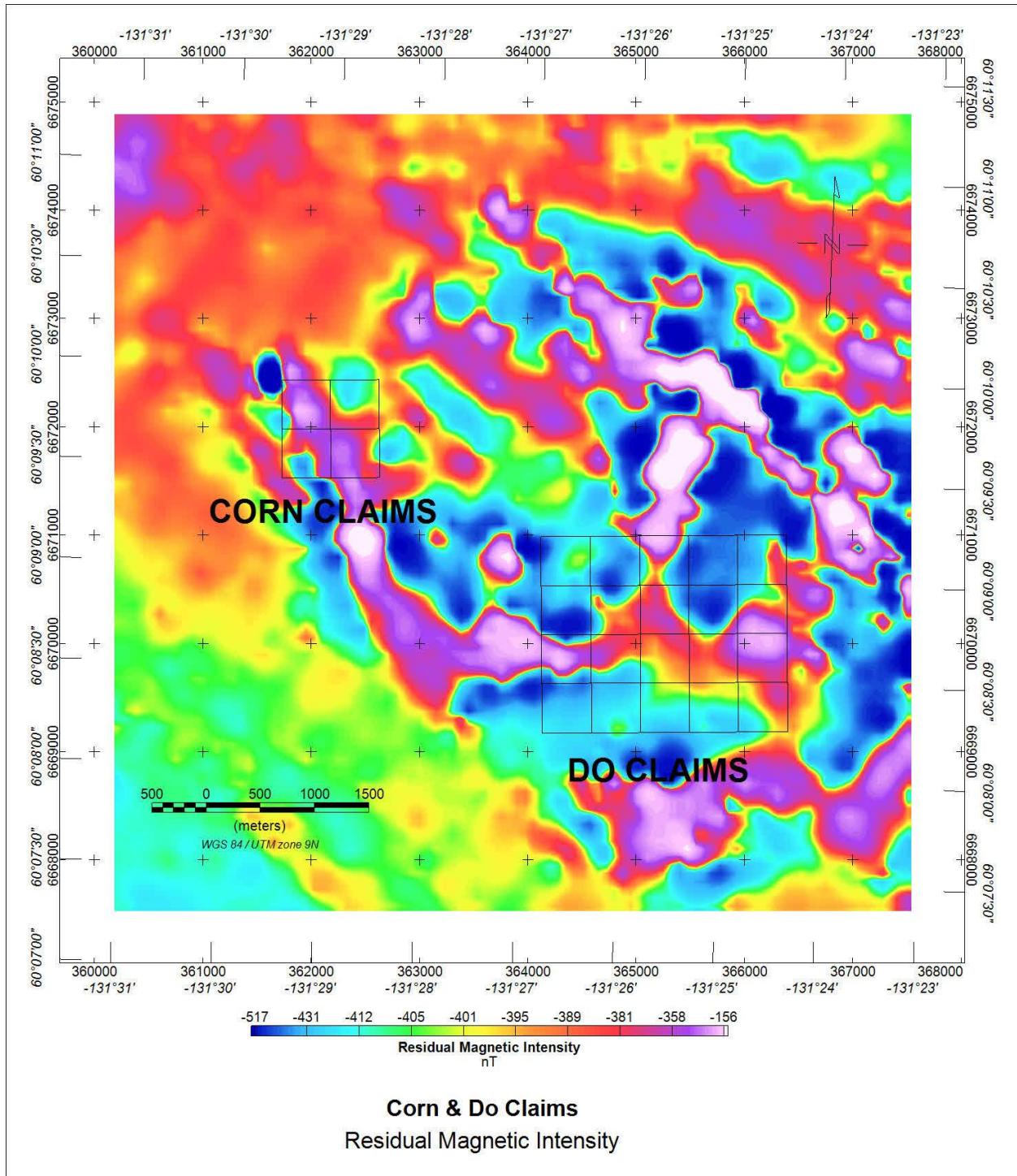


Figure 8. Residual Magnetic Intensity on the Corn and Do Claims

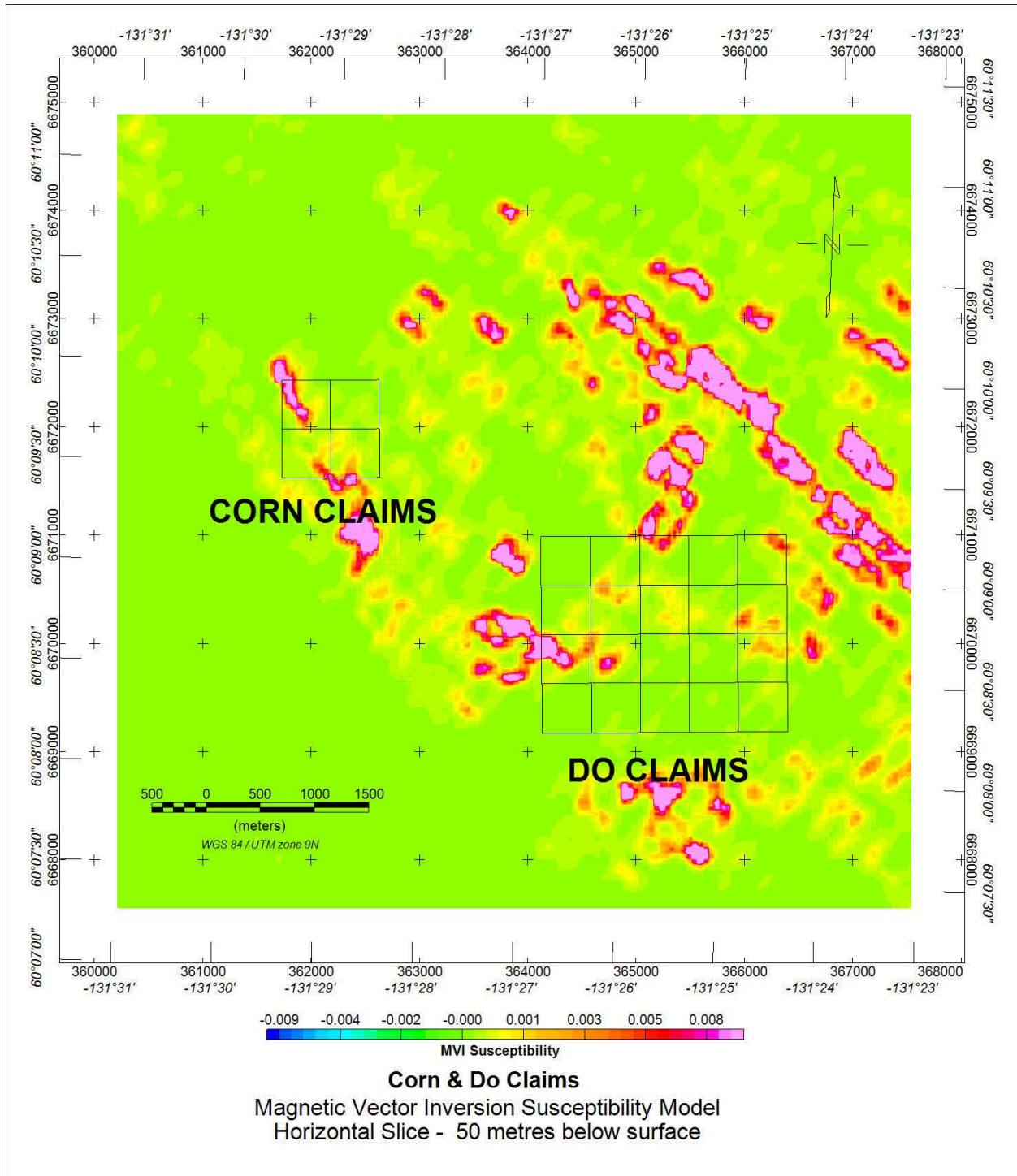


Figure 9. Magnetic Vector Inversion Susceptibility Model for the Corn and Do Claims

### ***11.2.2 Goods, Eccles and Milk Claims***

A 7500 metre by 7500 metre area of magnetic data windowed from the Seagull batholith aeromagnetic survey dataset and encompassing the Goods, Eccles and Milk Claims is examined and inversion modelled (Figures 10 and 11).

The residual magnetic intensity measured over the area ranges 1278 nT from -832nT to 446 nT with a mean value of -369 nT. Strongly positive magnetic readings form discontinuous anomalies approximately 200 metres in width and 600 metres length which trend northwest across the area. One such anomaly passes through the northeast portion of the Goods Claims. Both the Eccles and Milk Claims occupy areas of low magnetic relief. A gradational contact between slightly higher and lower magnetic intensity values is seen trending northeast through the Eccles Claims with a pronounced lobe near the centre of the block. A similar contact is seen traversing the Milk Claims.

The magnetic field inversion models a body of moderate magnetic susceptibility which explains the magnetic high anomaly observed on the Goods Claims. The body extends from surface to a depth of 150 metres and dips approximately 45° to the northeast. Magnetic inversion results from the Eccles and Milk Claims areas do not show elevated areas of magnetic susceptibility occurring on those claims.

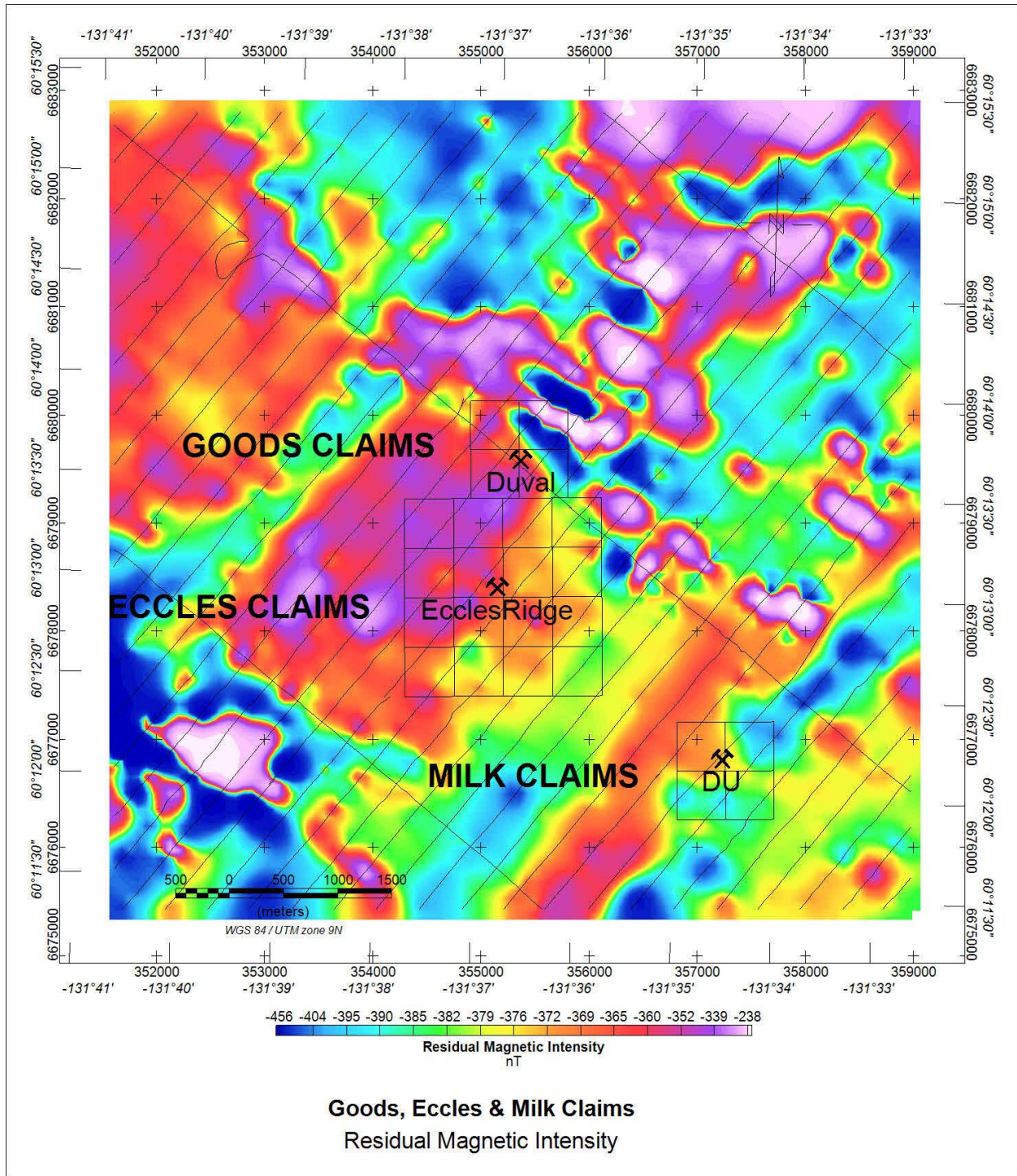


Figure 10. Residual Magnetic Intensity on the Goods, Eccles and Milk Claims

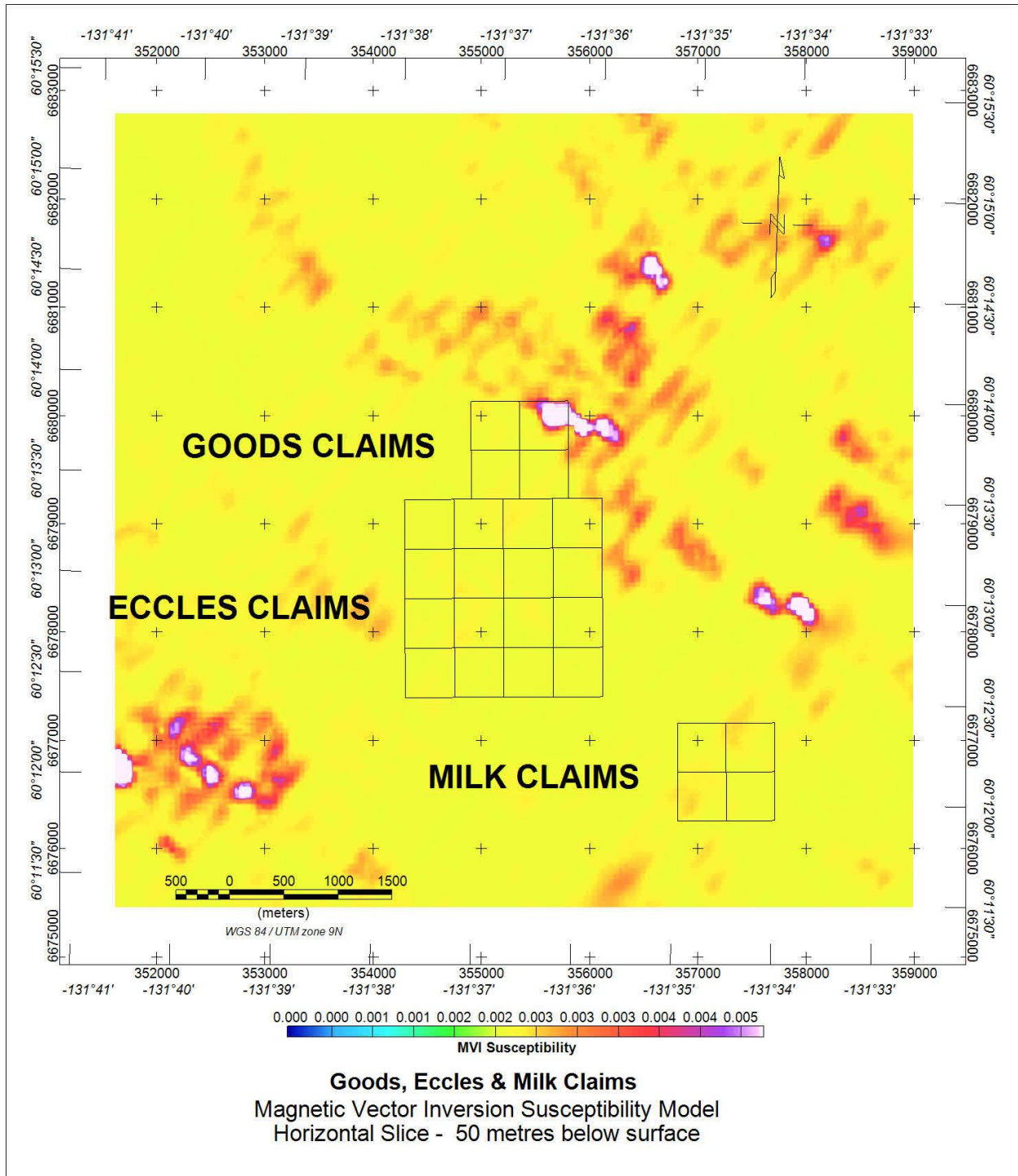


Figure 11. Magnetic Vector Inversion Susceptibility Model for the Goods, Eccles and Milk Claims

### **11.2.3 Fired and Milk Claims**

A 7500 metre by 7500 metre area of magnetic data windowed from the Seagull batholith aeromagnetic survey dataset and encompassing the Milk and Fired Claims is examined and inversion modelled (Figures 12 and 13).

The residual magnetic intensity measured over the area ranges 227 nT from -497nT to -270 nT with a mean value of -388 nT. The gridded magnetic intensity image is dominated by two parallel linear magnetic high anomalies striking northeast. The southern anomaly exhibits the strongest response while the northern anomaly is more subdued. The Fired Claims, located between the two magnetic features, shows low magnetic relief with an absence of any magnetic anomalies. The Milk Claims are divided by the northern magnetic lineament which trends through the claim block.

Inversion modelling of the magnetic data indicates that the causative sources for the magnetic linear anomalies are located at low elevations. In the area of the Milk Claims the magnetic source is buried approximately 400 metres below the highest topographic point located on the claims. The inversion model shows no significant magnetic sources situated within 50 metres of the surface.

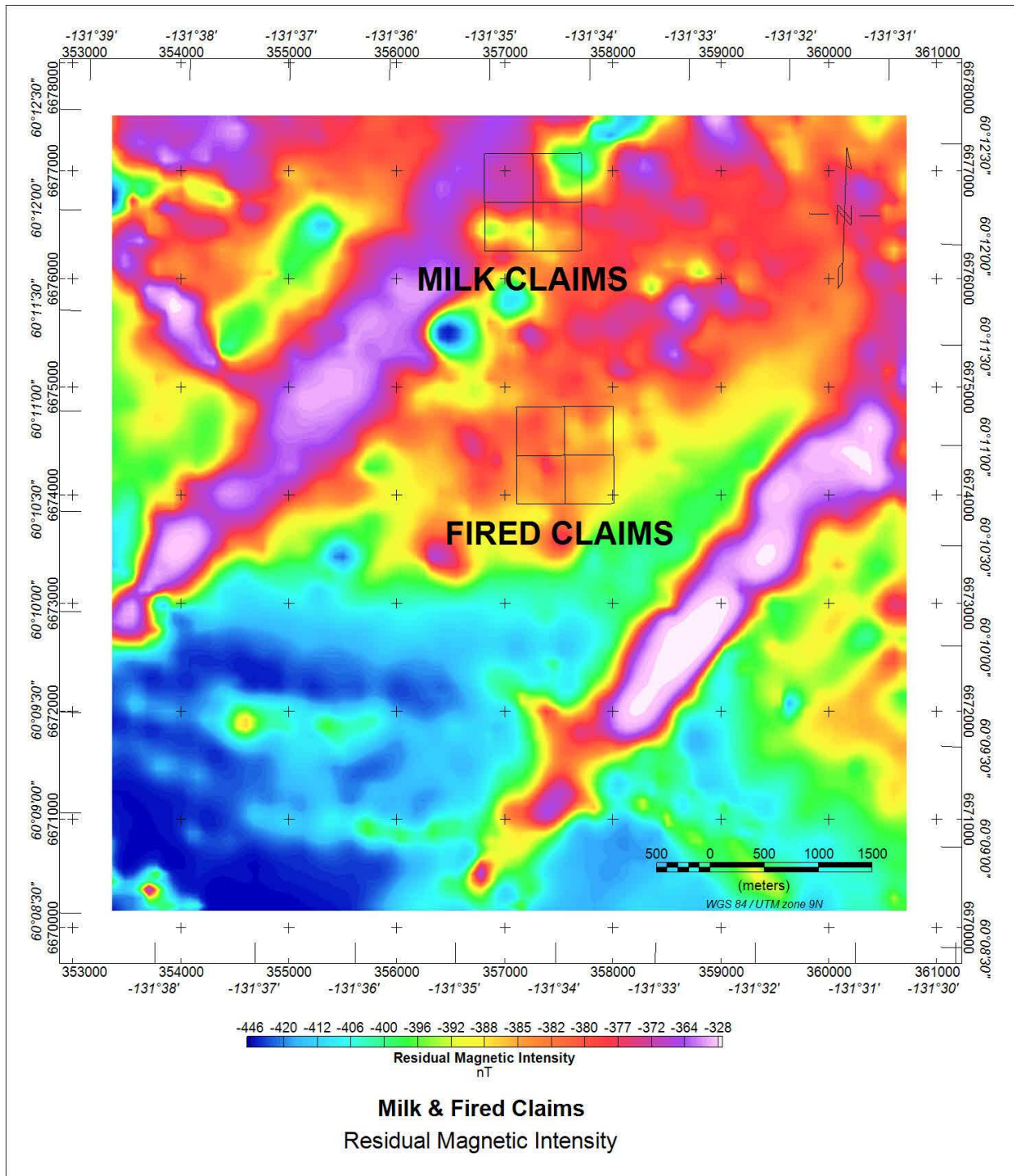


Figure 12. Residual Magnetic Intensity on the Milk and Fired Claims.

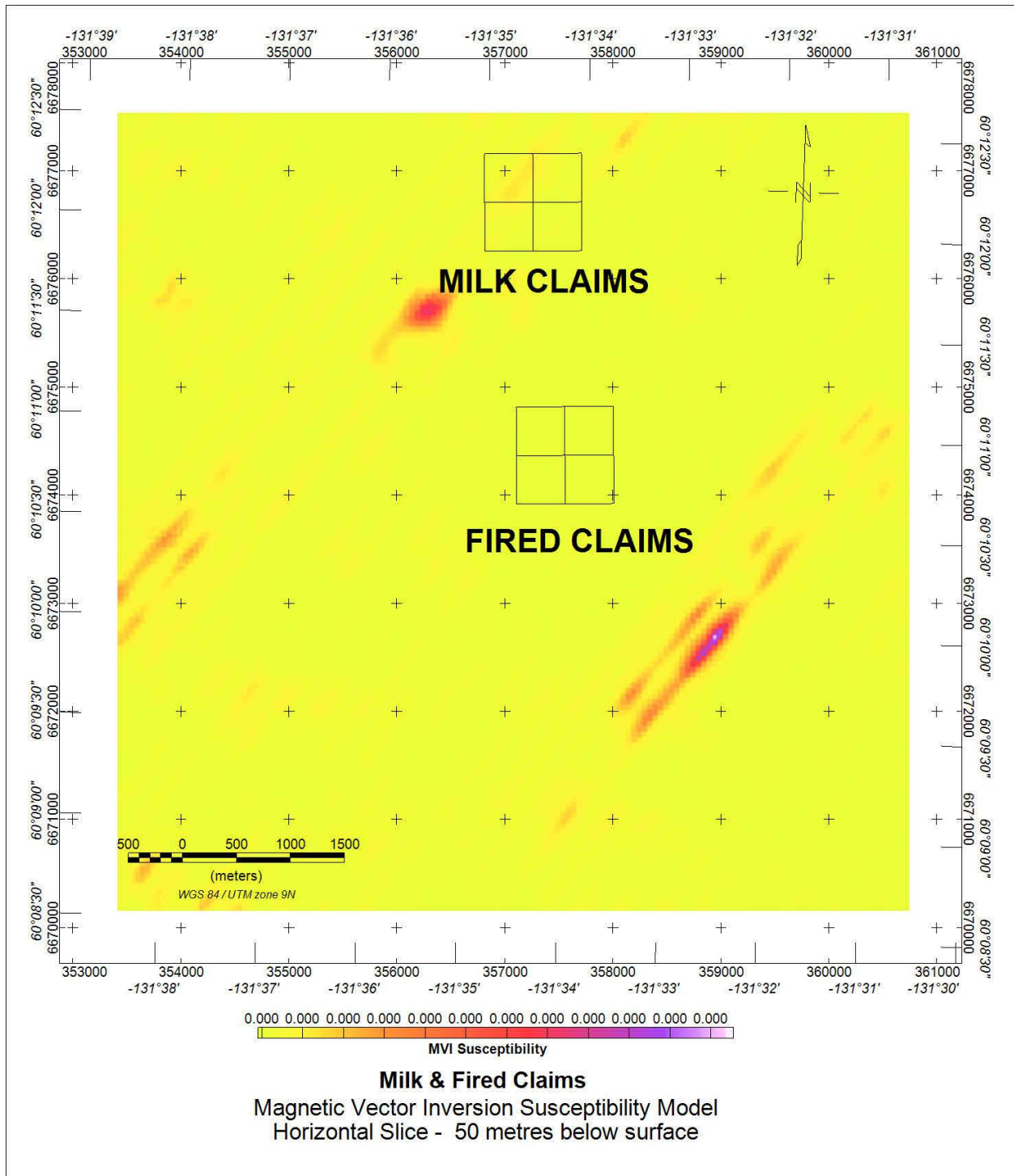


Figure 13. Magnetic Vector Inversion Susceptibility Model for the Milk and Fired Claims.

#### **11.2.4 Con Claims**

A 7500 metre by 7500 metre area of magnetic data windowed from the Seagull batholith aeromagnetic survey dataset and encompassing the Con Claims is examined and inversion modelled (Figures 14 and 15).

The residual magnetic intensity measured over the area ranges 4750 nT from -1569nT to 3181 nT with a mean value of -383 nT. The highest and lowest recorded values are associated with linear magnetic anomalies which strike northwest across the northern portion of the area and with a broad semi-circular anomaly located approximately 1000m north of the Con Claims. The Con Claims are centered on a magnetically quiet area exhibiting intensity values averaging -375 nT. The northeast, northwest and southwest corners of the claim block show slightly elevated magnetic readings.

Inversion modelling of the magnetic data indicates that the high amplitude magnetic anomalies located to the north of the Con Claims are the result of high magnetic susceptibility material forming zones 400 metres to 700 metres wide. The zones are located near surface and have an approximate depth extent of 350 metres. The recovered magnetic model shows no significant magnetic sources associated with the Con Claims.

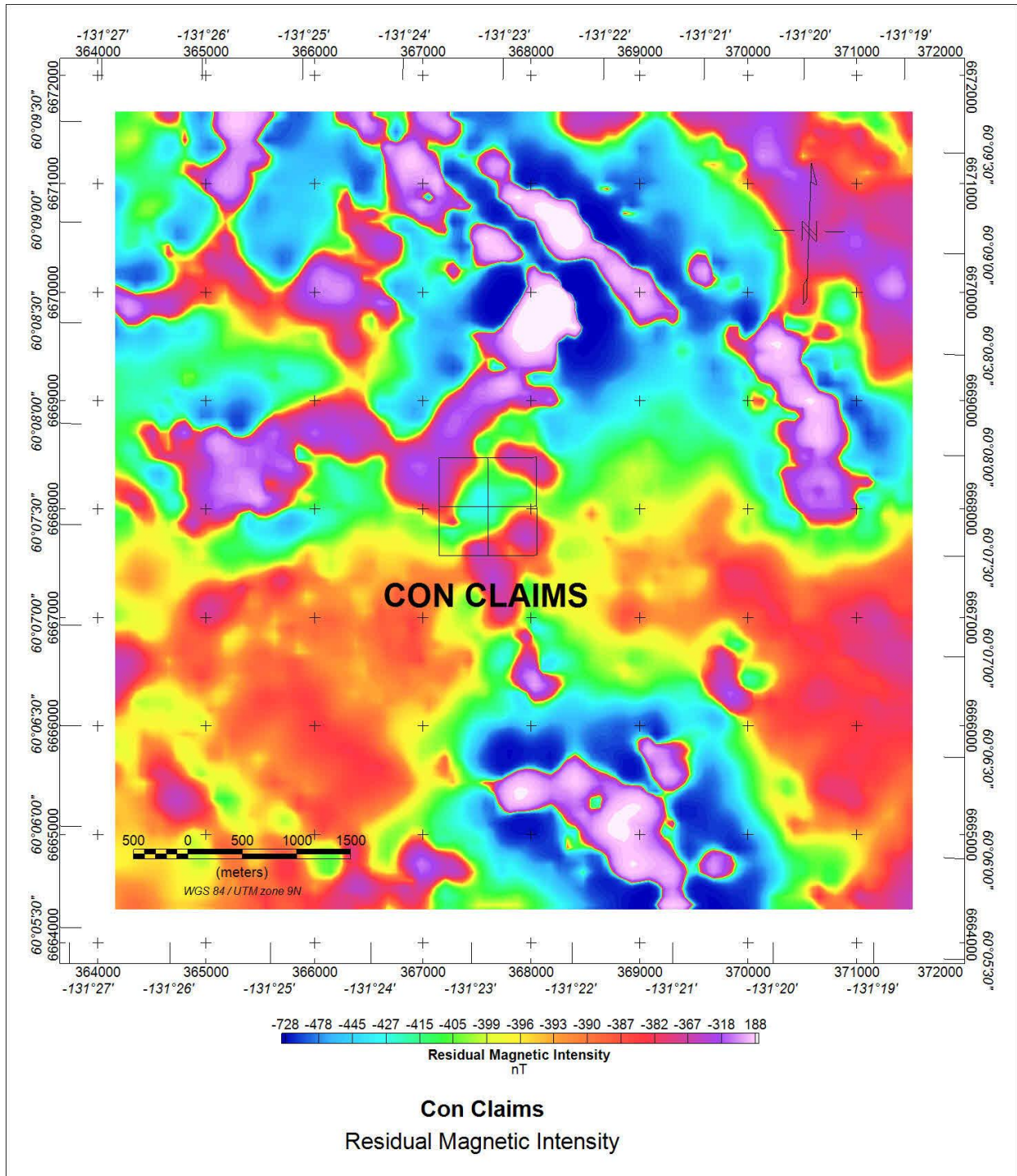


Figure 14. Residual Magnetic Intensity on the Con Claims.

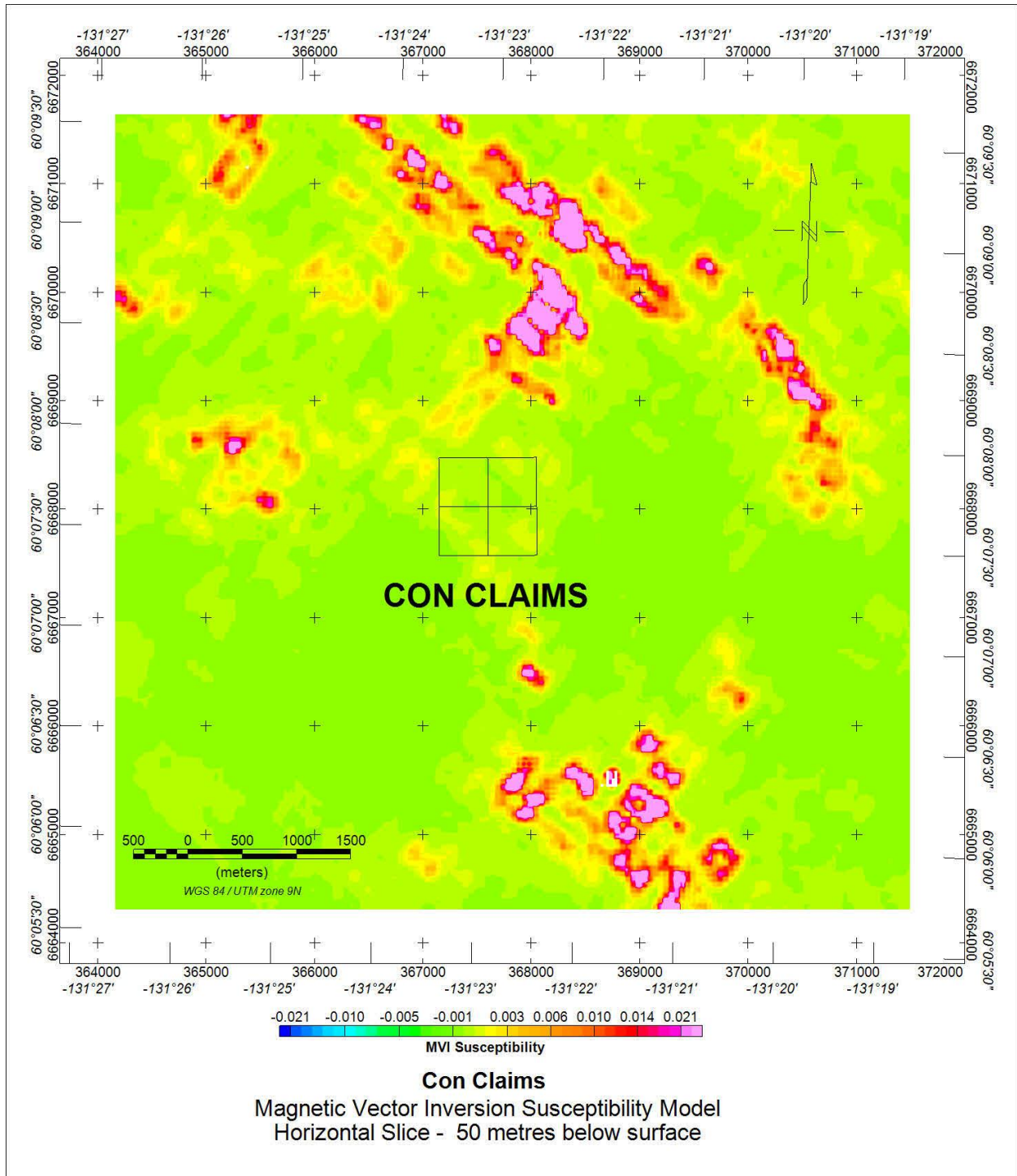


Figure 15. Magnetic Vector Inversion Susceptibility Model for the Con Claims.

### ***11.2.5 Beans and Music Claims***

A 7500 metre by 7500 metre area of magnetic data windowed from the Seagull batholith aeromagnetic survey dataset and encompassing the Beans and Music Claims is examined and inversion modelled (Figures 16 and 17).

The residual magnetic intensity measured over the area ranges 1936 nT from -1027nT to 910 nT with a mean value of -373 nT. The highest recorded values are observed on the eastern portions of the Beans Claim block where they form an irregular northwest trending magnetic high anomaly approximately 3000 metres long and up to 600 metres wide. Magnetic intensity values measured over the Music Claims are more subdued, but form a distinct magnetic high seen on the western half of the claim block.

Inversion modelling of the magnetic data indicates that the high amplitude magnetic anomalies located on the eastern portion of the Beans Claims are the result of high magnetic susceptibility material. The material forms a continuous near surface zone approximately 200 metres wide and has an approximate depth extent of 500 metres. The magnetic high anomaly located on the Music Claims is the result of weakly susceptible material located near surface and extending to approximately 400 metres depth below surface.

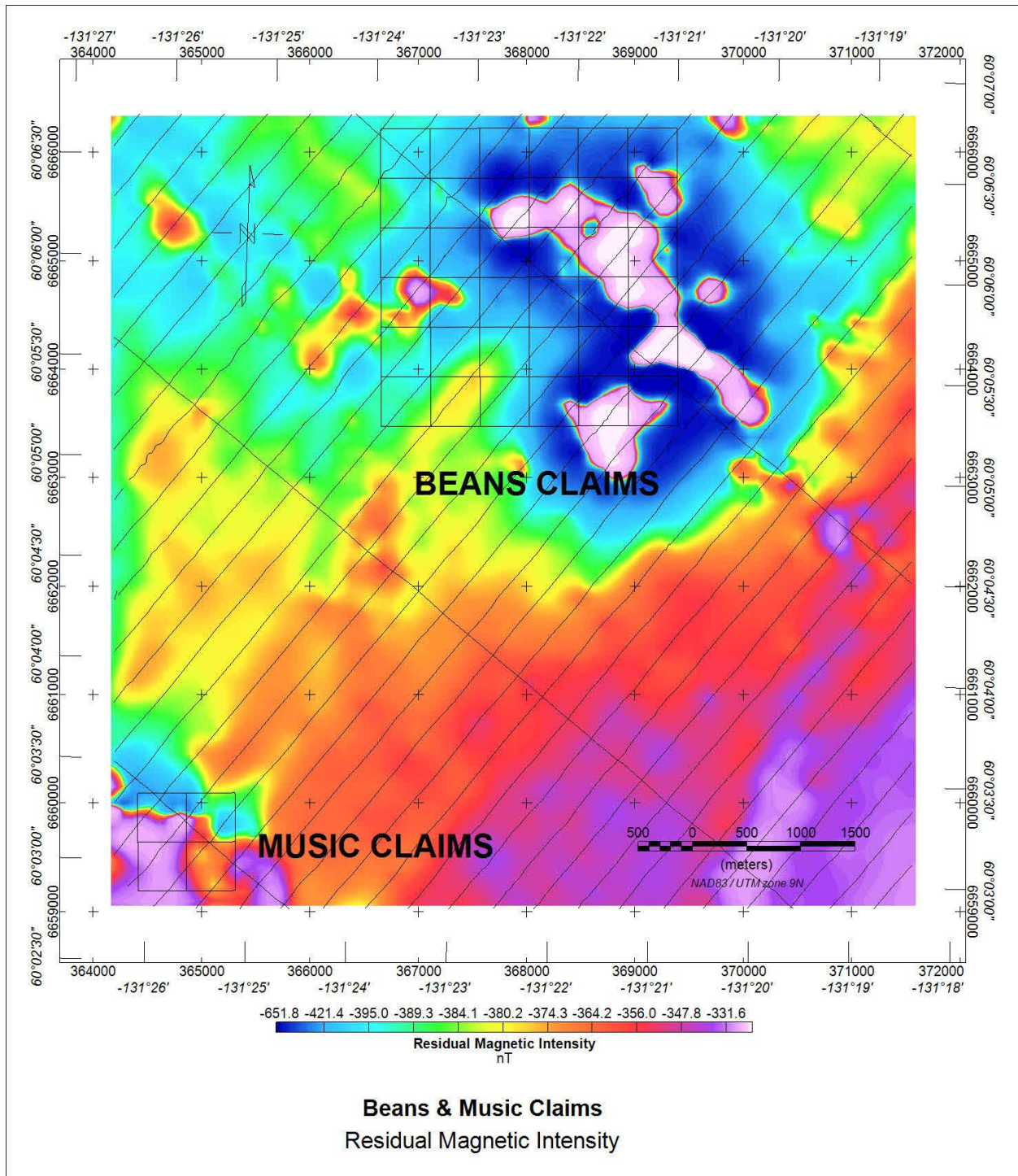


Figure 16. Residual Magnetic Intensity on the Beans and Music Claims.

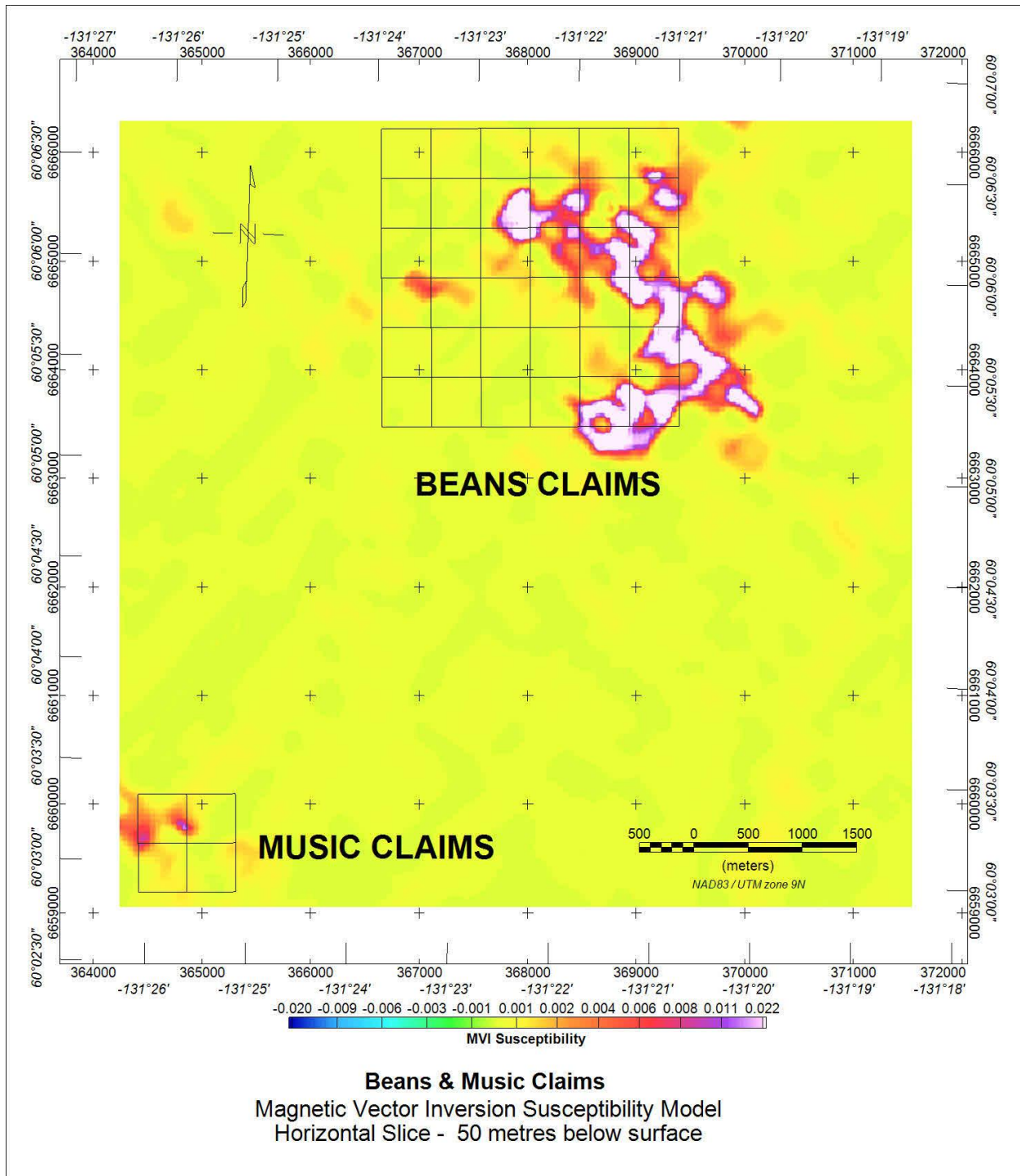


Figure 17. Magnetic Vector Inversion Susceptibility Model for the Beans and Music Claims.

### **11.2.6 Laughter Claims**

A 7500 metre by 7500 metre area of magnetic data windowed from the Seagull batholith aeromagnetic survey dataset and encompassing the Laughter Claims is examined and inversion modelled (Figures 18 and 19).

The residual magnetic intensity measured over the area ranges 1738 nT from -1024nT to 714 nT with a mean value of -343 nT. The highest recorded values form two closely spaced magnetic high anomalies located approximately 2000 metres to the west of the Laughter Claims. Besides those features the entire area shows only a gradual northwest to southeast trend from a lower to higher magnetic background. The magnetic relief over the Laughter Claims is slight and varies only by 10 nT.

The recovered magnetic model shows no significant magnetic sources associated with the Laughter Claims.

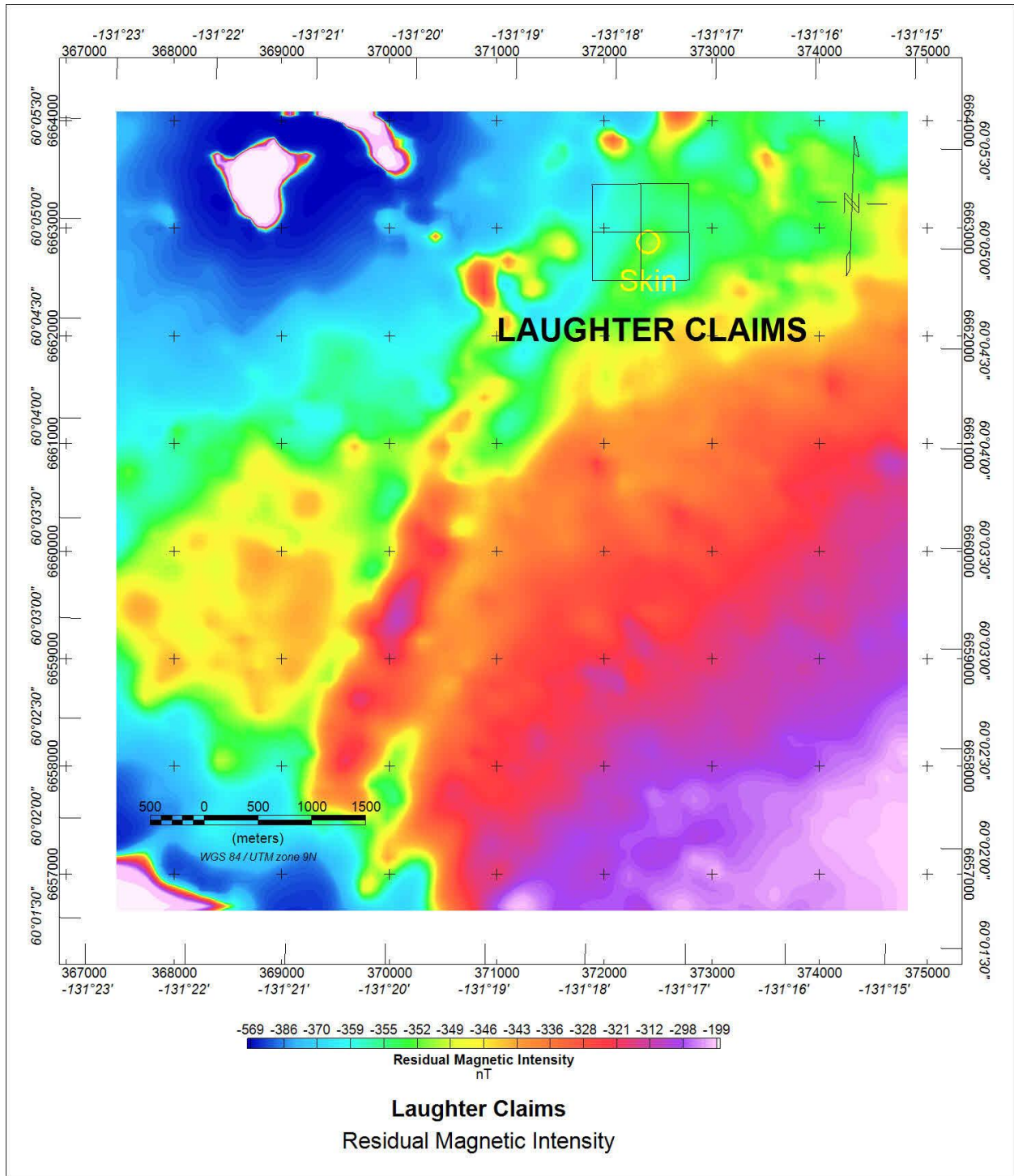


Figure 18. Residual Magnetic Intensity on the Laughter Claims.

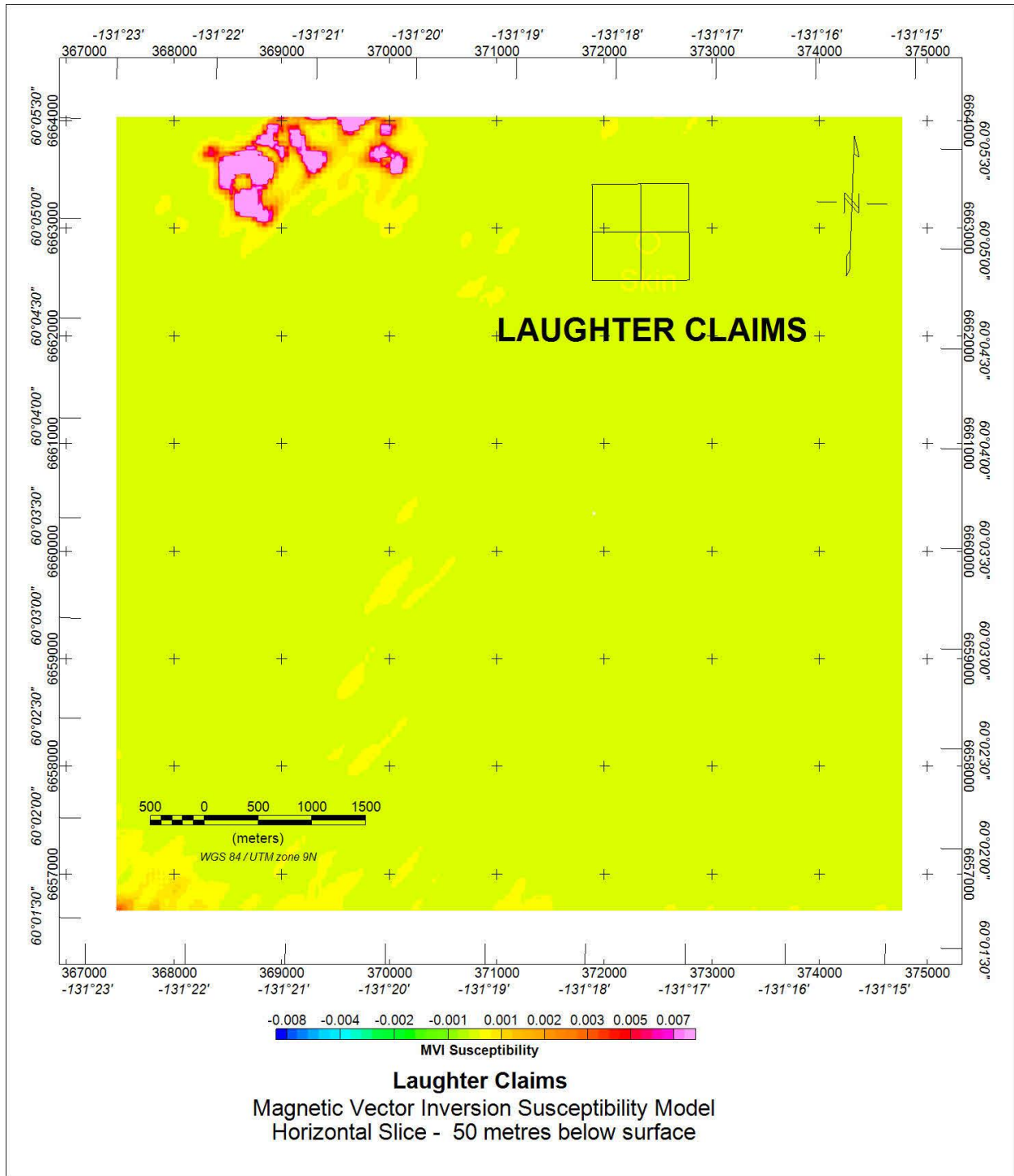


Figure 19. Magnetic Vector Inversion Susceptibility Model for the Laughter Claims.

### **11.2.7 Peas Claims**

A 7500 metre by 7500 metre area of magnetic data windowed from the Seagull batholith aeromagnetic survey dataset and encompassing the Peas Claims is examined and inversion modelled (Figures 20 and 21).

The residual magnetic intensity measured over the area ranges 3381 nT from -1045nT to 2336 nT with a mean value of -351 nT. A strongly positive magnetic anomaly with recorded values as high as 1044 nT and approximately 400 metres in width is observed striking west-northwest through the centre of the area before swinging to the northwest. The anomaly is located approximately 2000 metres to the northwest from the Peas Claims. The magnetic intensity recorded over the Peas Claims is subdued with values ranging between -450 and -350 nT. A curvilinear contact separating areas of higher and lower magnetic intensity strikes north south through the western portion of the claims block.

The results of the magnetic field inversion indicate that the strongly positive magnetic anomaly located to the northwest of the Peas Claims is caused by magnetically susceptible material occurring near surface and extending to approximately 700 metres below the surface. The recovered magnetic model shows no significant magnetic sources associated with the Peas Claims.

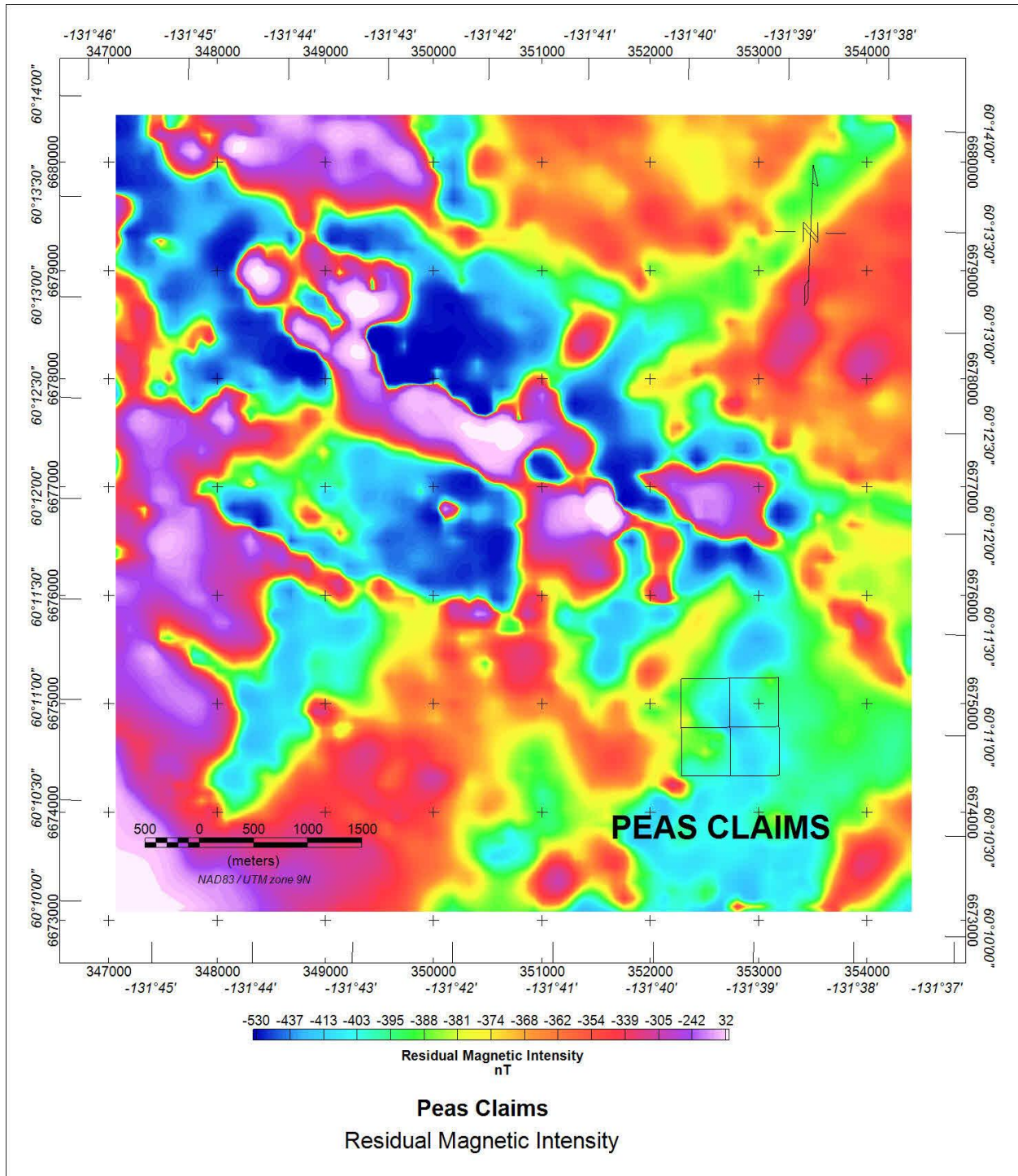


Figure 20. Residual Magnetic Intensity on the Peas Claims

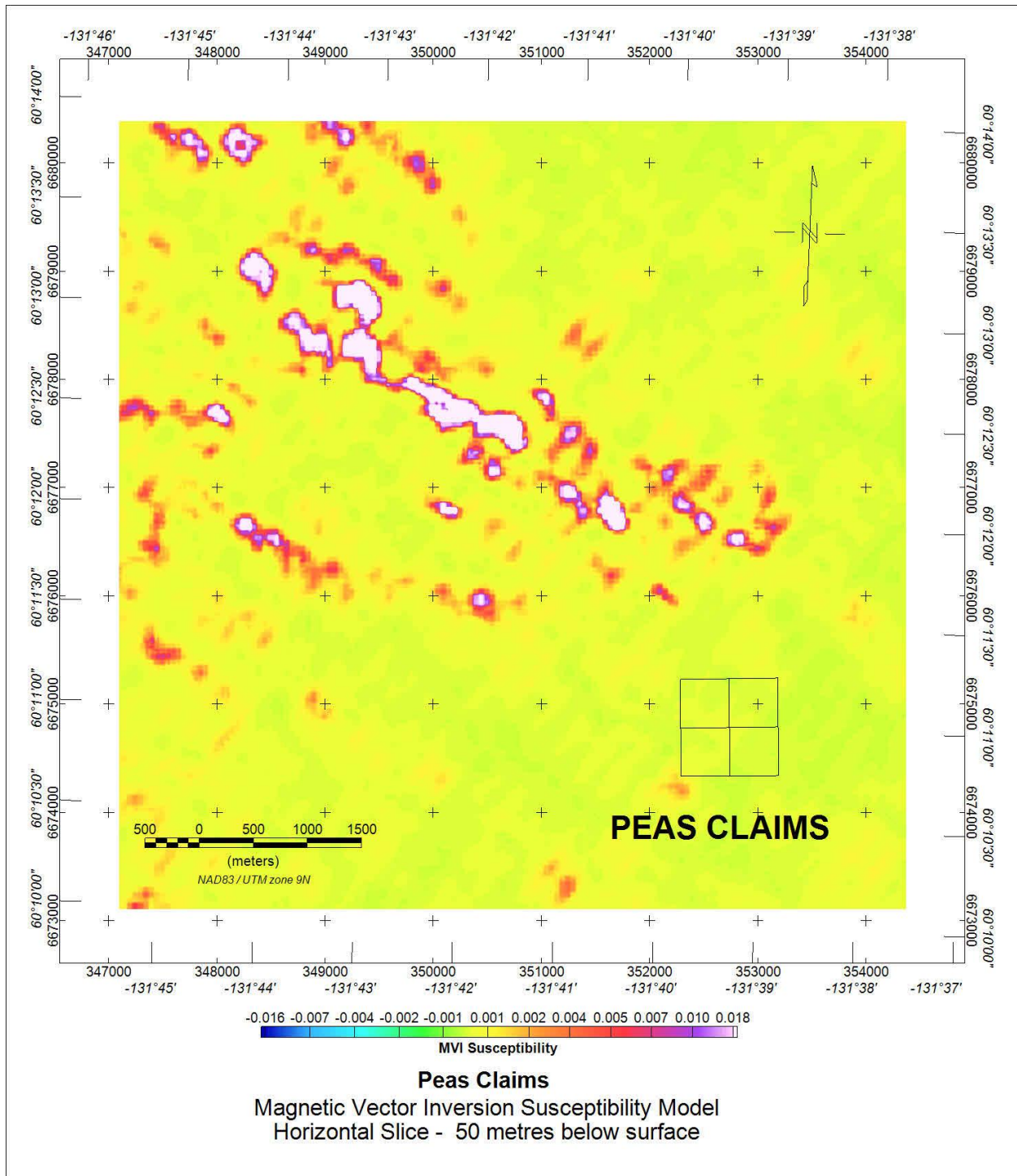


Figure 21. Magnetic Vector Inversion Susceptibility Model for the Peas Claims.

### ***11.2.8 Snip and Tuna Claims***

A 7500 metre by 7500 metre area of magnetic data windowed from the Seagull batholith aeromagnetic survey dataset and encompassing the Snip and Tuna Claims is examined and inversion modelled (Figures 22 and 23).

The residual magnetic intensity measured over the area ranges 534 nT from -549 nT to -15 nT with a mean value of -396 nT. The highest recorded values form an irregular shaped northeast trending magnetic high anomaly located approximately 1000 metres to the north of the Snip Claims. A series of well-defined lower amplitude magnetic high anomalies are measured over the Snip Claims. The anomalies trend southwest to northeast through the northern portion of the Snip Claims as well as southeast to northwest through the central southern portion of the claim block. The Tuna Claims host a northwest trending contact between high magnetic intensity values recorded over the southwestern half and low magnetic intensity values measured over the northeastern claims.

Inversion modelling of the magnetic data indicates that the high amplitude magnetic anomalies located north of the Snip Claims are the result of magnetically susceptible material forming near surface zones approximately 300 metres in width. The depth extent of the zones is limited to 300 metres to 500 metres below the surface. The Tuna Claims magnetic high anomaly is also the result of magnetic susceptible material which is contained in a steeply dipping body with a considerable depth extent of greater than 1000 metres. The top of the body is within 100m of the surface. The series of magnetic highs measured through the Snip Claims are modelled to be the result of weakly susceptible material buried approximately 250 metres below the surface.

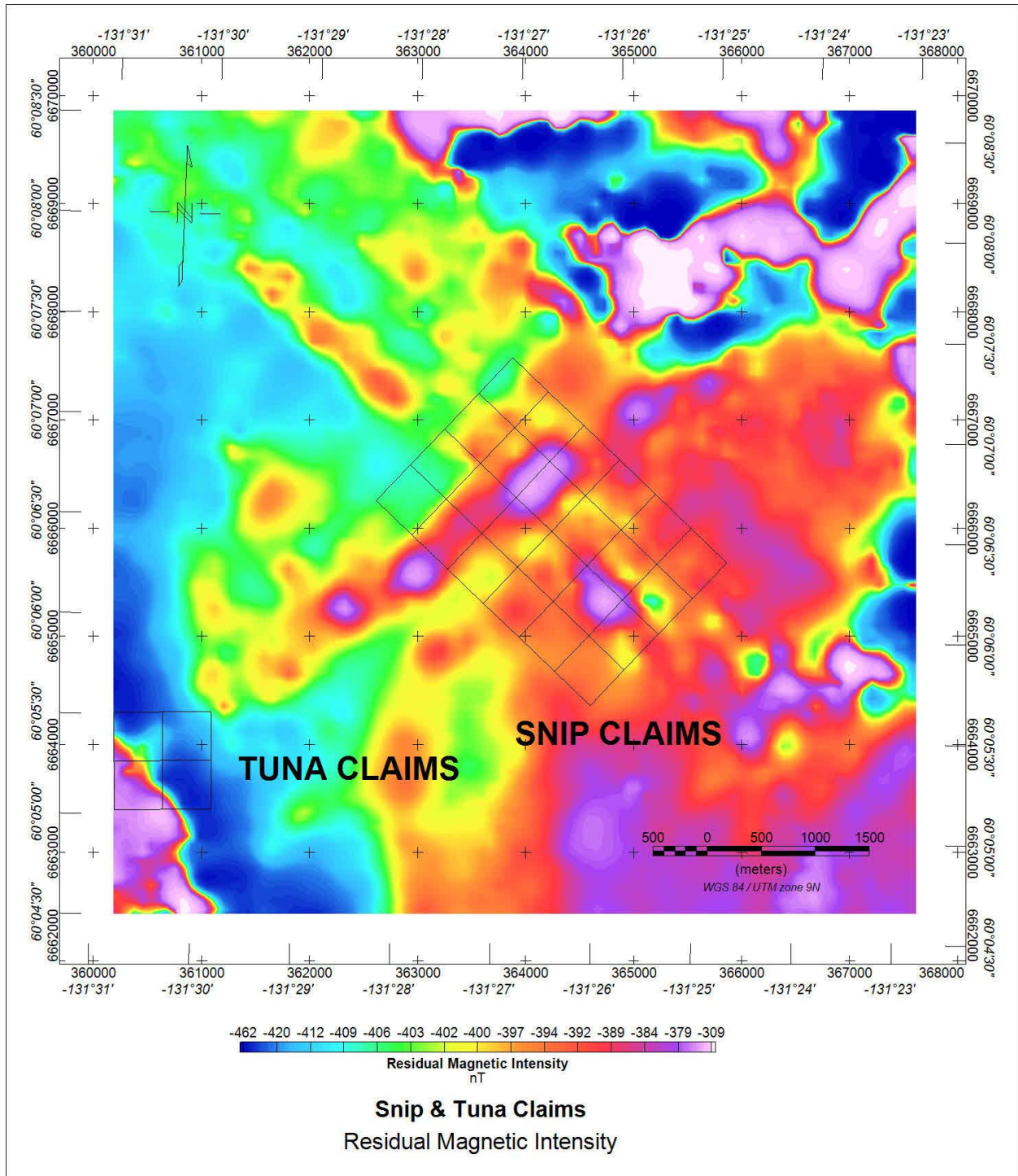


Figure 22. Residual Magnetic Intensity on the Snip and Tuna claims

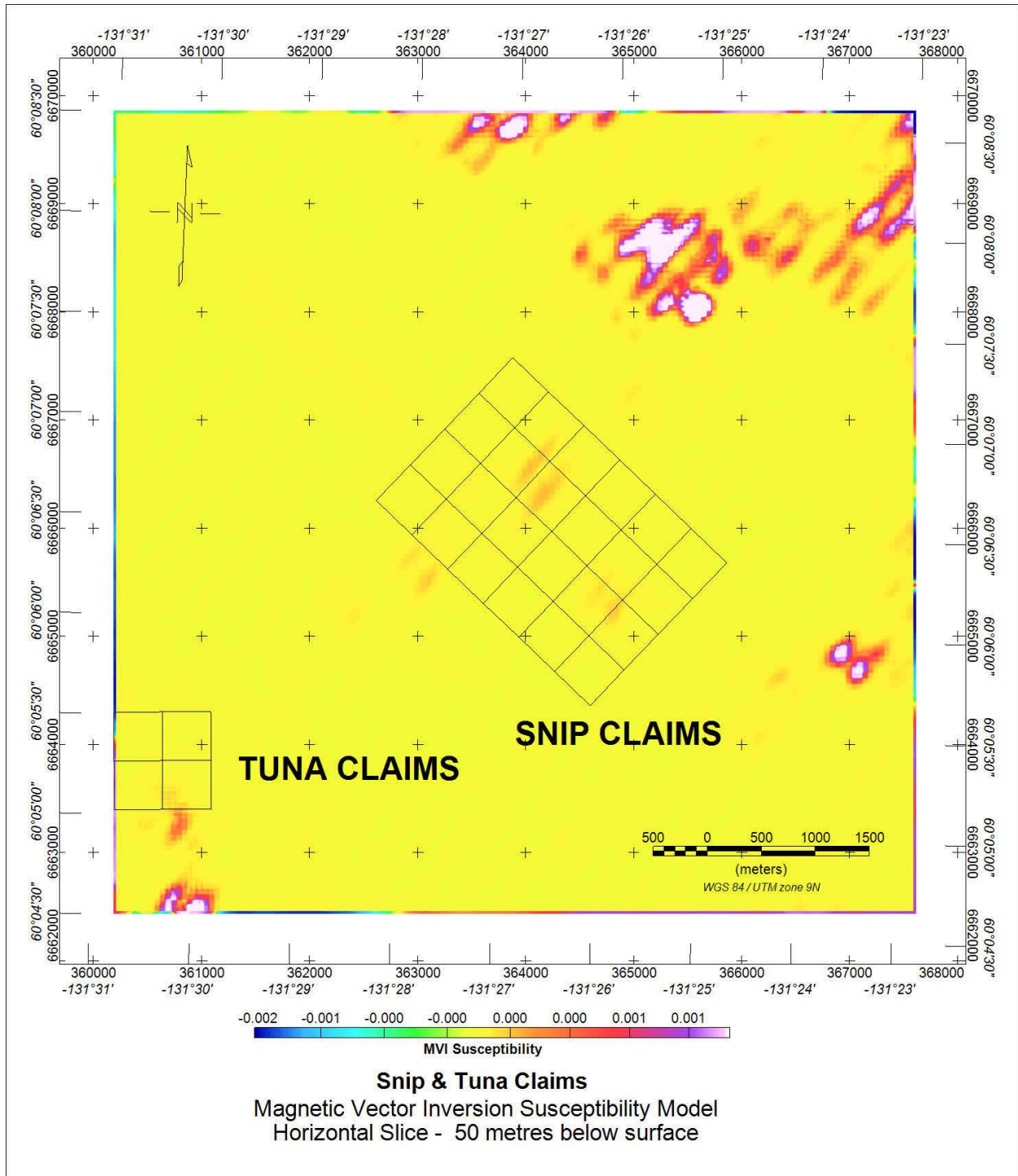


Figure 23. Magnetic Vector Inversion Susceptibility Model for the Snip and Tuna Claims.

## 12 INTERPRETATION AND CONCLUSIONS

The results of geological and geochemical surveys conducted on the Seagull Tin Project to date indicate that the area is highly prospective to host economic tin mineralization. The targets on the Do and Eccles Claims are currently the most promising targets with proximal bedrock mineralization. The 2013 airborne stream sediment survey defined a strong tin-tungsten anomaly on the Snip Claims in an area with no known bedrock mineralization. Additionally, contacts between higher and lower magnetic intensity areas produced by the airborne magnetic survey correlates well with lithological contacts and areas of known mineralization.

The results of the work to date support the following conclusions:

1. There is a large tin-in-soil anomaly covering a 250 square meter area along slope on the Do Claims. The geochemical anomaly is open upslope, towards the north, suggesting the likely source direction. Additionally, the highest tin value was acquired from a lone sample collected upslope and along the ridgeline, 300m northwest of the anomaly area. Magnetite-sulphide skarn mineralization was observed in this area during the 2011 prospecting and sampling program conducted by Panarc Resources Ltd. (Power, 2011). Additionally, this anomaly is associated with east-west trending residual magnetic high which swings towards northwest towards the Corn Claims and the Pont Showing. However, the source of this magnetic high, based on the magnetic vector inversion susceptibility model, is located approximately 400 west of the geochemical anomaly produced as a result of the soil sampling program. The source is interpreted as weakly susceptible material located near surface and limited to approximately 200 metres depth.
2. The weak tin anomaly on the Snips Claims suggests that the source of the strong focused tin-tungsten stream sediment geochemical anomaly observed during the 2012 stream sampling program is located on the northeast side of Tin Creek. A series of well-defined lower amplitude magnetic high anomalies are measured over the Snip Claims, but are not constrained to the northeast side of Tin Creek. These anomalies trend southwest to northeast through the northern portion of the Snip Claims as well as southeast to northwest through the central southern portion of the claim block. Additional investigation should be conducted northeast of Tin Creek to locate a bedrock source of the geochemical anomaly.
3. The Duval, Eccles Ridge and Du showings located on the Goods, Eccles and Milk Claims respectively, are observed to be located on the boundaries of a gradational contact between slightly higher and lower magnetic intensity values. The contact in the northeast margins of the Goods and Eccles Claims correlates with the lithological change between the Seagull batholith and the surrounding clastic and volcanic units as mapped by the Yukon Geological Survey (Gordey, 1999). Additionally, the Eccles Ridge showing, consisting of tin-bearing greisen-style mineralization, has been identified as immediately below the intrusive contact in the Seagull Batholith. Further exploration is warranted along the contact between the lower and higher

magnetic intensity values in this area in order to identify and expand areas of potential skarn and greisen-type mineralization.

4. Sample I841356 collected by Panarc Resources Ltd. in 2011 on the Con Claims and returned a tin value of 2700 ppm is located on a lobe-shaped contact between higher and lower magnetic intensity values. The sample is described to have been collected from a magnetite-bearing skarn boulder. The northeast, northwest and southwest corners of the claim block show slightly elevated magnetic readings, and warrant further exploration for magnetite-bearing skarn mineralization.
5. A weak contact between higher and lower magnetic intensity values is observed on the Peas and Tuna Claims that coincides with the boundary between the Seagull Batholith and surrounding carbonate and clastic units, as mapped by the YGS (Gordey, 1999). Both the JC and Hollister Minfile showings on the Peas and Tuna Claims, respectively, are located on this magnetic contact. The JC Minfile showing in particular is described as a skarn bearing patches of massive pyrrhotite and chalcopyrite, along with disseminated magnetite, cassiterite, arsenopyrite, pyrite and pyrrhotite, and would have a higher magnetic intensity value. However, a brief traverse of both claim blocks by Panarc Resources Ltd. in 2011 failed to locate any mineralization.

## 13 RECOMMENDATIONS

The conclusions of this report support the following recommendations:

1. Additional airborne magnetic surveys to decrease the line spacing distance and increase the resolution of the geophysical model overlying the target area. A line spacing of 50 or 75 metres is recommended in order to allow for a 10 metre cell size.
2. In the absence of a high resolution airborne magnetic survey, ground magnetic geophysics is recommended on claims where magnetite and pyrrhotite has been associated with mineralization (Tuna, Music, Con and Do Claims), and where magnetic intensity is associated with the contact between the Seagull Batholith and the surrounding clastic and carbonate units and greisen zones (Con, Eccles, Goods, Milk, Peas and Tuna Claims).
3. Induced Polarization ground geophysics is recommended in areas where the tin mineralization is closely associated with sulphide mineralization, such as the Beans, Do and Con claims.
4. Additional mapping and prospecting along contacts between the Seagull Batholith granite and clastic, carbonate and greisen units and focusing on the contacts between lower and higher magnetic intensity would be beneficial to identifying new mineralized areas.
5. Soil sampling and prospecting on the Snips Claims, northeast of Tin Creek in order to locate the bedrock source of the identified stream and soil geochemical anomalies.

Respectfully submitted,  
**PANARC RESOURCES LTD.**



Tomasz Kalkowski, B.Sc. (hons), G.I.T.

## 14 REFERENCES

- Abbot, G. (1981).** Geology of Seagull Tin District.  
in: Yukon Exploration and Geology 1981. INAC Yukon Region.
- Environment Canada (2014).** [http://climate.weatheroffice.gc.ca/climate\\_normals](http://climate.weatheroffice.gc.ca/climate_normals)
- Gordey, S. P. and A. J. Makepeace (1999).** Yukon Digital Geology.  
Geological Survey of Canada Open File D3826.
- Heon, D. (compiler)(2003).** Regional Stream Geochemistry, Second Edition. Exploration and Geological Services Division, Indian and Northern Affairs Canada.
- Poole, W.H., J.A. Roddick, L.H. Green (1960).** Geology of the Wolf Lake Map Area.  
Geological Survey of Canada Map 10-1960.
- Power, M. (2011).** Prospecting, Geological and Geochemical Surveys at the Seagull Tin Property.  
Internal Assessment report.
- Sillitoe, R.H., C. Halls and J.N. Grant. (1975).** Porphyry tin deposits in Bolivia.  
Economic Geology Vol. 70. pp 913-927.
- Smith, M. (1980).** Klinkit Joint Venture.  
Yukon Mining Recorder: Assessment report AR090557
- Taylor, R.G. (1979).** Geology of Tin Deposits. New York: Elsevier.
- Xiangzhao, H. L. Xinge, H. Xuefeng (1996).** Origin and petrology on Yinyan tin-bearing granite porphyry. Jiangshu Science and Technology Press.

**Appendix I**

**Statement of Qualifications**

---

## STATEMENT OF QUALIFICATIONS

I, Tomasz Kalkowski, with business address and residence in Yellowknife, Northwest Territories do hereby certify that:

1. I am a graduate of the University of Ottawa, having graduated in 2012 with an Honours Bachelor of Science with Specialization in Geology-Physics.
2. I am a Geologist in Training registered with the Northwest Territories and Nunavut Association of Professional Engineers and Geoscientists (Number T307).
3. Since 2011, I have worked on numerous projects with Aurora Geosciences, assisting in and conducting both geological and geophysical surveys. My experience includes all aspects of geological surveying, including prospecting, mapping, geochemical sampling and drill target acquisition.
4. I have worked on the Seagull Tin Project in 2011, and I co-authored this report.
5. I have not received, nor do I expect to receive, any direct or indirect interest in the Seagull Tin Properties or the securities of Ucore Rare Metals Inc.

**Certificate dates January 20, 2015 in Yellowknife, NT.**



---

Respectfully Submitted,  
**Tomasz Kalkowski, B.Sc.(Hons)**

## STATEMENT OF QUALIFICATIONS

I, Franz Dziuba, of the City of Yellowknife, in the Northwest Territories, Canada,

HEREBY CERTIFY:

1. That my address is 3506 McDonald Drive, Yellowknife, NT, X1A 2H1
2. This certificate applies to the report titled "Assessment Report – Staking, Soil Sampling, Prospecting and Airborne Geophysics – Seagull Tin Project" and dated January 21, 2015.
3. That I am a graduate of the University of British Columbia with a B.Sc. in geophysics obtained in 1986.
4. That I have been practicing Geophysics since 1988
5. That I am a registered Professional Geophysicist in the Northwest Territories.
6. That I am not aware of any material fact or material change with respect to technical aspects of the report which is not reflected in the report.
7. That, as of the 21st day of January, 2015 to the best of my knowledge, information and belief, the Assessment Report contains all scientific and technical information that is required to be disclosed to make the technical report not misleading.

Respectfully Submitted,

--- *signed* ---

---

Franz Dziuba B.Sc. P.Geoph

**Appendix II**

**Project Log**

---

**Airborne Magnetic and Radiometric Survey Conducted 7<sup>th</sup> October to 22<sup>nd</sup> October, 2014.****Geochemical Sampling Crew Project Log**

October 7 <sup>th</sup> , 2014	Instrument and equipment checks. Mobe to Rancheria.
October 8 <sup>th</sup> , 2014	Fuel positioning near the continental divide. Some weather issues.
October 9 <sup>th</sup> , 2014	Weather day.
October 10 <sup>th</sup> , 2014	Late start due to weather conditions. Sampled NE claim line on the SNIPS Property.
October 11 <sup>th</sup> , 2014	Sampled the SW claim line on the SNIPS Property.
October 12 <sup>th</sup> , 2014	Sampled on the DO Property.
October 13 <sup>th</sup> , 2014	Fuel positioning and sorting data.
October 14 <sup>th</sup> , 2014	Ridgeline prospecting on the DO Property.
October 15 <sup>th</sup> , 2014	Demobe to Whitehorse.

**Geochemical Sampling Crew:**

Name	Address
Phil Jackson	c/o 34A Laberge Road, Whitehorse, YT, Y1A 5Y9
Shane Carlos	c/o 34A Laberge Road, Whitehorse, YT, Y1A 5Y9

**Appendix III**

**Statement of Expenditures**

---

**2014 Seagull Tin Project Statement of Expenditures*****Airborne Geophysics Survey***

Surveying: 2,421 line km	\$169,470.00	
Fuel positioning fee	\$3,443.00	
Mobe, set-up, calibration, report	\$12,500.00	
Standby time: 3 days	<u>\$6,600.00</u>	
	\$192,013.00	\$192,013.00

***Soil Sampling and Propecting Survey***

Job Prep and Equipment Checks	\$1,000.00	
Project Management: 12 hours	\$1,200.00	
Expediting: 4 hours	\$340.00	
Accommodation & meals: 9 days	\$2,356.19	
Fuel	\$424.22	
Sampling Crew: 9 days	\$9,000.00	
Equipment Rentals: 9 days	\$1,750.00	
Vehicle Rental: 9 days	\$1,400.00	
Field Supplies	\$500.00	
Helicopter Support	\$7,840.00	
Shipping	<u>\$211.47</u>	
	\$26,021.88	\$26,021.88

***Analyses and report***

Airborne interpretation/inversion	\$8,000.00	
Geophysical report compilation	\$1,000.00	
Data compilation for reports	\$1,500.00	
Assessment report, 43-101	\$15,000.00	
Mineralogy report: Lee Groat	\$5,000.00	
Assaying costs	<u>\$3,640.00</u>	
	\$34,140.00	<u>34,140.00</u>

***Total project expenditures***

\$252,174.88

I certify that this statement of expenditures is complete and true to the best of my knowledge.



Tomasz Kalkowski, B.Sc. G.I.T.

**Appendix IV**

**Precision GeoSurveys Airborne Magnetism and Radiometrics Survey Report**

---

# AIRBORNE GEOPHYSICAL SURVEY REPORT



## Seagull Batholith Survey Block Prepared for Ucore Rare Metals Inc.

Jenny Poon, B.Sc., G.I.T.  
Precision GeoSurveys Inc.  
[www.precisiongeosurveys.com](http://www.precisiongeosurveys.com)  
520-355 Burrard St., Vancouver, BC  
Canada V6C 2G8  
604-484-9402

November 2014

## Table of Contents

1.0	Introduction.....	1
1.1	Survey Area.....	2
1.2	Survey Specifications.....	4
2.0	Geophysical Data.....	5
2.1	Magnetic Data.....	5
2.2	Radiometric Data.....	5
3.0	Survey Operations.....	7
3.1	Operations Base and Crew.....	8
3.2	Base Station Specifications.....	9
3.3	Field Processing and Quality Control.....	11
4.0	Aircraft and Equipment.....	14
4.1	Aircraft.....	14
4.2	Equipment.....	15
4.2.1	AGIS.....	15
4.2.2	Magnetometer.....	16
4.2.3	Spectrometer.....	17
4.2.4	Base Station.....	18
4.2.5	Laser Altimeter.....	19
4.2.6	Pilot Guidance Unit.....	20
4.2.7	GPS Navigational System.....	20
5.0	Data Acquisition Equipment Checks and Calibration.....	21
5.1	Magnetometer Checks.....	21
5.1.1	Compensation Flight Test.....	21
5.1.2	Lag Test.....	22
5.1.3	Heading Error Test.....	22
5.2	Gamma-ray Spectrometer Checks and Calibrations.....	23
5.2.1	Calibration Pad Test.....	23
5.2.2	Cosmic Flight Test.....	23
5.2.3	Breckenridge Test Range.....	24
6.0	Data Processing.....	24
6.1	Magnetic Processing.....	24
6.1.1	IGRF Removal and Calculation of the First Vertical Derivative.....	25
6.2	Radiometric Processing.....	25
7.0	Deliverables.....	27
7.1	Digital Data.....	27
7.2	KMZ Grids.....	28
7.3	Maps.....	28
7.4	Report.....	29

Appendix A: Equipment Specifications ..... A-1

Appendix B: Digital File Descriptions ..... B-1

Appendix C: Seagull Batholith Survey Block Maps ..... C-1

**List of Figures**

Figure 1: Seagull Batholith survey block location map.....1

Figure 2: Seagull Batholith survey block boundary in red.....2

Figure 3: Plan View – Seagull Batholith survey block with actual survey and tie lines displayed in yellow, and the block boundary in red.....3

Figure 4: Terrain View – Seagull Batholith survey block with actual survey and tie lines displayed in yellow.....3

Figure 5: Survey map of Seagull Batholith survey area showing proposed survey and tie lines.....4

Figure 6: Seagull Batholith survey block displaying survey and tie lines plotted in green flown on and after October 13. Snow accumulations on and after October 13 have affected gamma signal.....6

Figure 7: Seagull Batholith survey block displaying survey and tie lines plotted in blue flown before October 13. Most of the area covered by these survey lines was free of snow, so that snow attenuation of gamma data was minimal.....7

Figure 8: Map showing base of operations at Rancheria Lodge relative to Seagull Batholith survey block.....8

Figure 9: GEM 2 (left) and GEM 4 (right) magnetic base station locations.....10

Figure 10: GEM 2 and GEM 4 magnetic base station locations north of the Rancheria Lodge.....11

Figure 11: Histogram showing survey elevation vertically above ground summary.....12

Figure 12: Profile plot of Line 470 flight 3 displaying X and Y coordinates (top), laser altimeter readings in meters (middle), and compensated magnetic intensity (bottom) profiles.....13

Figure 13: Profile plot of Line 470 flight 22 displaying X and Y coordinates (top), laser altimeter readings in meters (middle), and compensated magnetic intensity (bottom) profiles.....13

Figure 14: Profile plot of Line 470 flight 24 displaying X and Y coordinates (top), laser altimeter readings in meters (middle), and compensated magnetic intensity (bottom) profiles.....14

Figure 15: Eurocopter AS350 helicopter equipped with mag stinger for magnetic data acquisition, and internal spectrometer crystals for radiometric data acquisition .....15

Figure 16: AGIS operator display installed in the Eurocopter AS350.....16

Figure 17: View of the mag stinger.....17

Figure 18: IRIS strapped in the back seat of the Eurocopter AS350.....18

Figure 19: GEM GSM-19T proton precession magnetometer.....19

Figure 20: Opti-Logic RS800 laser altimeter.....19

Figure 21: Pilot Guidance Unit.....20  
Figure 22: Hemisphere GPS – Mini Max.....21  
Figure 23: Heading data results in .tbl format in Geosoft table.....23

**List of Tables**

Table 1: Seagull Batholith survey area flight line specifications.....4  
Table 2: Seagull Batholith survey block polygon coordinates using WGS 84 in Zone  
9N.....5  
Table 3: Base station specifications.....9  
Table 4: Contract re-flight specifications.....12  
Table 5: Figure of Merit maneuver test results for compensation flight flown on  
October 10, 2014.....22  
Table 6: Heading error test data format flown on October 8, 2014.....22

## 1.0 Introduction

This report outlines the geophysical survey operations and data processing procedures taken during the high resolution airborne magnetic and radiometric survey flown at the Seagull Batholith survey block for Ucore Rare Metals Inc. The survey area is located 60 km east of Teslin, YT and 15 km west of Rancheria Lodge, YT. The survey block covers 652.8 km<sup>2</sup> (Figure 1). The geophysical survey was flown from October 07, 2014 to October 22, 2014.



Figure 1: Seagull Batholith survey block location map.

Radiometric data were collected simultaneously along with the acquisition of magnetic data. However, survey and tie lines flown after October 13 and lines above 6000 feet have variable amounts of fresh snow, thus radiometric data are compromised. Therefore the radiometric data were corrected to the best approximate concentrations and should be used with discretion.

## 1.1 Survey Area

Seagull Batholith survey block is located approximately 30 km west of Rancheria Lodge, YT. It covers a rectangular area of 16.4 km by 32.3 km (Figure 2). A total of 2421 line kilometers of magnetic and radiometric data were collected; this total includes tie lines and survey lines.

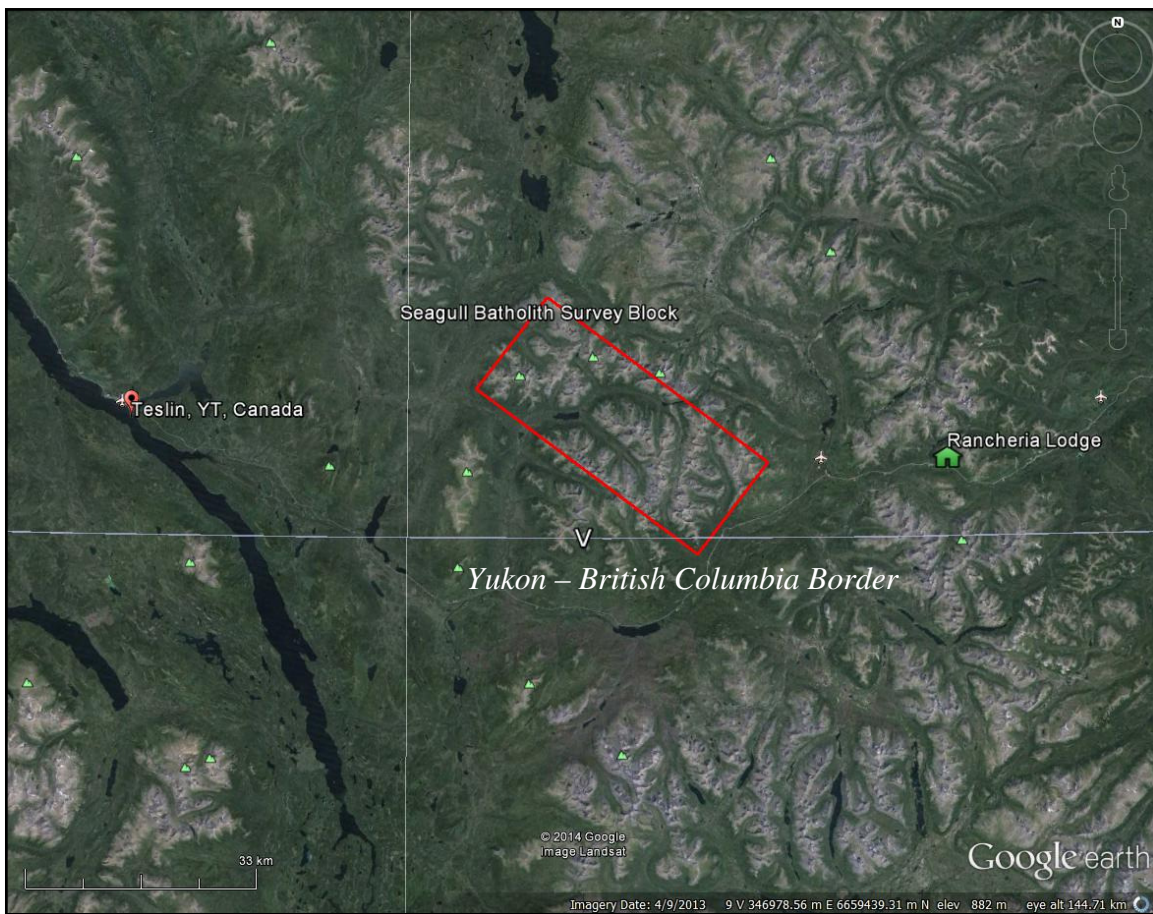


Figure 2: Seagull Batholith survey block boundary in red.

The survey was flown at 300 meter spacing at a 040°/220° heading; the tie lines were flown at 3000 meter spacing at a heading of 130°/310° (Figures 3 and 4).

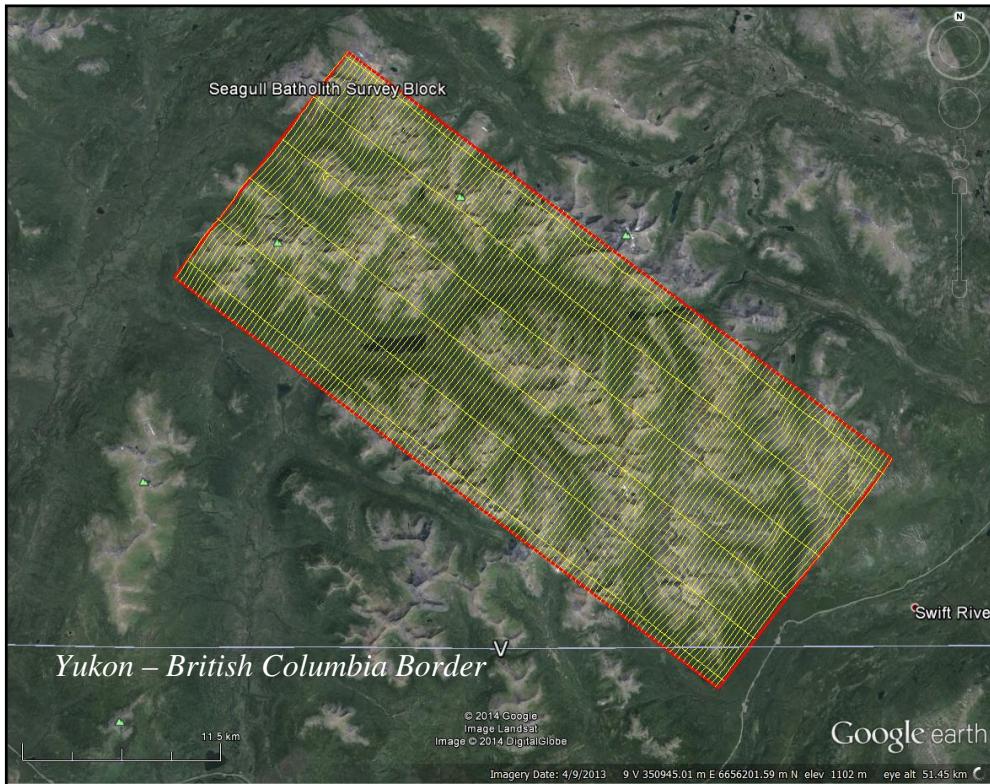


Figure 3: Plan View – Seagull Batholith survey block with actual survey and tie lines displayed in yellow, and the block boundary in red.

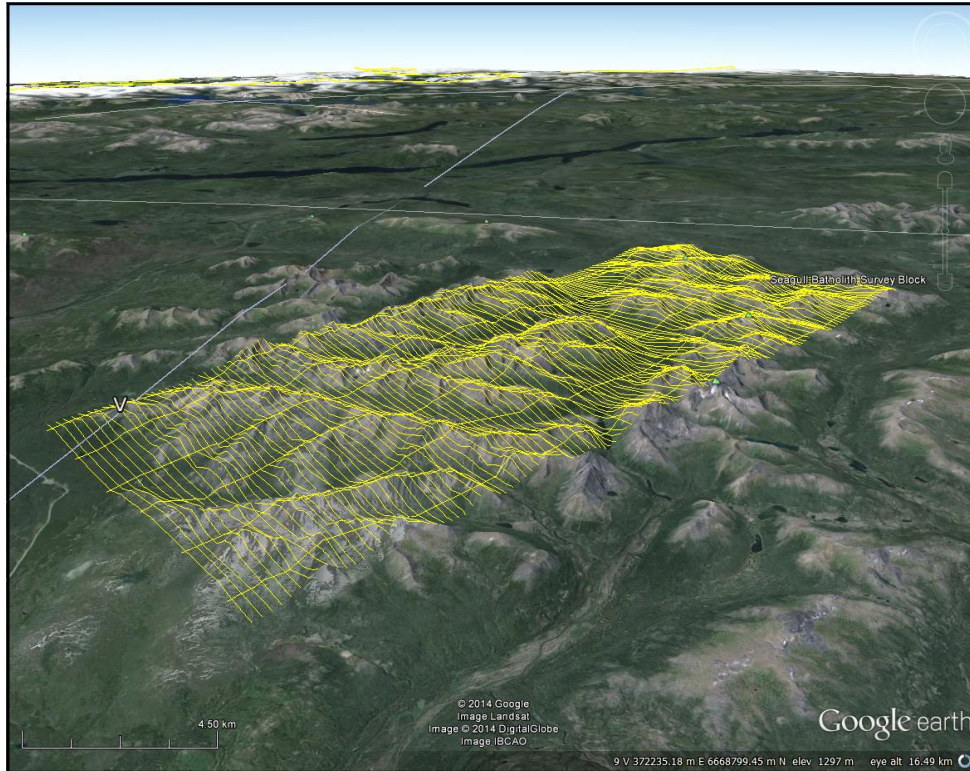


Figure 4: Terrain View – Seagull Batholith survey block with actual survey and tie lines displayed in yellow.

## 1.2 Survey Specifications

The geodetic system used for this survey is WGS 84 and the area is contained in zone 9N. A total of 2421 line km was flown (Figure 5). The survey data acquisition specifications and coordinates for the survey are specified as follows (Tables 1 and 2).

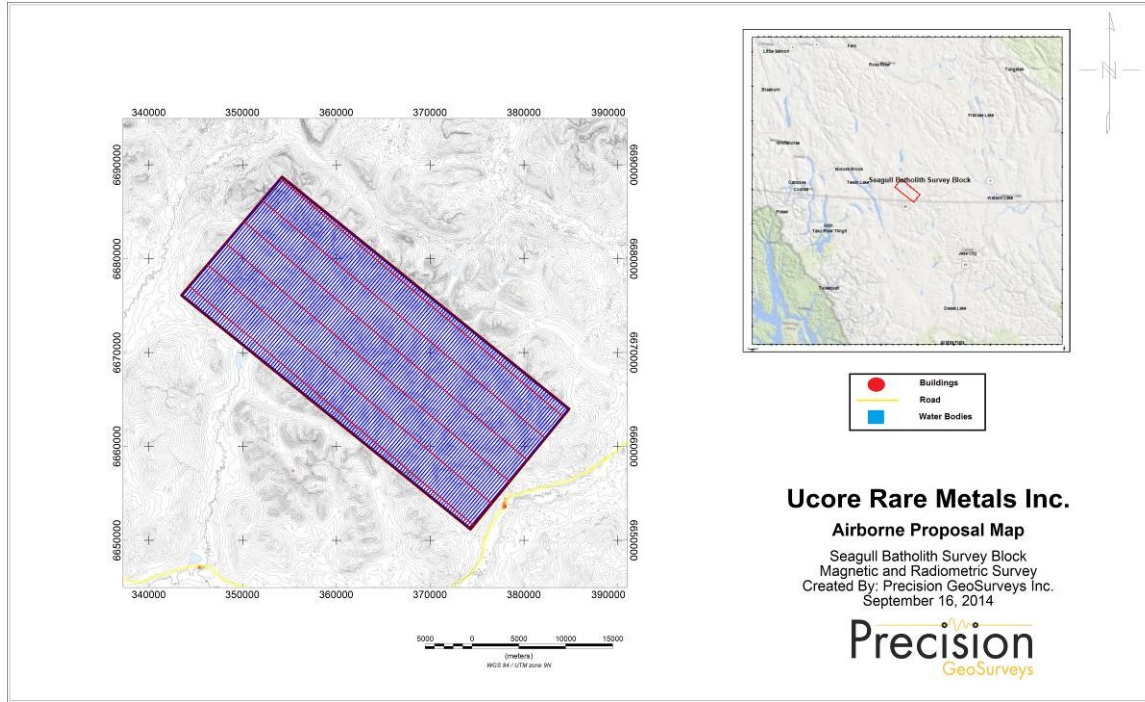


Figure 5: Survey map of Seagull Batholith survey area showing proposed survey and tie lines.

Survey Block	Area (km <sup>2</sup> )	Planned Line Spacing (m)	Planned Survey Line (km)	Planned Tie Line (km)	Survey Line Orientation	Nominal Survey Height (m)	Actual Survey Height (m)	Total Planned Line (km)	Total Actual Flown (km)
Seagull Batholith	652.8	300	2184	237	040°/220°	40	44.8	2421	2421
Total	652.8							2421	2421

Table 1: Seagull Batholith survey area flight line specifications.

Longitude	Latitude	Easting	Northing	N/S	E/W
131.63903780	60.30862013	354200	6688700	N	W
131.07162486	60.09682404	384800	6664000	N	W
131.25244451	59.97889044	374300	6651200	N	W
131.82269691	60.19164008	343500	6676100	N	W

Table 2: Seagull Batholith survey block polygon coordinates using WGS 84 in zone 9N.

## 2.0 Geophysical Data

Geophysical data are collected in a variety of ways and are used to aid in determination of geology, mineral deposits, oil and gas deposits, geotechnical investigations, contaminated land sites and UXO detection.

For the purposes of this survey, airborne magnetic and radiometric data were collected to serve in the exploration for potential gold and copper mineralization.

### 2.1 Magnetic Data

Magnetic surveying is probably the most common airborne survey type to be conducted for both mineral and hydrocarbon exploration. Aeromagnetic surveys measure and record the total intensity of the magnetic field at the magnetometer sensor, which is a combination of the desired magnetic field generated in the Earth as well as tiny variations due to the temporal effects of the constantly varying solar wind and the magnetic field of the survey aircraft. By subtracting the solar, regional, and aircraft effects, the resulting aeromagnetic map shows the spatial distribution and relative abundance of magnetic minerals (most commonly the iron oxide mineral magnetite) in the upper levels of the Earth's crust. The type of survey specifications, instrumentation, and interpretation procedures depend on the objectives of the survey. Typically magnetic surveys are performed for:

1. Geological Mapping - to aid in mapping lithology, structure and alteration.
2. Depth to Basement Mapping - for exploration in sedimentary basins or mineralization associated with the basement surface.

### 2.2 Radiometric Data

Radiometric surveys detect and map natural radioactive emanations, called gamma rays, from rocks and soils. All detectable gamma radiation from earth materials come from the natural decay products of three primary elements; uranium (U), thorium (Th), and potassium (K). The purpose of radiometric surveys is to determine either the absolute or relative amounts of U, Th, and K in surface rocks and soils which are then useful in mapping lithology, alteration, and structure.

In this case, the counts for U, Th, and K have been affected as the ground was covered with variable amounts of fresh snow. The survey and tie lines flown after October 13 were covered with fresh snow (Figure 6), thus radiation from the ground is significantly attenuated and thus the counts measured are reduced. For example, 10 cm of fresh snow will attenuate gamma rays as effectively as 10 m of air (IAEA, 2003).

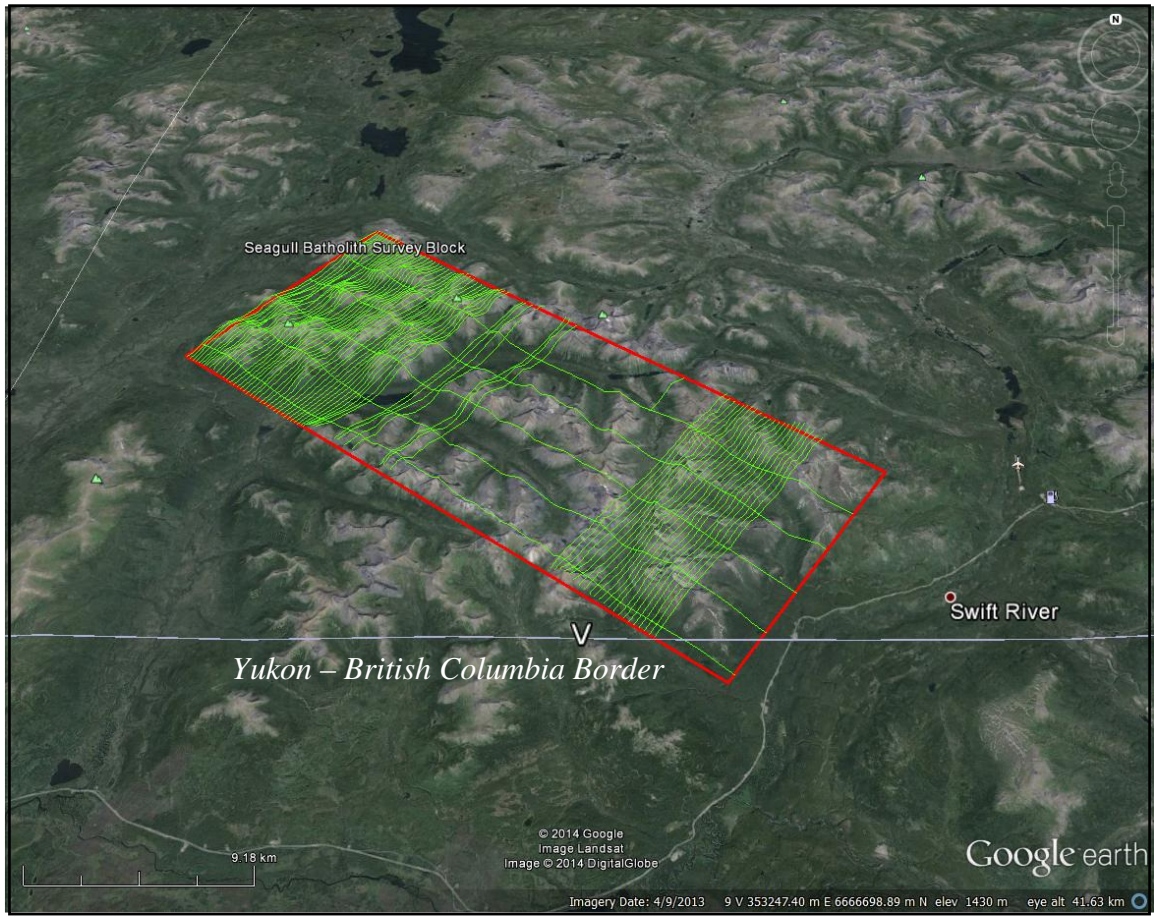


Figure 6: Seagull Batholith survey block displaying survey and tie lines plotted in green flown on and after October 13. Snow accumulations on and after October 13 have affected gamma signal.

Survey and tie lines flown before October 13 were not covered by snow, except north slopes over 6000 feet (1800 m ASL); therefore the radiometric data were not compromised (Figure 7). The gamma rays were not attenuated and the counts measured were not reduced.

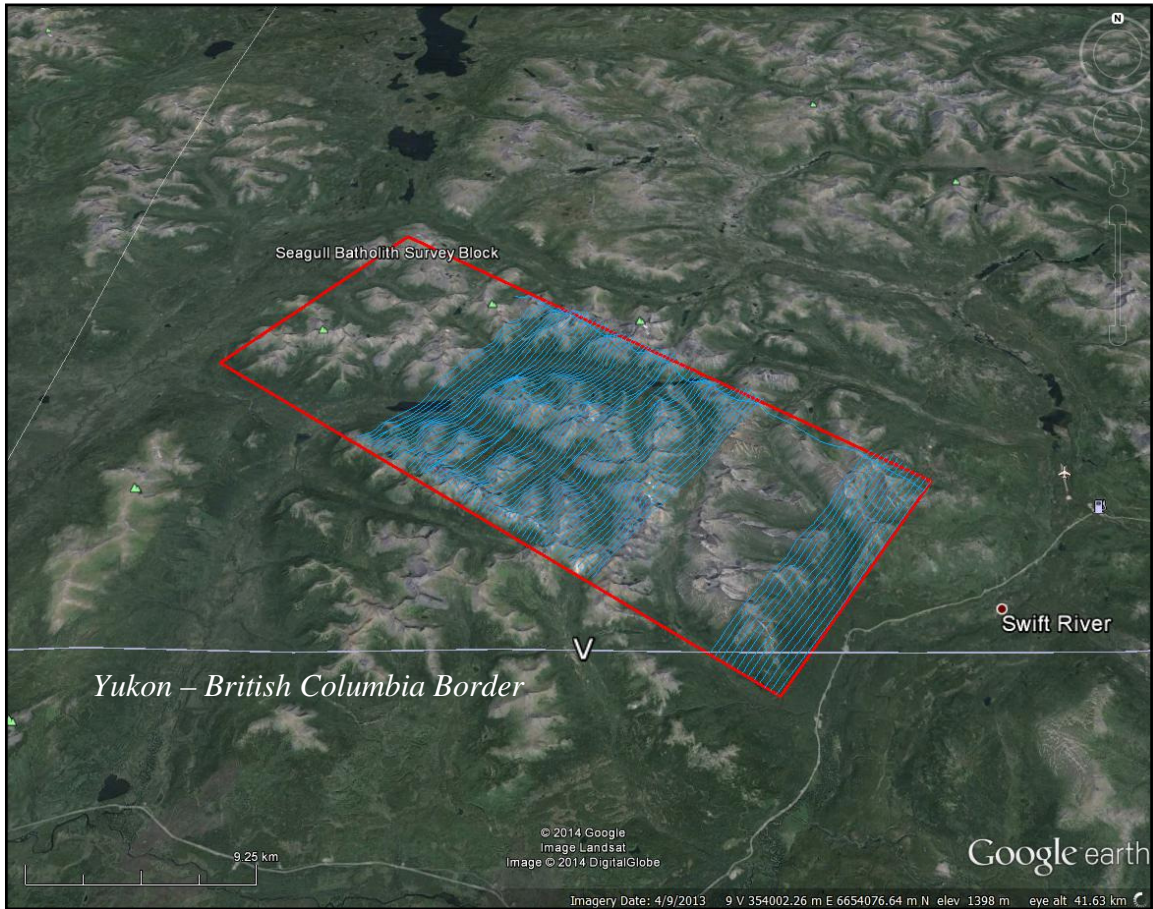


Figure 7: Seagull Batholith survey block displaying survey and tie lines plotted in blue flown before October 13. Most of the area covered by these survey lines was free of snow, so that snow attenuation of gamma data was minimal.

### 3.0 Survey Operations

Precision GeoSurveys flew the Seagull survey out of Rancheria Lodge, YT. The experience of the pilot helped to ensure that the data quality objectives were met and that the safety of the flight crew was never compromised given the potential risks involved in airborne geophysical surveying. Field processing and quality control checks were done daily.

### 3.1 Operations Base and Crew

The survey was based at the Rancheria Lodge, at km 1142 (mile 710) on the Alaska Highway (Figure 8).



Figure 8: Map showing base of operations at Rancheria Lodge relative to Seagull Batholith survey block.

The Precision geophysical crew consisted of four members:

Harmen Keyser – Pilot

Phil Jackson and Matt Greening – Geophysical operators

Jenny Poon – Geophysicist and data processor

The survey was flown from October 07, 2014 to October 22, 2014. The survey encountered several days of delays caused by freezing rain and low clouds which resulted in poor flight conditions.

### 3.2 Base Station Specifications

Two base station magnetometers were set up before the survey to ensure that diurnal magnetic activity were recorded during the survey flights. In this case, two GEM GSM 19T base stations (Figure 9), GEM 2 (Serial # 2105650) and GEM 4 (Serial # 2065370), were located in the bushes across the Alaska Highway north of the Rancheria Lodge (see Table 3 and Figure 10).

Station name	Easting/ Northing	Longitude/ Latitude	Datum/ Projection
GEM 2 (Serial # 2105650)	0410754E, 6662383N	130° 36' 15.98" W 60° 05' 19.64" N	WGS 84, Zone 9N
GEM 4 (Serial # 2065370)	0410758E, 6662368N	130° 36' 19.18 " W 60° 05' 19.18" N	WGS 84, Zone 9N

Table 3: Base station specification.

Base station readings were reviewed at regular intervals to ensure that no data were collected during periods with high diurnal activity (greater than 5 nT per minute). The magnetic base stations were installed at a magnetically noise-free area, away from metallic items such as ferromagnetic objects, vehicles, or power lines that could affect the diurnal or survey data.



Figure 9: GEM 2 (left) and GEM 4 (right) magnetic base station locations.



Figure 10: GEM 2 and GEM 4 magnetic base station locations north of the Rancheria Lodge.

The diurnal magnetic variations recorded by the stationary base station were removed from the magnetic data recorded in flight to ensure that the anomalies seen were real and not due to solar activity.

### 3.3 Field Processing and Quality Control

On a flight-by-flight basis, the survey data were transferred from the helicopter's data acquisition system onto a USB flash drive and copied onto a field data processing laptop. The raw data files were in PEI binary data format and were converted into Geosoft GDB database format. Using Geosoft Oasis Montaj 8.2, the quality of the data was inspected to see if it met the contract specifications (Table 4). Navigational accuracy (left/right or up/down) for all survey and tie lines were within contract specifications (Figure 11), and no re-flights were required due to navigational error. All suspect anomalies, especially those found on a single flight line, were re-flown. Re-flight lines were a minimum of 1500 m long, so that survey line re-flights crossed at least two tie lines, and tie line re-flights crossed at least 15 survey lines. All data were confirmed and verified by a geophysicist before the survey helicopter and crew demobilized on October 22, 2014.

Specification	Parameter	Details
Line Spacing	Position	Flight line deviation from flight path by more than 15 m left/ right for 1 km or more.
Height		Flight line deviation from height by more than 10 up/down with a nominal flight height of 40 m above ground for 1 km or more, except for extreme topography.
GPS		Any flight lines where 3 or less GPS satellites received for distances of greater than 1 km, provided signal loss is not due to topography.
Diurnal Variations	Magnetics	Non-linear magnetic diurnal variations exceed 10nT from a linear chord of length one (1) minute.
Normalized 4 <sup>th</sup> Difference		Magnetic data exceeding 0.25 nT peak to peak for distances greater than 1 km or more (provided noise is not due to geological or cultural features).
Test Line Data	Radiometrics	If signal from the four spectrometer windows (K, Th, U, and TC) over the test line vary by more than 12%, the flights shall be re-flown or suspended.

Table 4: Contract re-flight specifications.

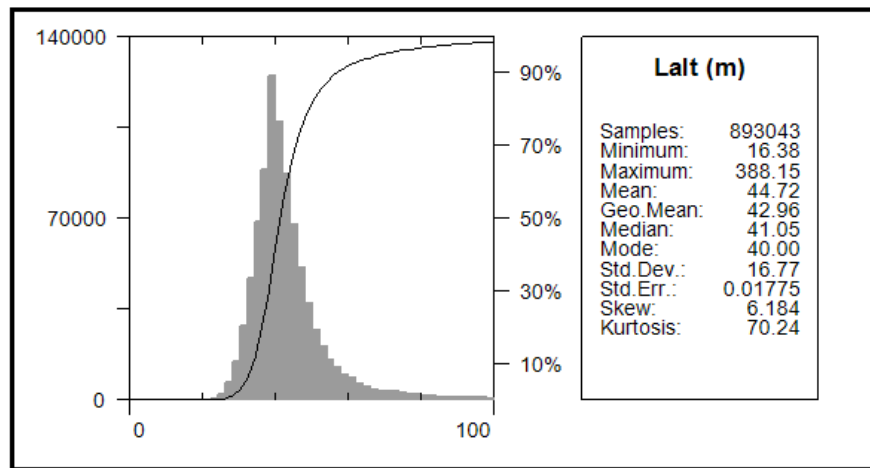


Figure 11: Histogram showing survey elevation vertically above ground.

Several linear magnetic anomalies closely coincident with the direction and location of survey lines were recognized. L470 was flown three times (Figures 12, 13 and 14) in the same direction and the data consistently display the same magnetic profile. A similar magnetic high coincident with L330 was also re-flown, and the data confirm that the NE-trending linear magnetic highs are real.

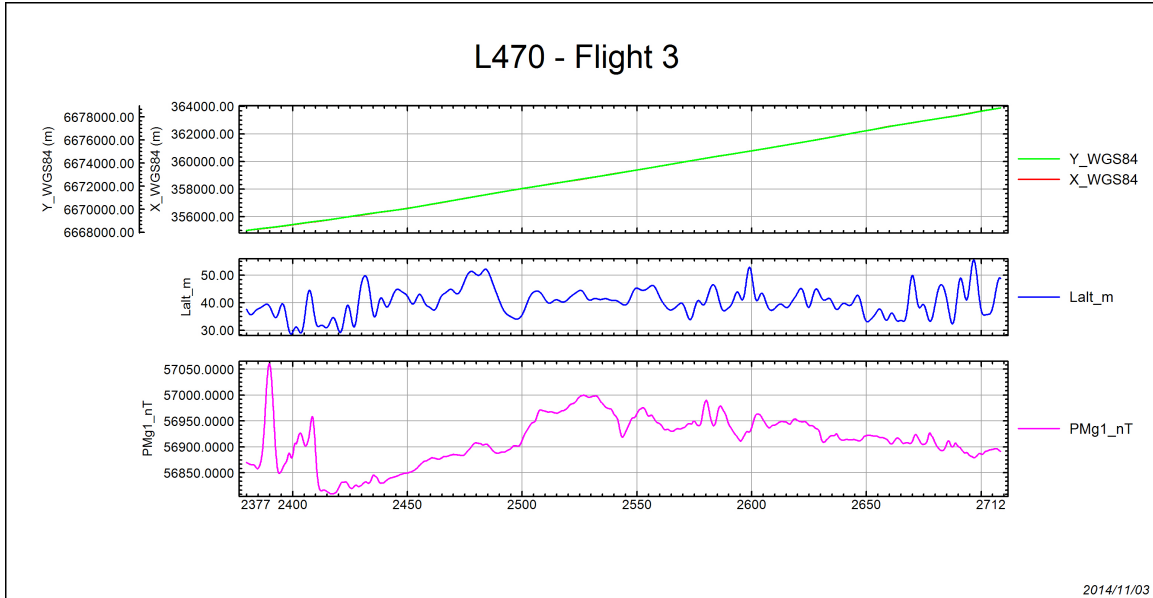


Figure 12: Plot of Line 470 flight 3 displaying X and Y UTM coordinates (top), laser altimeter readings in meters AGL (middle), and compensated magnetic intensity (bottom) profiles.

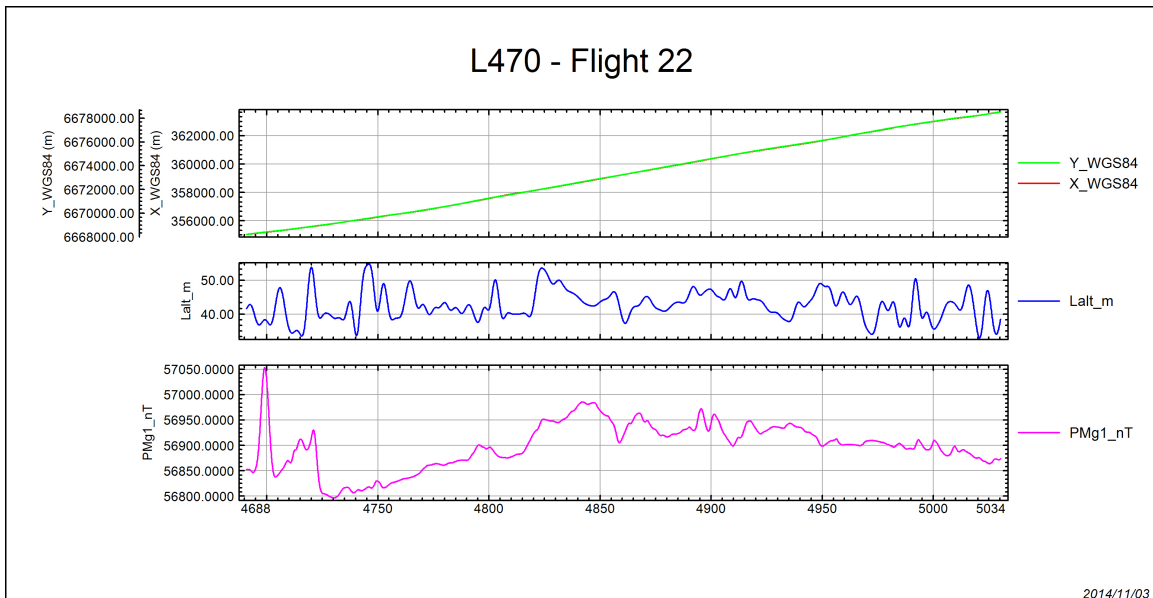


Figure 13: Plot of Line 470 flight 22 displaying X and Y UTM coordinates (top), laser altimeter readings in meters AGL (middle), and compensated magnetic intensity (bottom) profiles.

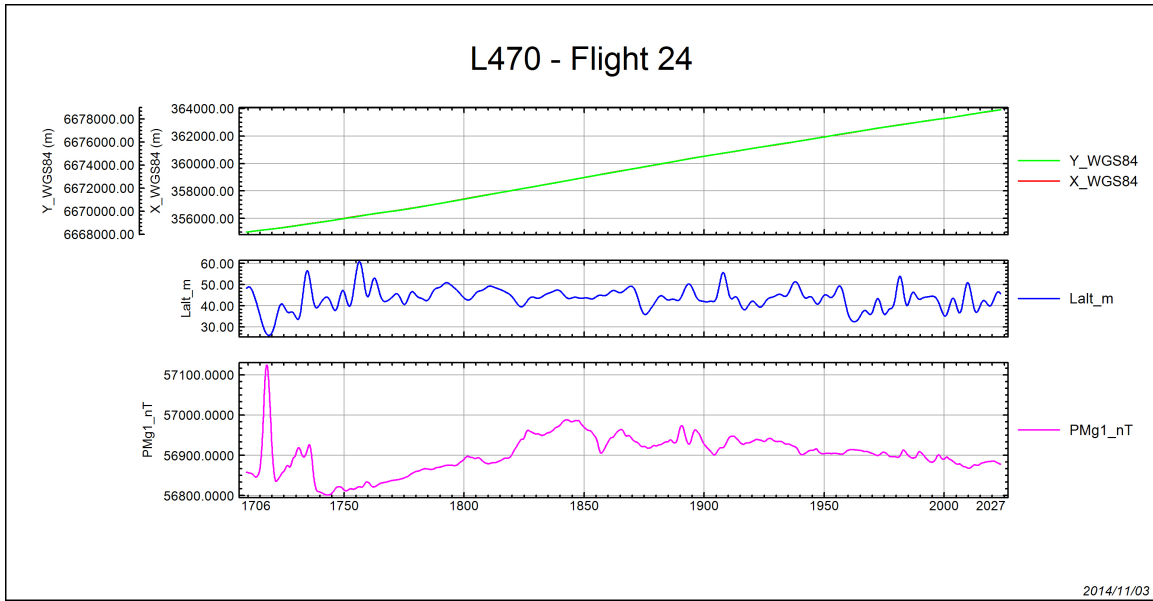


Figure 14: Plot of Line 470 flight 24 displaying X and Y UTM coordinates (top), laser altimeter readings in meters AGL (middle), and compensated magnetic intensity (bottom) profiles.

## 4.0 Aircraft and Equipment

All geophysical and subsidiary equipment are carefully installed on Precision GeoSurveys aircraft. For this survey, a magnetometer, a spectrometer, a data acquisition system, laser altimeter, magnetic compensation system, a pilot guidance unit (PGU), and magnetic base stations were required to carry out the survey and collect quality, high resolution data. The survey magnetometer was carried in an approved “stinger” configuration to enhance flight safety and improve data quality in this mountainous terrain.

### 4.1 Aircraft

Precision GeoSurveys flew the Seagull Batholith survey block using a Eurocopter AS350 helicopter (Figure 15), registration C-GOHK. The survey lines were flown at a nominal line spacing of three hundred (300) meters spacing and the tie lines were flown at three thousand (3000) meters spacing for both the magnetometer and spectrometer.



Figure 15: Eurocopter AS350 helicopter equipped with mag stinger for magnetic data acquisition, and internal spectrometer crystals for radiometric data acquisition.

## 4.2 Equipment

### 4.2.1 AGIS

The Airborne Geophysical Information System, AGIS, (Figure 16), is the main computer used in data recording, data synchronizing, displaying real-time QC data for the geophysical operator, and the generation of navigation information for the pilot and operator display system. Information such as magnetic field, total gamma count, counts of various radioelements (K, U, Th, etc.), temperature, cosmic radiation, barometric pressure, atmospheric humidity and survey altitude can all be monitored on the AGIS monitor for immediate QC.



Figure 16: AGIS operator display installed in the Eurocopter AS350.

The AGIS was manufactured by Pico Envirotec; therefore the system uses standardized Pico software and external sensors are connected to the system via RS-232 serial communication cables. The AGIS data format is easily converted into Geosoft or ASCII file formats by a supplied conversion program called PEIView. Additional Pico software allows for post or real time magnetic compensation and survey quality control procedures.

#### 4.2.2 Magnetometer

The airborne magnetic sensor used by Precision GeoSurveys is a Scintrex cesium vapor CS-3 magnetometer. The system was housed in a front mounted “stinger” (Figure 17). The CS-3 is a high sensitivity/low noise magnetometer with automatic hemisphere switching and a wide voltage range, the static noise rating for the unit is +/- 0.01 nT. On the AGIS monitor the operator can view the raw magnetic response, the magnetic fourth difference, compensated and uncompensated data, aircraft position, and the survey altitude for immediate QC of the magnetic data. The magnetic data are recorded at 10 Hz. A magnetic compensator is also used to remove noise created by the movement of the helicopter as it pitches, rolls and yaws within the Earth’s geomagnetic field.



Figure 17: View of the mag stinger.

### 4.2.3 Spectrometer

The IRIS, or Integrated Radiometric Information System, is a fully integrated, gamma radiation detection system containing 8.4 litres of NaI (T1) synthetic downward looking crystals (Figure 18) with 256 channel output at 1 Hz sampling rate. The downward-looking crystals are designed to measure gamma rays from below the aircraft and are equipped with upward-shielding high density RayShield® gamma-attenuating blankets to minimize cosmic and solar gamma noise. Real time data acquisition, navigation and communication tasks are integrated into a single unit that is installed in the rear cabin of the aircraft as indicated below.

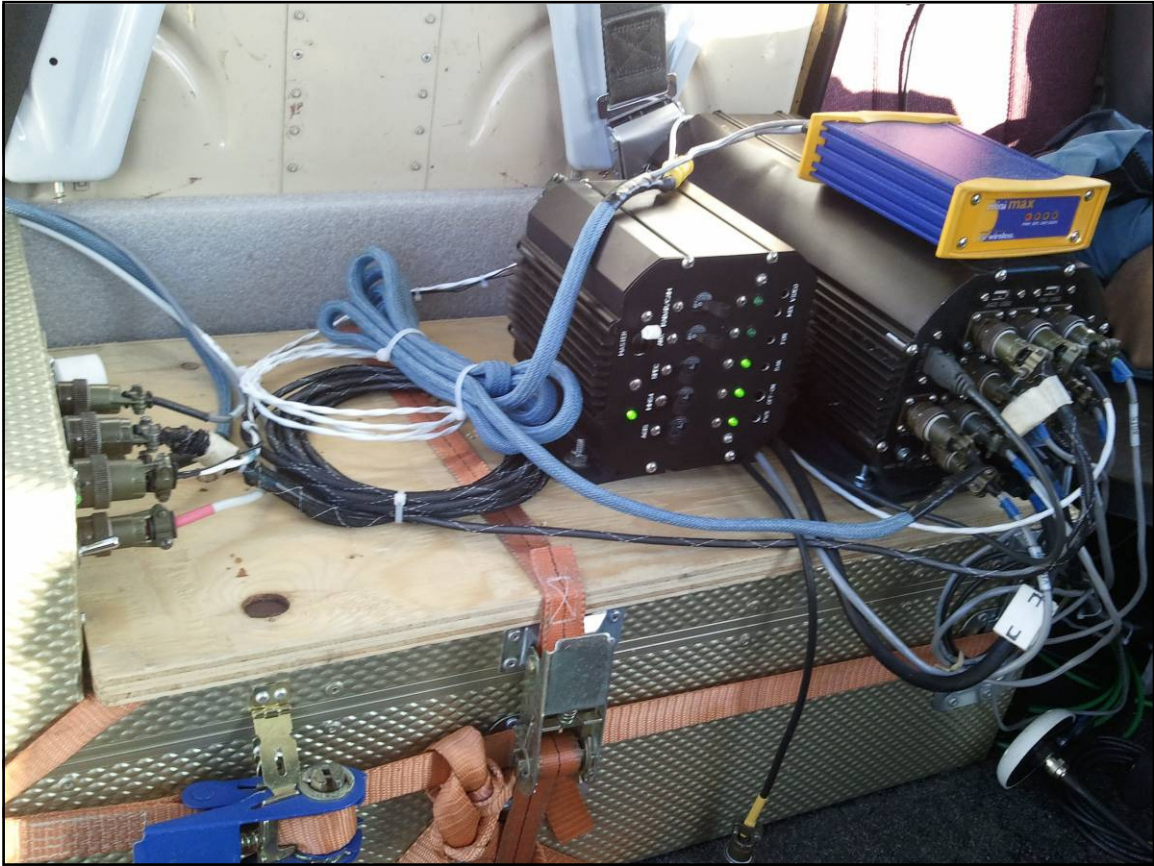


Figure 18: IRIS strapped in the back seat of the Eurocopter AS350.

#### 4.2.4 Base Station

For monitoring and recording of the Earth's diurnal magnetic field variation, Precision GeoSurveys operates two GEM GSM-19T magnetometer base stations continuously throughout the airborne data acquisition operation. The base stations were positioned north of Rancheria Lodge, hidden within the trees and in a region with low magnetic gradient, to give accurate magnetic field readings. The base stations were located in an area away from electric transmission power lines and moving ferrous objects, such as aircraft and motor vehicles that could affect the survey data integrity.

The GEM GSM-19T magnetometer with integrated GPS (Figure 19) time synchronization uses proton precession technology with a rate of 0.5 Hz sampling rate. The GSM-19T has an accuracy of +/- 0.2 nT at 1 Hz. Base station data are recorded on the internal solid-state memory, and downloaded onto a field laptop computer using a serial cable and GEMLink 5.0 software. Profile plots of the base station readings are generated and updated at the end of each survey day.



Figure 19: GEM GSM-19T proton precession magnetometer.

#### 4.2.5 Laser Altimeter

The pilot is provided with terrain guidance and clearance information from an Opti-Logic RS800 laser altimeter (Figure 20). This is attached at the aft end of the magnetometer boom. The RS800 sensor is a time-of-flight sensor that measures distance by a rapidly-modulated and collimated laser beam that creates a dot on the target surface. The maximum range of the laser altimeter is 700 m off of natural surfaces with an accuracy of +/- 1 meter on 1 x 1 m<sup>2</sup> diffuse target with 50% (+/- 20%) reflectivity. Within the sensor unit, reflected signal light is collected by the lens and focused onto a photodiode. Through serial communications and digital outputs, the ground clearance data are transmitted to an RS-232 compatible port and recorded and displayed by the AGIS and PGU at 10 Hz.

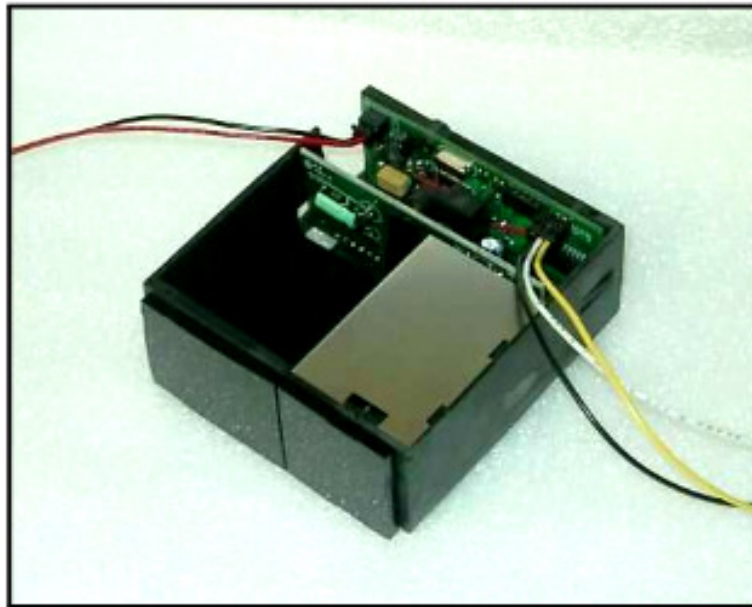


Figure 20: Opti-Logic RS800 laser altimeter.

#### 4.2.6 Pilot Guidance Unit

The PGU (Pilot Guidance Unit) is a graphical display type unit that provides continuous steering and elevation information to the pilot (Figure 21). It is mounted remotely from the data system on top of the helicopter's instrument panel. The PGU assists the pilot in keeping the helicopter on the flight path and at the desired ground clearance.



Figure 21: Pilot Guidance Unit.

The LCD monitor measures 7 inches, with a full VGA 800 x 600 pixel display. The CPU for the PGU is housed in the PC-104 console and uses Windows XP Embedded operating system control, with input from the GPS antenna, laser altimeter, and AGIS.

#### 4.2.7 GPS Navigation System

A Hemisphere GPS Mini Max navigation system integrated with the pilot display (PGU) and AGIS provided navigational information and control. The Hemisphere GPS Mini Max is composed of a receiver with an MGL-3 antenna (Figure 22). It has a position accuracy to within 1 meter and supports SBAS (WAAS, EGNS, and others), Beacon, and Satloc's patented e-Dif.



Figure 22: Hemisphere GPS – Mini Max

A differential correction signal (DGPS –Differential GPS) is applied to the GPS signal received through the MGL-3 antenna and can be applied up to 5 times per second (5 Hz). Therefore, the high- performance Mini Max differential correction provides positional accuracy on the order of 1 meter or less.

## 5.0 Data Acquisition Equipment Checks and Calibration

Airborne equipment tests were conducted at the start of the survey. There are three tests conducted for the airborne magnetometer: compensation flight, lag test, and heading error test. Gamma ray spectrometer checks and calibrations are also conducted prior to the start of the survey. The three tests conducted were the calibration pad test, cosmic flight test, and the Breckenridge test range.

### 5.1 Magnetometer Checks

#### 5.1.1 Compensation Flight Test

During aeromagnetic surveying a small but significant amount of noise is introduced to the magnetic data by the aircraft itself, as the magnetometer is within the helicopter's magnetic field. Movement of the aircraft (roll, pitch and yaw) and the permanent magnetization of certain aircraft parts (engine and other ferromagnetic objects) contribute to this noise. To remove noise generated by the aircraft a process called magnetic compensation is implemented. The magnetic compensation process starts with a test flight at the beginning of the survey, close to the Seagull survey block, where the aircraft flies in the four orthogonal headings required for the survey ( $040^{\circ}/220^{\circ}$  and  $130^{\circ}/310^{\circ}$  in the case of this survey) at a sufficient altitude (typically  $> 1,500$  m AGL) where the Earth's magnetic field becomes nearly uniform at the scale of the compensation flight. In each heading direction, three specified roll, pitch, and yaw maneuvers are performed by the pilot at constant elevation so that any magnetic variation recorded by the airborne magnetometer can be attributed to the aircraft movement. The variations recorded by

these maneuvers provide the data that are required to calculate the necessary parameters for compensating the magnetic data and removing the aircraft noise.

Pre-Compensation					Post-Compensation				
Heading	Roll	Pitch	Yaw	Total	Heading	Roll	Pitch	Yaw	Total
039	10.9008	2.2448	1.3390	14.4846	039	0.1904	0.2392	0.2035	0.6331
132	11.6529	5.0659	3.6687	20.3875	132	0.1712	0.1599	0.1676	0.4987
211	8.8287	5.3775	2.1865	16.3927	211	0.2331	0.2227	0.2377	0.6935
306	7.6775	2.8717	1.4458	11.9950	306	0.2172	0.2347	0.2172	0.6691
<b>Total</b>	39.0599	15.5599	8.6400		<b>Total</b>	0.8119	0.8565	0.8260	
<b>FOM = 63.2598 nT</b>					<b>FOM = 2.4944 nT</b>				

Table 5: Figure of Merit maneuver test results for compensation flight flown on October 10, 2014.

### 5.1.2 Lag Test

A lag test was performed to determine the relationship between the time the digital reading was recorded by the instrument magnetic sensor and the time for the position fix that the fiducial of the reading was obtained by the GPS system.

The test was flown in the four orthogonal headings over an identifiable magnetic anomaly (ie. Truck, Trailer, etc.) at survey speed and height. A lag of 10 fiducials (1.0 seconds) was determined from the lag test.

### 5.1.3 Heading Error Test

To determine the magnetic heading effect a cloverleaf pattern flight test was conducted. The cloverleaf test was flown in the same orthogonal headings as the survey and tie lines (040°/220° and 130°/310°) at >1000 m AGL in an area with low magnetic gradient. For all four directions the survey helicopter must pass over the same mid-point all four times at the same elevation (Table 6 and Figure 23).

Line Number	Fiducials	Heading	Mag (nT)	Average (nT)
L040	6942.7	NE- 040°	57076.2590	
L130	6651.8	SE - 130°	57087.8508	
L220	6896.5	SW - 220°	57067.7282	
L310	6538.9	NW - 310°	57059.9088	
				57072.9367

Table 6: Heading error test data format flown on October 08, 2014.

```

/Geosoft Heading Correction Table

/
/=Direction:real:i
/=Correction:real
/
/Direction Correction
040    -3.3223
130    -14.9141
220    +5.2085
310    +13.0279

```

Figure 23: Heading data results in .tbl format in Geosoft table.

## 5.2 Gamma-ray Spectrometer Checks and Calibrations

Pre-survey calibrations and testing of the GRS-10 airborne gamma-ray spectrometry system were carried out prior to the start of the survey. The calibration of the spectrometer system involved three tests which enabled the conversion of airborne data to ground concentration of natural radioactive elements. These tests were the calibration pad test, cosmic flight test, and the Breckenridge test range. The measurements were made in accordance with IAEA technical report series No. 323, “Airborne Gamma Ray Spectrometer Surveying”, and AGSO Record 1995/60, “A Guide to the Technical Specification for Airborne Gamma-Ray Surveys”.

### 5.2.1 Calibration Pad Test

The calibration pad test was conducted by Pico Envirotec at the GSC (Geological Survey of Canada) testing facility in Ottawa, Ontario over the approved GSC calibration pad. It is a slab of concrete containing known concentrations of the radioelements (K, Th, and U) and is ideally used to simulate a geological source of radiation. The measurements collected from the calibration pad test are used to determine the Compton scattering and Grasty Backscatter (spectral overlap between element windows) coefficients.

### 5.2.2 Cosmic Flight Test

While the background source of gamma radiation from the aircraft itself is essentially constant, the amount of signal detected from ground sources varies with ground clearance. As the height of the aircraft increases, the distance between the ground and the spectrometer crystals increase, and the proportion of cosmic radiation in each spectral window increases exponentially due to radiation of cosmic origin. The cosmic flight test is conducted to determine the aircraft’s background attenuation coefficients for the detector crystal packs and the cosmic coefficients. The pilot is required to fly over the same location repeatedly in opposite directions starting from 1,500 m to 3,000 m at 500 m intervals for approximately 2

minutes each to collect gamma data used to determine the amount of non-terrestrial gamma signal.

### 5.2.3 Breckenridge Test Range

The Breckenridge test range is very similar to the cosmic flight test but is conducted at lower elevations (from ground level). The pilot is required to fly over the same location at the following elevations in meters above ground; 30, 50, 100, 150, 200, 250, and 300. As the distance of the aircraft increases away from the radioactive ground source, the source signature exponentially degrades. As a result, this test is used to determine the altitude attenuation coefficients and the radio-element sensitivity of the airborne spectrometer system.

## 6.0 Data Processing

After all the data were collected from a survey flight several procedures were undertaken to ensure that the data met a high standard of quality. All data were processed using Pico Envirotec software and Geosoft Oasis Montaj 8.2 geophysical processing software along with proprietary processing algorithms.

### 6.1 Magnetic Processing

The data obtained from the compensation flight test were applied to the raw magnetic data before any further processing and editing. A computer program called PEIComp was used to create a model from the compensation flight test for each survey to remove the noise induced by aircraft movement; this model was applied to each survey flight so the data could be further processed.

Over glassy water or fog, the laser altimeter is unable to record a valid reading and a zero is recorded; therefore all data points recorded at zero were replaced with a nominal height of 40 m. Filtering was then applied to the laser altimeter data to remove vegetation clutter and to show the actual ground clearance. To remove vegetation clutter a Rolling Statistic filter was applied to the laser altimeter data and a low pass filter was used to smooth out the laser altimeter profile to eliminate isolated noise. As a result, filtering the data will yield a more uniform surface in close conformance with the actual terrain. A digital terrain model channel was calculated by subtracting the filtered laser altimeter data from the filtered GPS altimeter data defined by the WGS 84 ellipsoidal height.

The processing of the magnetic data first involved the correction for diurnal variations. The base station data were edited, plotted and merged into a Geosoft (.gdb) database on a daily basis. The airborne magnetic data were corrected for diurnal variations by subtracting the observed magnetic base station deviations. Following the diurnal correction, a lag correction was applied. A lag correction of 1.0 seconds was applied to the total magnetic field data to compensate for the combination of lag in the recording system and the magnetometer sensor flying 5.70 m ahead of the GPS antenna. Lastly, a

heading correction was applied to the data. As a result, after all corrections have been applied the initial Total Magnetic Intensity (TMI) data was generated.

The initial Total Magnetic Intensity (TMI) data from the survey and tie lines were used to level the entire survey dataset. Two forms of leveling were applied to the corrected data: conventional leveling and micro-leveling. There were two components to conventional leveling; the first involved statistical leveling of magnetic data to correct miss ties (intersection errors) followed by specific patterns or trends. For the second component, tie lines were brought to a common regional base value using the mean value of the cross-level error. To obtain the best possible leveled data, individual corrections were edited at selected intersections. Lastly, micro-leveling was applied to the corrected conventional leveled data. This will remove any residual noise related to flight line direction, and any low amplitude component of flight line noise, that still remained in the data after tie line leveling.

### 6.1.1 IGRF Removal and Calculation of the First Vertical Derivative

The International Geomagnetic Reference Field (IGRF) model is the empirical representation of the Earth's magnetic field (main core field without external sources) collected and disseminated from satellites and from observatories around the world. The IGRF is generally revised and updated every five years by a group of modelers associated with the International Association of Geomagnetism and Aeronomy (IAGA). In this case, the IGRF values were calculated from model year 2010 and the actual survey dates were obtained from the "Date" channel.

With the removal of the IGRF from the observed Total Magnetic Intensity (TMI) a Residual Magnetic Intensity (RMI) was generated. This created a more valid model of individual near surface anomalies and the data will not be referenced to a time which can be easily incorporated into databases of magnetic data acquired in the past or in the future.

The first vertical derivative was computed from the Total Magnetic Intensity (TMI) data. Long wavelengths and vertical rate of change were suppressed in the magnetic field. Therefore, the edges of magnetic anomalies were highlighted and spatial resolution was increased.

## 6.2 Radiometric Processing

Radiometric surveys map the concentration of radioelements at or near the earth's surface; typically up to 1.5 meters below surface. Thus, the first step which is vital before processing of the airborne radiometric data was to calibrate the spectrometer system. Once calibration of the system was complete, the radiometric data were processed by windowing the full spectrum to create channels for U, K, Th and total count. A 5-point Hanning filter was applied to the Cosmic window before going any further with processing the radiometric data.

Aircraft background and cosmic stripping corrections were applied to all three elements, and total count using the following formula:

$$C_{ac} = C_{lt} - (a_c + b_c * \text{Cos}_f)$$

where:  $C_{ac}$  is the background and cosmic corrected channel  
 $C_{lt}$  is the live time corrected channel  
 $a_c$  is the aircraft background for this channel  
 $b_c$  is the cosmic stripping coefficient for this channel  
 $\text{Cos}_f$  is the filtered cosmic channel

The radon backgrounds were first removed followed by Compton stripping. Spectral overlap corrections were applied on to potassium, uranium, and thorium as part of the Compton stripping process. This was done by using the stripping ratios that have been calculated for the spectrometer by prior calibration; this breaks the corrected elemental values down into the apparent radioelement concentrations. Lastly, attenuation corrections were applied to the data which involves nominal survey altitude corrections, in this case 44.72 metres is applied to total count, potassium, uranium, and thorium data.

With all corrections applied to the radiometric data, the final step was to convert the corrected potassium, uranium, and thorium to apparent radioelement concentrations using the following formula:

$$eE = C_{cor} / s$$

where:  $eE$  is the element concentration K(%) and equivalent element concentration of U(ppm) & Th(ppm)  
 $s$  is the experimentally determined sensitivity  
 $C_{cor}$  is the fully corrected channel

Finally, the natural air exposure rate was determined by using the following formula:

$$E = [(13.08 * K + 5.43 * eU + 2.69 * eTh) / 8.69]$$

where:  $E$  is the absorption dose rate in  $\mu\text{R/h}$   
 $K$  is the concentration of potassium (%)  
 $eU$  is the equivalent concentration of uranium (ppm)  
 $eTh$  is the equivalent concentration of thorium (ppm)

To calculate for radiometric ratios the guidelines of the IAEA were followed. Due to statistical uncertainties in the individual radioelement measurements, some care was taken in the calculation of the ratio in order to obtain statistically significant values. Following IAEA guidelines, the method of determining ratios of the eU/eTh, eU/K and eTh/K was as follows:

1. Any data points where the potassium concentration was less than 0.25% were removed.
2. The element with the lowest corrected count rate was determined.
3. The element concentrations of adjacent points on either side of each data point were summed until they exceeded a pre-determined threshold value. This threshold was set to be equivalent to 100 counts of the element with the lowest count rate. Additional minimum thresholds of 1.6% for potassium, 20 ppm for thorium, and 30 ppm for uranium were established to ensure meaningful ratios.
4. The ratios were calculated using the accumulated sums.

With this method, the errors associated with the calculated ratios were minimized and comparable for all data points.

The inverse was taken for both of these eTh/K and eU/K ratios. Therefore, K/eTh and K/eU are gridded to help identify relative potassium enrichments.

Gamma rays detected during airborne surveys emanate from near the ground surface. With a few centimeters of surficial cover (ie heavy vegetation or snow cover), some of the radiation from the rocks beneath are attenuated. Therefore, radiometric data collected should be used cautiously.

## 7.0 Deliverables

All digital data are presented on a compact disc (CD) and USB memory stick with the logistic report. The survey data are presented as digital databases, maps, and a report.

### 7.1 Digital Data

The file format will be provided in two (2) formats, the first will be a .GDB file for use in Geosoft Oasis Montaj, the second format will be a .XYZ file, this is text file. A complete file provided in each format will contain magnetic and radiometric data separately. Full description of the digital data and contents are included in the report (Appendix B).

The digital data are represented into grids. The following grids are prepared for the Seagull Batholith survey block at 75 m cell size listed below:

- Digital terrain model (DTM)
- Total magnetic intensity (TMI)
- Residual magnetic intensity (RMI) – removal of IGRF from TMI
- Calculated vertical gradient (CVG) - first vertical derivative of TMI
- Potassium (%K) - radiometric data in percentage
- Thorium (eTh) - radiometric data in concentrations
- Uranium (eU) - radiometric data in concentrations
- Total count (TCcor) – radiometric data in equivalent dose rate
- Total count (TCexp) – radiometric data in exposure rate
- Thorium over Potassium ratio (eTh/%K) – radiometric ratios
- Uranium over Potassium ratio (eU/%K) – radiometric ratios
- Uranium over Thorium ratio (eU/eTh) – radiometric ratios
- Potassium over Thorium ratio (%K/eTh) – radiometric ratios
- Potassium over Uranium ratio (%K/eU) – radiometric ratios

## 7.2 KMZ Grids

The digital data represented into grids were exported into kmz files which can be displayed using Google Earth. The grids can be draped onto topography and rendered to give a 3D view.

## 7.3 Maps

Digital maps were created for the Seagull Batholith survey block. The following map products were prepared:

Survey Overview Maps (colour images with elevation contour lines):

- Actual flight lines
- Digital terrain model

Magnetic Maps (colour images with elevation contour lines):

- Total magnetic intensity
- Total magnetic intensity with plotted flight lines
- Residual magnetic intensity
- Calculated vertical gradient of the total magnetic intensity

Radiometric Maps (colour images with elevation contour lines):

- Potassium – percentage
- Thorium – equivalent concentration
- Uranium – equivalent concentration
- Total Count – equivalent dose rate
- Total Count – exposure rate
- Thorium over Potassium ratio
- Uranium over Potassium ratio
- Uranium over Thorium ratio
- Potassium over Thorium ratio
- Potassium over Uranium ratio
- Ternary – an element ratio map of K, Th, and U

All maps were prepared in WGS 84 and UTM zone 9N.

#### 7.4 Report

The logistics report provides information on the acquisition procedures, magnetic processing, radiometric processing, and presentation of the Seagull Batholith survey block data. A pdf copy of the report is included along with the digital data and maps that are provided on the CD and USB stick.

## **Appendix A**

### Equipment Specifications

- GEM GSM-19T Proton Precession Magnetometer (Base Station)
- Hemisphere GPS – Mini Max
- Opti-Logic RS800 Laser Altimeter
- Scintrex CS-3 Survey Magnetometer
- Bartington Mag-03 three-axis fluxgate magnetic field sensor
- Pico Envirotec GRS-10 Gamma Spectrometer
- Pico Envirotec AGIS data recorder system (for Navigation, Gamma spectrometer, VLF-EM and Magnetometer Data Acquisition)

**GEM GSM-19T Proton Precession Magnetometer (Base Station)**

<b>Configuration Options</b>	15
<b>Cycle Time</b>	999 to 0.5 sec
<b>Environmental</b>	-40 to +60 ° Celsius
<b>Gradient Tolerance</b>	7,000 nT/m
<b>Magnetic Readings</b>	299,593
<b>Operating Range</b>	10, 000 to 120,000 nT
<b>Power</b>	12 V @ 0.62 A
<b>Sensitivity</b>	0.1 nT @ 1 sec
<b>Weight (Console/ Sensor)</b>	3.2 Kg
<b>Integrated GPS</b>	Yes

**Hemisphere GPS – Mini Max**

<b>GPS Sensor Specifications</b>	Receiver Type	LI, C/A code, with carrier phase smoothing
	Channels	I2-channel, parallel tracking ( 10-channel when tracking SBAS)
	WAAS Tracking	2-channel, parallel tracking
	Update Rate	1 Hz default, 5 Hz max
	Horizontal Accuracy	< 1 m 95% confidence (DGPS) < 5 m 95% confidence (autonomous, no SA)
	Cold Start	1 min typical
	Antenna Input Impedance	50 $\Omega$
<b>Beacon Sensor Specifications</b>	Channels	2-channel, parallel tracking
	Frequency Range	283.5 to 325 kHz
	Channel Spacing	500 Hz
	MSK Bit Rates	50, 100, and 200 bps
	Operating Modes	Manual, automatic, semi-automatic
	Cold Start Time	< 1 minute typical
	Reacquisition Time	< 2 seconds typical
	Demodulation	Minimum shift keying (MSK)
	Sensitivity	2.5 $\mu$ V for 6dB SNR @ 200 bps
	Dynamic Range	100dB
	Frequency Offset	$\pm$ 8 Hz (~ 27 ppm)
	Adjacent Channel Rejection	61 dB $\pm$ 1dB @ fo $\pm$ 400 Hz
<b>Communications</b>	Serial ports	2 full duplex
	Interface Level	RS-232C
	Baud Rates	4800, 9600, 19200
	Correction Input/ Output Protocol	RTCM SC-104
	Raw Measurement Data	Proprietary binary (RINEX utility available)
	Timing Output	1 PPS (HCMOS, active high, rising edge sync, 10k $\Omega$ , 10pF load)
<b>Environmental</b>	Operating Temperature	-32 $^{\circ}$ C to +74 $^{\circ}$ C
	Storage Temperature	-40 $^{\circ}$ C to +85 $^{\circ}$ C
	Humidity	95% non-condensing
	EMC	FCC Part I 5, Subpart B, Class B CISPR 22
<b>Power</b>	Input Voltage Range	9 to 32 VDC
	Reverse Polarity Protection	Yes
	Power Consumption	3W
	Current Consumption	<250 mA @ 12 VDC
	Antenna Short Circuit Protection	Yes

**Opti-Logic RS800 Laser Altimeter**

<b>Accuracy</b>	+/- 1 yard
<b>Com. Protocol</b>	RS232-8,N,1
<b>Baud Rate</b>	19200
<b>Raw Data Rate</b>	~200 Hz
<b>Calibrated Data Rate</b>	~10 Hz
<b>Laser</b>	Class I (eye-safe) 905nm +/- 10nm
<b>Power</b>	7-to-9 Vdc
<b>Typical Range</b>	400 yards
<b>Laser Wavelength</b>	905 nm +/- 10 nm
<b>Laser Divergence</b>	Vertical axis -- 3.5 mrad half- angle divergence Horizontal axis -- 1 mrad half- angle divergence (Approximate beam footprint at 100 m is 5 cm x 5 cm)
<b>Data Rate</b>	~200 Hz raw counts for un-calibrated operation ~10 Hz for calibrated operation (averaging algorithm seeks 8 good readings)
<b>Dimensions</b>	32 x 78 x 84 mm (lens face cross section is 32 x 78 mm)
<b>Casing</b>	RS100/RS400/RS800 units are supplied as OEM modules consisting of an open chassis containing optics and circuit boards. Custom housings can be designed and built on request.

**Scintrex CS-3 Survey Magnetometer**

<b>Operating Principal</b>	Self-oscillation split-beam Cesium Vapor (non-radioactive Cs-133)
<b>Operating Range</b>	15,000 to 105,000 nT
<b>Gradient Tolerance</b>	40,000 nT/metre
<b>Operating Zones</b>	10° to 85° and 95° to 170°
<b>Hemisphere Switching</b>	a) Automatic b) Electronic control actuated by the control voltage levels (TTL/CMOS) c) Manual
<b>Sensitivity</b>	0.0006 nT $\sqrt{\text{Hz}}$ rms.
<b>Noise Envelope</b>	Typically 0.002 nT P-P, 0.1 to 1 Hz bandwidth
<b>Heading Error</b>	+/- 0.25 nT (inside the optical axis to the field direction angle range 15° to 75° and 105° to 165°)
<b>Absolute Accuracy</b>	<2.5 nT throughout range
<b>Output</b>	a) continuous signal at the Larmor frequency which is proportional to the magnetic field (proportionality constant 3.49857 Hz/nT) sine wave signal amplitude modulated on the power supply voltage b) square wave signal at the I/O connector, TTL/CMOS compatible
<b>Information Bandwidth</b>	Only limited by the magnetometer processor used
<b>Sensor Head</b>	Diameter: 63 mm (2.5") Length: 160 mm (6.3") Weight: 1.15 kg (2.6 lb)
<b>Sensor Electronics</b>	Diameter: 63 mm (2.5") Length: 350 mm (13.8") Weight: 1.5 kg (3.3 lb)
<b>Cable, Sensor to Sensor Electronics</b>	3m (9' 8"), lengths up to 5m (16' 4") available
<b>Operating Temperature</b>	-40°C to +50°C
<b>Humidity</b>	Up to 100%, splash proof
<b>Supply Power</b>	24 to 35 Volts DC
<b>Supply Current</b>	Approx. 1.5A at start up, decreasing to 0.5A at 20°C
<b>Power Up Time</b>	Less than 15 minutes at -30°C

**Bartington Mag-03 three-axis fluxgate magnetic field sensor**

<b>Number of Axes</b>	3
<b>Bandwidth</b>	0 to 3kHz at 50 $\mu$ T peak
<b>Internal Noise:</b> <b>Basic version</b> <b>Standard version</b> <b>Low Noise version</b>	>10 to 20pTrms/ $\sqrt$ Hz at 1Hz 6 to $\leq$ 10pTrms/ $\sqrt$ Hz at 1Hz <6pTrms/ $\sqrt$ Hz at 1Hz
<b>Scaling error (DC)</b>	< $\pm$ 0.5%
<b>Orthogonality error</b>	<0.1 $^\circ$
<b>Alignment error (Z axis to reference face)</b>	<0.1 $^\circ$
<b>Linearity error</b>	<0.0015%
<b>Frequency response</b>	0 to 1kHz maximally flat, $\pm$ 5% maximum at 1kHz
<b>Input voltage</b>	$\pm$ 12V to $\pm$ 17V
<b>Supply current</b>	+30mA, -10mA (+1.4mA per 100 $\mu$ T for each axis)
<b>Power supply rejection ratio</b>	5 $\mu$ V/V (-106dB)
<b>Analog output</b>	$\pm$ 10V ( $\pm$ 12V supply) swings to within 0.5V of supply voltage
<b>Output impedance</b>	10 $\Omega$
<b>Operating temperature range</b>	-40 $^\circ$ C to +70 $^\circ$ C
<b>Environmental protection</b>	IP51
<b>Dimensions (W x H x L)</b>	32 x 32 x 152mm
<b>Weight</b>	160g
<b>Enclosure material</b>	Reinforced epoxy
<b>Connector</b>	ITT Cannon DEM-9P-NMB
<b>Mating connector</b>	ITT Cannon DEM-9S-NMB
<b>Mounting</b>	2 x M5 fixing holes

**Pico Envirotec GRS-10 Gamma Spectrometer**

<b>Crystal volume</b>	8.4 litres of NaI (Tl) synthetic downward looking crystals
<b>Resolution</b>	256/512 channels
<b>Tuning</b>	Automatic using peak determination algorithm
<b>Detector</b>	Digital Peak
<b>Calibration</b>	Fully automated detector
<b>Real Time</b>	Linearization and gain stabilization
<b>Communication</b>	RS232
<b>Detectors</b>	Expandable to 10 detectors and digital peak
<b>Count Rate</b>	Up to 60,000 cps per detector
<b>Count Capacity per channel</b>	65545
<b>Energy detection range:</b>	36 KeV to 3 MeV
<b>Cosmic channel</b>	Above 3 MeV
<b>Upward Shielding</b>	RayShield® non-radioactive shielding on downward looking crystals
<b>Spectra</b>	Collected spectra of 256/512 channels, internal spectrum resolution 1024
<b>Software</b>	Calibration: High voltage adjustment, linearity correction coefficients calculation, and communication test support Real Time Data Collection: Automatic Gain real time control on natural isotopes, and PC based test and calibration software suite
<b>Sensor</b>	Each box containing two (2) gamma detection NaI(Tl) crystals – each 4.2 liters. (256 cu in.) (approx. 100 x 100 x 650 mm) Total volume of approx 8.4 litres or 512 cu in with detector electronics
<b>Spectra Stabilization</b>	Real time automatic corrections on radio nuclei: Th, Ur, K. No implanted sources.

**Pico Envirotec AGIS data recorder system**

(for Navigation, Gamma spectrometer, VLF-EM and Magnetometer Data Acquisition)

<b>Functions</b>	Airborne Geophysical Information System (AGIS) with integrated Global Positioning System Receiver (GPS) and all necessary navigation guidance software. Inputs for geophysical sensors - portable gamma ray spectrometer GRS-10, MMS4 Magnetometer, Totem 2A EM, A/D converter, temperature probe, humidity probe, barometric pressure probe, and laser altimeter. Output for the 2 line Pilot Indicator
<b>Display</b>	Touch screen with display of 800 x 600 pixels; customized keypad and operator keyboard. Multi-screen options for real-time viewing of all data inputs, fiducial points, flight line tracking, and GPS channels by operator.
<b>GPS Navigation</b>	Garmin 12-channel, WAAS-enabled
<b>Data Sampling</b>	Sensor dependent
<b>Data Synchronization</b>	Synchronized to GPS position
<b>Data File</b>	PEI Binary data format
<b>Storage</b>	80 GB
<b>Supplied Software</b>	PEIView: Allows fast data Quality Control (QC) Data Format: Geosoft GBN and ASCII output PEIConv: For survey preparation and survey plot after data acquisition
<b>Software</b>	Calibration: High voltage adjustment, linearity correction coefficients calculation, and communication test support Real Time Data Collection: Automatic Gain real time control on natural isotopes and PC based test and calibration software suite
<b>Power Requirements</b>	24 to 32 VDC
<b>Temperature</b>	Operating:-10 to +55 deg C; storage:-20 to +70 deg C

## **Appendix B**

### Digital File Descriptions

- Magnetic database description
- Radiometric database description
- Grids
- Maps

Magnetic Database:

Abbreviations used in the GDB files listed below:

<b>Channel</b>	<b>Units</b>	<b>Description</b>
<b>X_WGS84</b>	m	UTM Easting – WGS 84 Zone 9 North
<b>Y_WGS84</b>	m	UTM Northing – WGS 84 Zone 9 North
<b>Lon_deg</b>	deg	Longitude
<b>Lat_deg</b>	deg	Latitude
<b>Date</b>	yyyy/mm/dd	Dates of the survey flight(s)
<b>FLT</b>		Flight Line numbers
<b>STL</b>		Number of satellite(s)
<b>LineNo</b>		Line numbers
<b>GPSfix</b>		GPS fix
<b>GPStime</b>	Hours:min:secs	GPS time (UTC)
<b>Geos_m</b>	m	Geoidal separation
<b>GHead_deg</b>	deg	Heading of the helicopter
<b>XTE_m</b>	M	Flight line cross distance
<b>Galt</b>	m	GPS height – WGS 84 Zone 9 North
<b>Lalt</b>	m	Laser Altimeter readings
<b>DTM</b>	m	Digital Terrain Model
<b>basemag</b>	nT	Base station diurnal data
<b>IGRF</b>		International Geomagnetic Reference Field 2010
<b>Declin</b>	Decimal deg	Calculated declination of magnetic field
<b>Inclin</b>	Decimal deg	Calculated inclination of magnetic field
<b>TMI</b>	nT	Total Magnetic Intensity
<b>RMI</b>	nT	Residual Magnetic Intensity

Radiometric Database:

Abbreviations used in the GDB files listed below:

<b>Channel</b>	<b>Units</b>	<b>Description</b>
<b>X_WGS84</b>	m	UTM Easting – WGS 84 Zone 9 North
<b>Y_WGS84</b>	m	UTM Northing – WGS 84 Zone 9 North
<b>Lon_deg</b>	deg	Longitude
<b>Lat_deg</b>	deg	Latitude
<b>Date</b>	yyyy/mm/dd	Dates of the survey flight(s)
<b>FLT</b>		Flight numbers
<b>STL</b>		Number of satellite(s)
<b>LineNo</b>		Line numbers
<b>GPStime</b>	Hours:min:secs	GPS time (UTC)
<b>Geos_m</b>	m	Geoidal separation
<b>GPSFix</b>		GPS fix
<b>GHead_deg</b>	deg	Heading of the helicopter
<b>XTE_m</b>	m	Flight line cross distance
<b>Galt</b>	m	GPS height – WGS 84 Zone 9 North
<b>Lalt</b>	m	Laser Altimeter readings
<b>DTM</b>	m	Digital Terrain Model
<b>BaroSTP_Kp</b>	KiloPascal	Barometric Altitude (Press and Temp Corrected)
<b>Temp_degC</b>	Degrees C	Air Temperature
<b>Press_kP</b>	KiloPascal	Atmospheric Pressure
<b>COSFILT</b>	counts/sec	Spectrometer - Filtered Cosmic
<b>Kcor</b>	%	Equivalent Concentration - Potassium
<b>THcor</b>	ppm	Equivalent Concentration - Thorium
<b>Ucor</b>	ppm	Equivalent Concentration - Uranium
<b>TCcor</b>	μR	Equivalent Dose Rate
<b>TCexp</b>	μR/hour	Exposure Rate - SUM(%k, eU, eTh) * determined factors
<b>THKratio</b>		Spectrometer – eTh/%K ratio
<b>UKratio</b>		Spectrometer – eU/%K ratio
<b>UTHratio</b>		Spectrometer – eU/eTh ratio
<b>KTHratio</b>		Spectrometer –%K/eTh ratio
<b>KUratio</b>		Spectrometer –%K/eU ratio

Grids: Seagull Batholith survey block, WGS 84 Datum, Zone 9N

FILE NAME	DESCRIPTION
Seagull Batholith_DTM_75m.grd	Seagull Batholith survey block digital terrain model gridded at 75 m cell size
Seagull Batholith_TMI_75m.grd	Seagull Batholith survey block total magnetic intensity gridded at 75 m cell size
Seagull Batholith_RMI_75m.grd	Seagull Batholith survey block residual magnetic intensity gridded at 75 m cell size
Seagull Batholith_CVG_75m.grd	Seagull Batholith survey block calculated vertical gradient of TMI gridded at 75 m cell size
Seagull Batholith_Kcor_75m.grd	Seagull Batholith survey block potassium (Kcor) percentage gridded at 75 m cell size
Seagull Batholith_Thcor_75m.grd	Seagull Batholith survey block Thorium (Thcor) equivalent concentration gridded at 75 m cell size
Seagull Batholith_Ucor_75m.grd	Seagull Batholith survey block Uranium (Ucor) equivalent concentration gridded at 75 m cell size
Seagull Batholith_TCcor_75m.grd	Seagull Batholith survey block Total Count (TCcor) equivalent dose rate gridded at 75 m cell size
Seagull Batholith_TCexp_75m.grd	Seagull Batholith survey block Total Count (TCexp) exposure rate gridded at 75 m cell size
Seagull Batholith_ThKratio_75m.grd	Seagull Batholith survey block thorium over potassium ratio (eTh/%K) gridded at 75 m cell size
Seagull Batholith_UKratio_75m.grd	Seagull Batholith survey block uranium over potassium ratio (eU/%K) gridded at 75 m cell size
Seagull Batholith_UTHratio_75m.grd	Seagull Batholith survey block uranium over thorium ratio (eU/eTh) gridded at 75 m cell size
Seagull Batholith_KTHratio_75m.grd	Seagull Batholith survey block potassium over thorium ratio (%K/eTh) gridded at 75 m cell size
Seagull Batholith_KUratio_75m.grd	Seagull Batholith survey block potassium over uranium ratio (%K/eU) gridded at 75 m cell size

Maps: Seagull Batholith survey block, WGS 84 Datum, Zone 9N (jpegs and pdfs)

FILE NAME	DESCRIPTION
Seagull Batholith_ActualFlightLines_75m	Seagull Batholith Survey block plotted actual flown flight lines
Seagull Batholith_DTM_75m	Seagull Batholith Survey block digital terrain model gridded at 75 m cell size
Seagull Batholith_TMI_75m	Seagull Batholith Survey block total magnetic intensity gridded at 75 m cell size
Seagull Batholith_TMI_with_FlightLines_75m	Seagull Batholith Survey block total magnetic intensity with plotted actual flight lines gridded at 75 m cell size
Seagull Batholith_RMI_75m	Seagull Batholith Survey block residual magnetic intensity gridded at 75 m cell size
Seagull Batholith_CVG_75m	Seagull Batholith Survey block calculated vertical gradient of TMI gridded at 75 m cell size
Seagull Batholith_%Kcor_75m	Seagull Batholith Survey block potassium (Kcor) percentage gridded at 75 m cell size
Seagull Batholith_Thcor_75m	Seagull Batholith Survey block Thorium (Thcor) equivalent concentration gridded at 75 m cell size
Seagull Batholith_Ucor_75m	Seagull Batholith Survey block Uranium (Ucor) equivalent concentration gridded at 75 m cell size
Seagull Batholith_TCcor_75m	Seagull Batholith Survey block Total Count (TCcor) equivalent dose rate gridded at 75 m cell size
Seagull Batholith_TCexp_75m	Seagull Batholith Survey block Total Count (TCexp) exposure rate gridded at 75 m cell size
Seagull Batholith_eTh%K_Ratio_75m	Seagull Batholith Survey block thorium over potassium ratio (%K/eTh) gridded at 75 m cell size
Seagull Batholith_eU%K_Ratio_75m	Seagull Batholith Survey block uranium over potassium ratio (eU/%K) gridded at 75 m cell size
Seagull Batholith_eUeTh_Ratio_75m	Seagull Batholith Survey block uranium over thorium ratio (eU/eTh) gridded at 75 m cell size
Seagull Batholith_%KeTh_Ratio_75m	Seagull Batholith Survey block potassium over thorium ratio (%K/eTh) gridded at 75 m cell size
Seagull Batholith_%KeU_Ratio_75m	Seagull Batholith Survey block potassium over uranium ratio (%K/eU) gridded at 75 m cell size
Seagull Batholith_TernaryMap_75m	Seagull Batholith Survey block displaying ratios of all three elements (%K, eTh, eU)

## **Appendix C**

### Seagull Batholith Survey Block Maps

Survey Overview Maps (colour image with elevation contour lines):

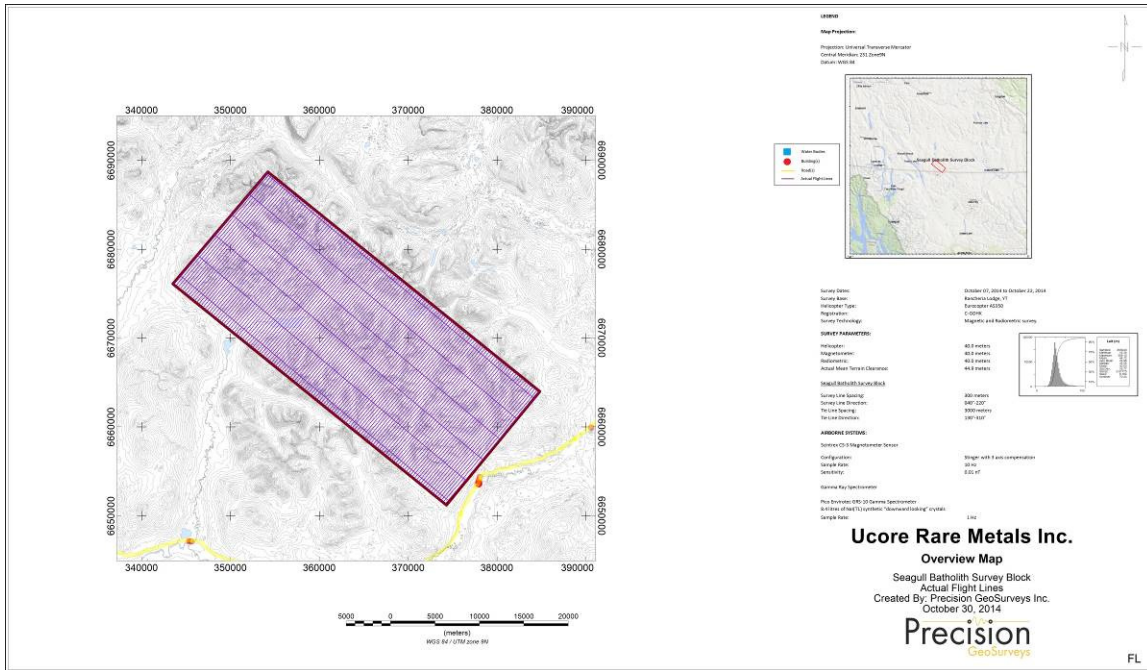
- Flight Lines (FL)
- Digital Terrain Model (DTM)

Magnetic Maps (colour image with elevation contour lines):

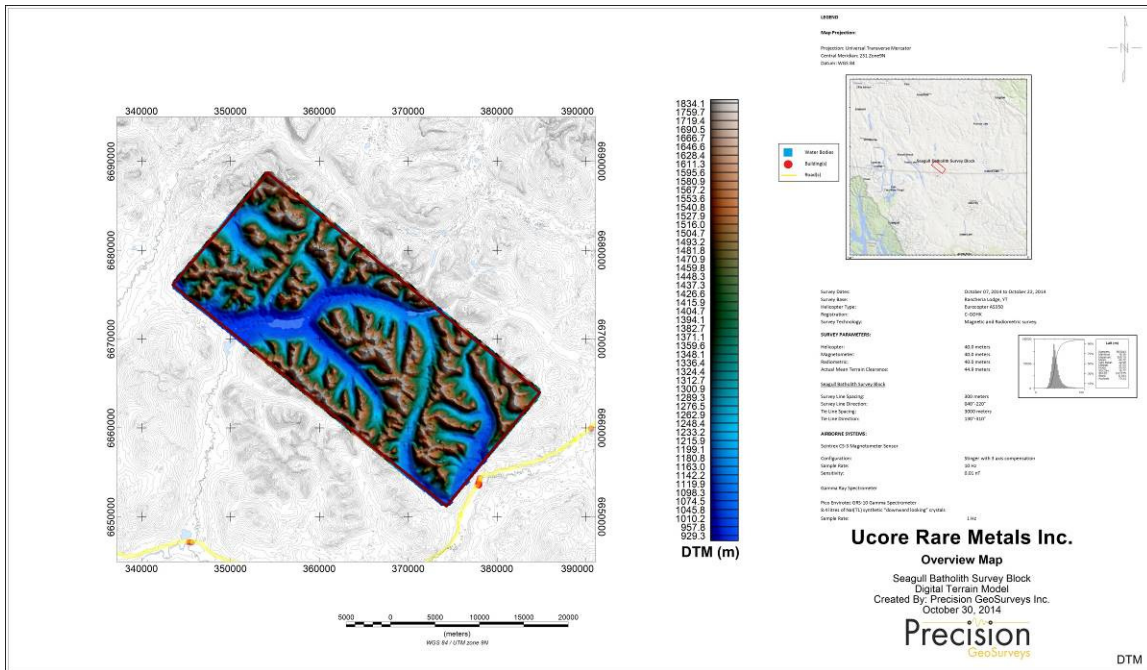
- Total Magnetic Intensity (TMI)
- Total Magnetic Intensity (TMI\_wFL) with flight lines
- Residual Magnetic Intensity (RMI)
- Calculated Vertical Gradient (CVG) of TMI

Radiometric Maps (colour image with elevation contour lines):

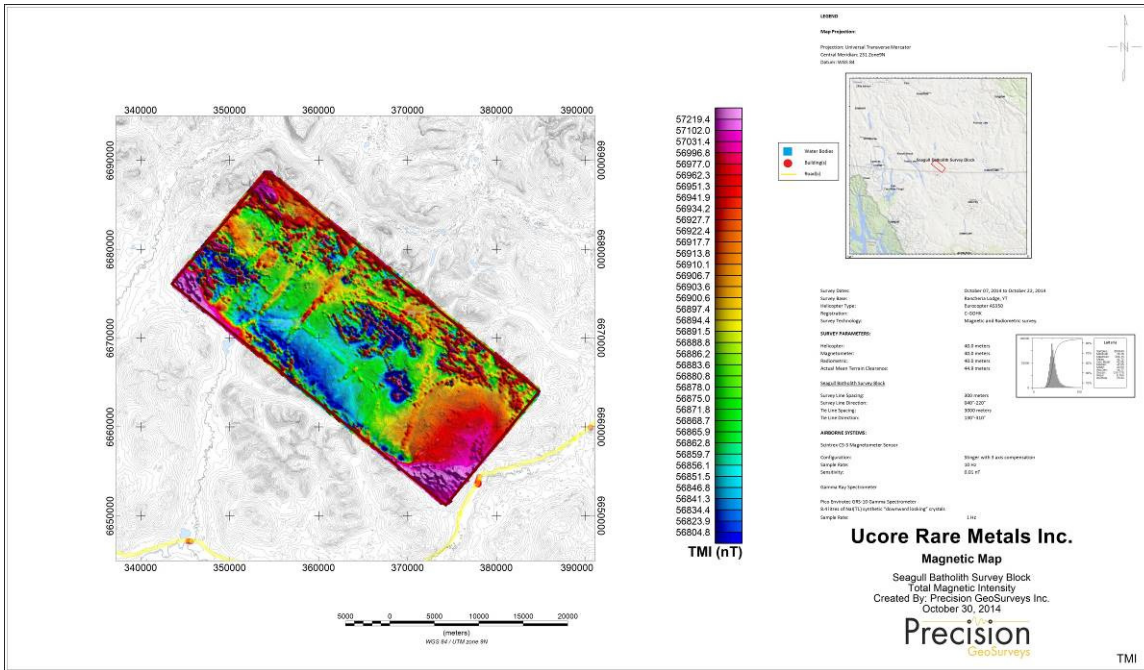
- Potassium – Equivalent Concentration (%K)
- Thorium – Equivalent Concentration (eTh)
- Uranium – Equivalent Concentration (eU)
- Total Count –Equivalent Dose Rate (TCcor)
- Total Count – Exposure Rate (TCexp)
- Thorium over Potassium Ratio - Spectrometer - eTh/%K ratio
- Uranium over Potassium Ratio - Spectrometer - eU/%K ratio
- Uranium over Thorium Ratio - Spectrometer - eU/eTh ratio
- Potassium over Thorium Ratio - Spectrometer - %K/eTh ratio
- Potassium over Uranium Ratio - Spectrometer - %K/eU ratio
- Ternary (TM)



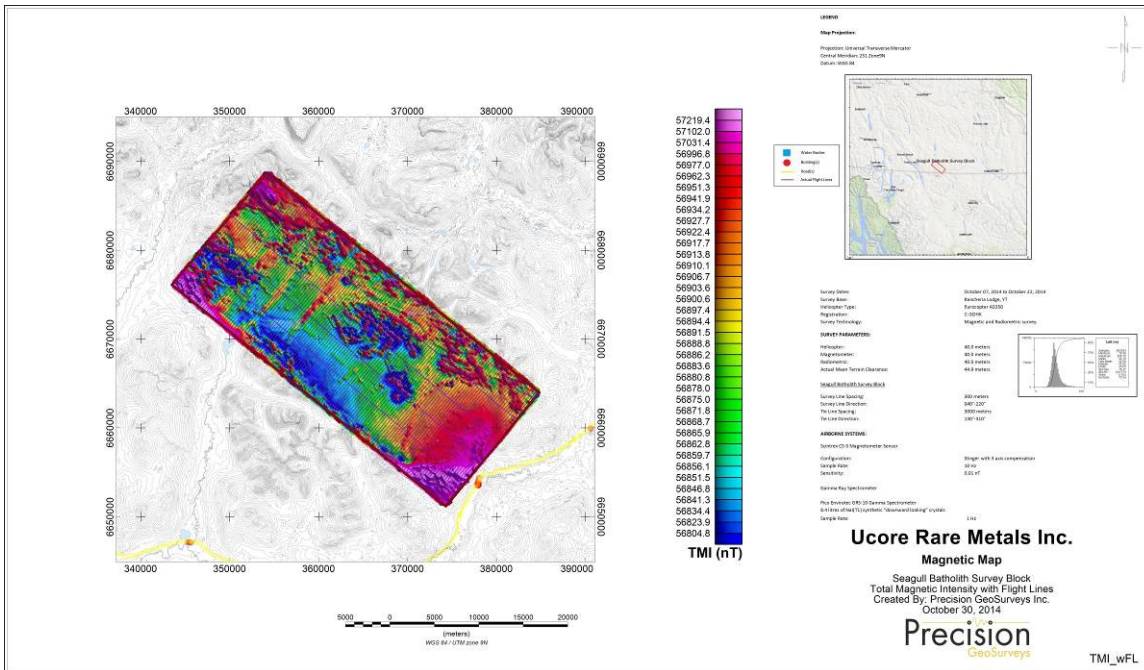
Map 1: Seagull Batholith survey block actual flight lines.



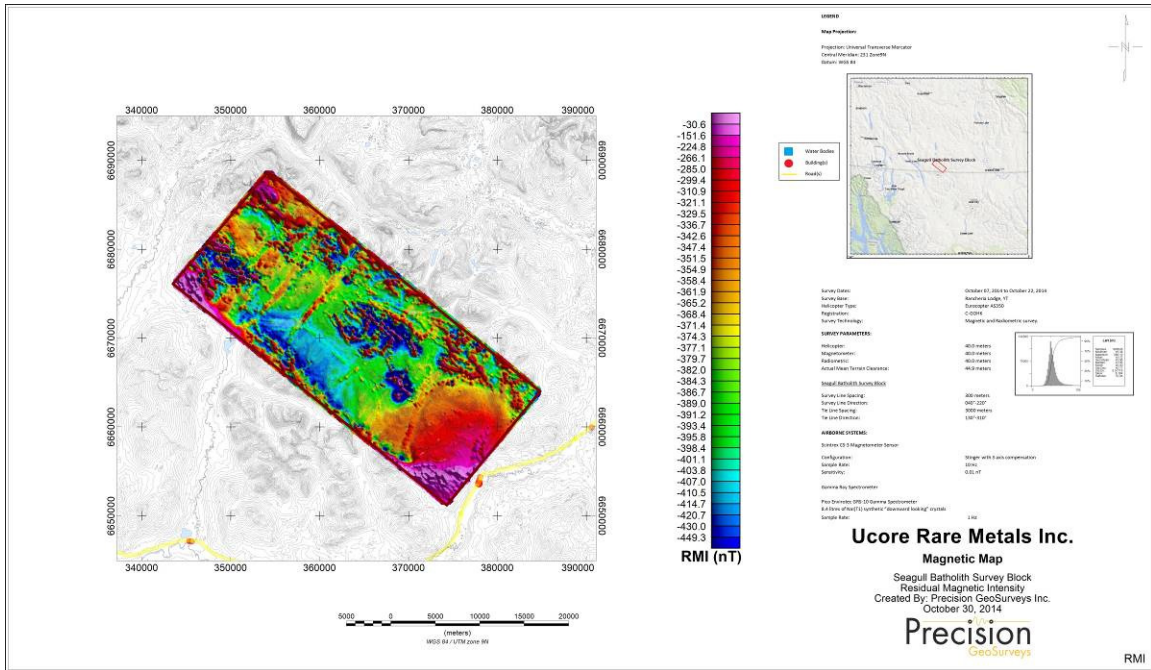
Map 2: Seagull Batholith survey block digital terrain model.



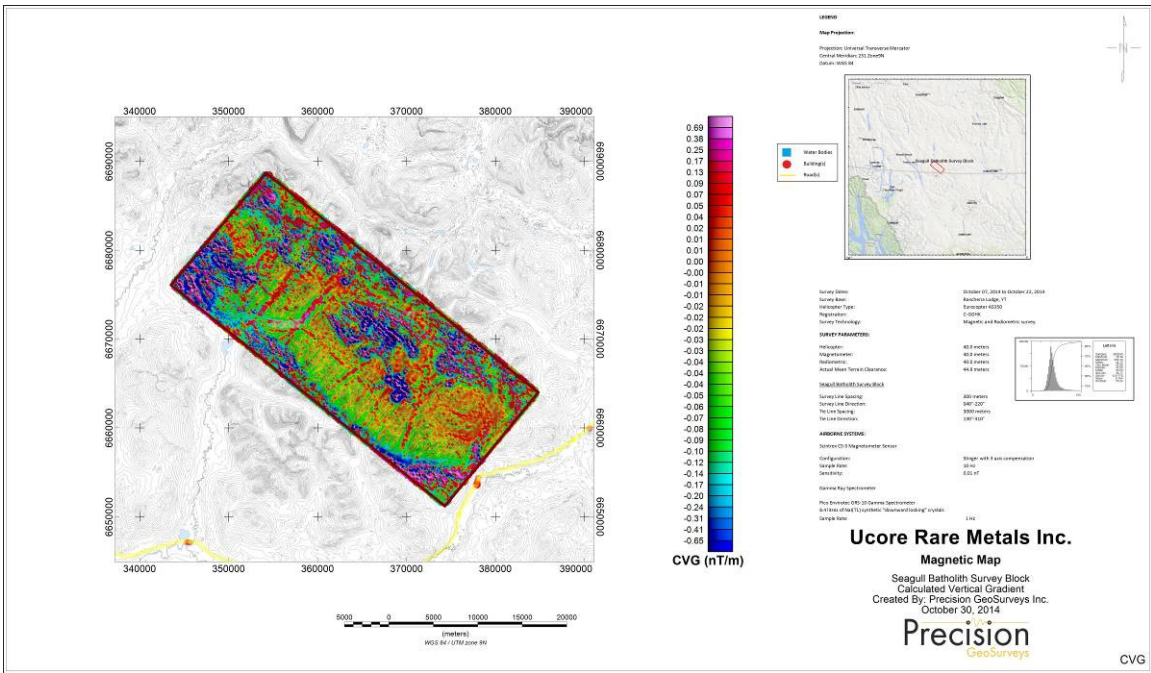
Map 3: Seagull Batholith survey block total magnetic intensity.



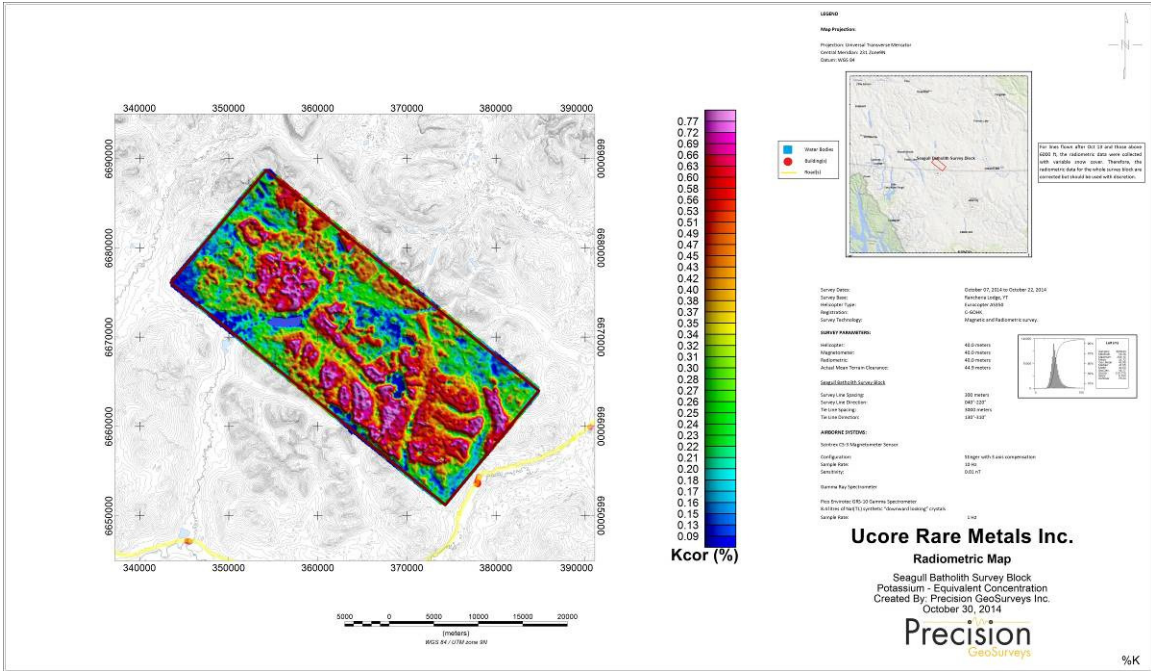
Map 4: Seagull Batholith survey block total magnetic intensity with plotted actual flight lines.



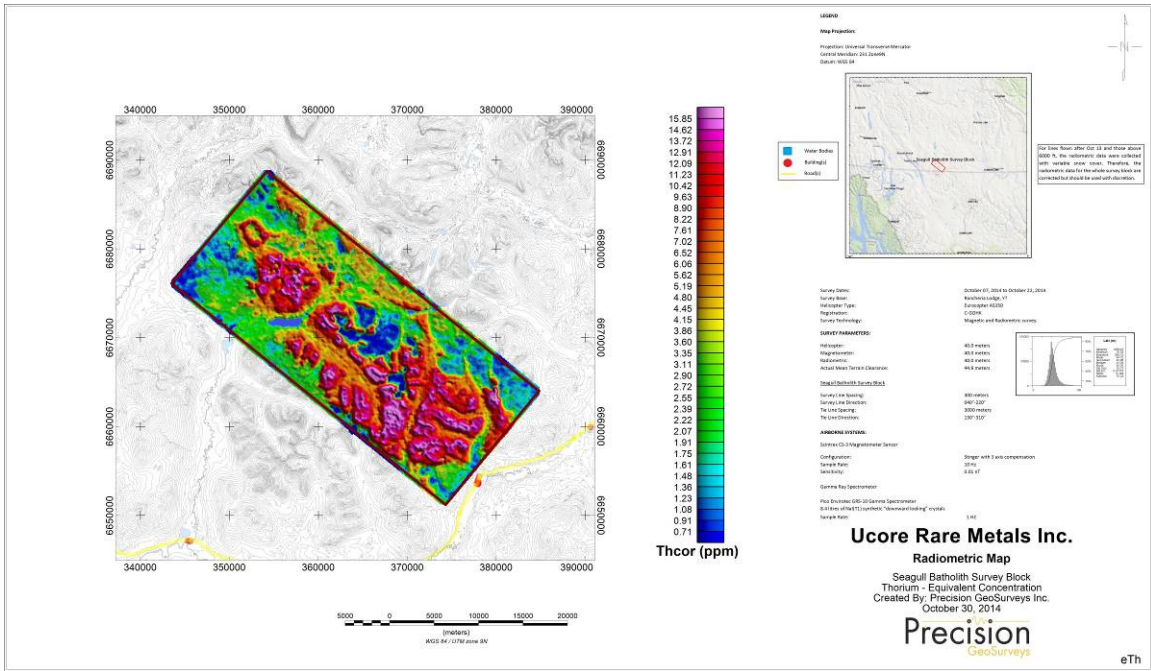
Map 5: Seagull Batholith survey block residual magnetic intensity.



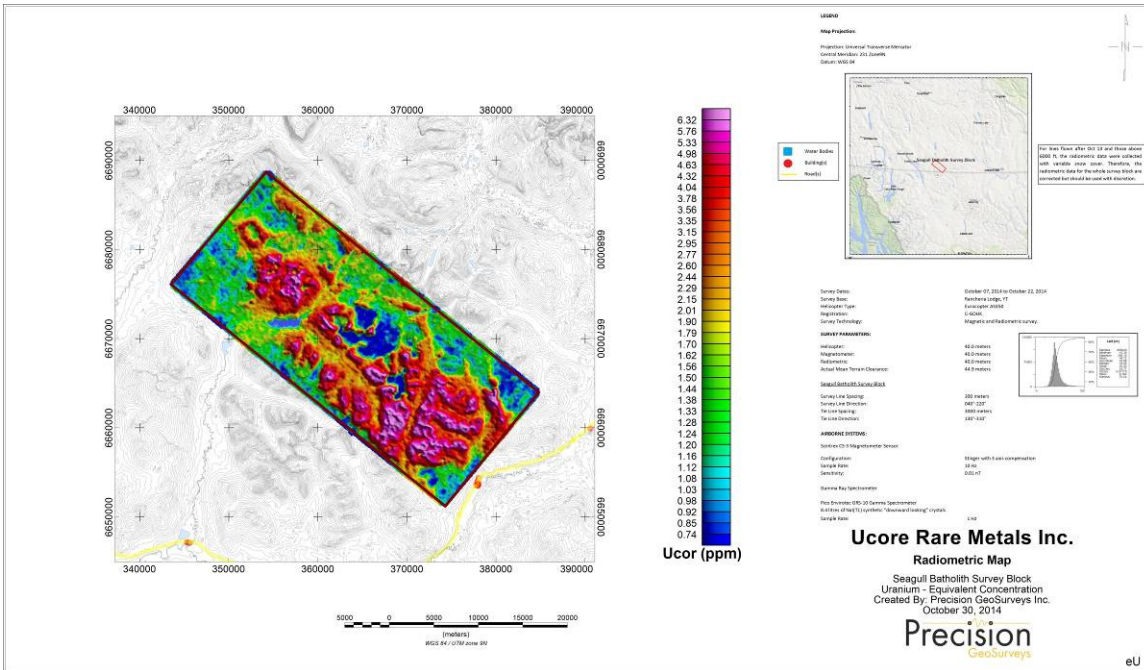
Map 6: Seagull Batholith survey block calculated vertical gradient of the total magnetic intensity.



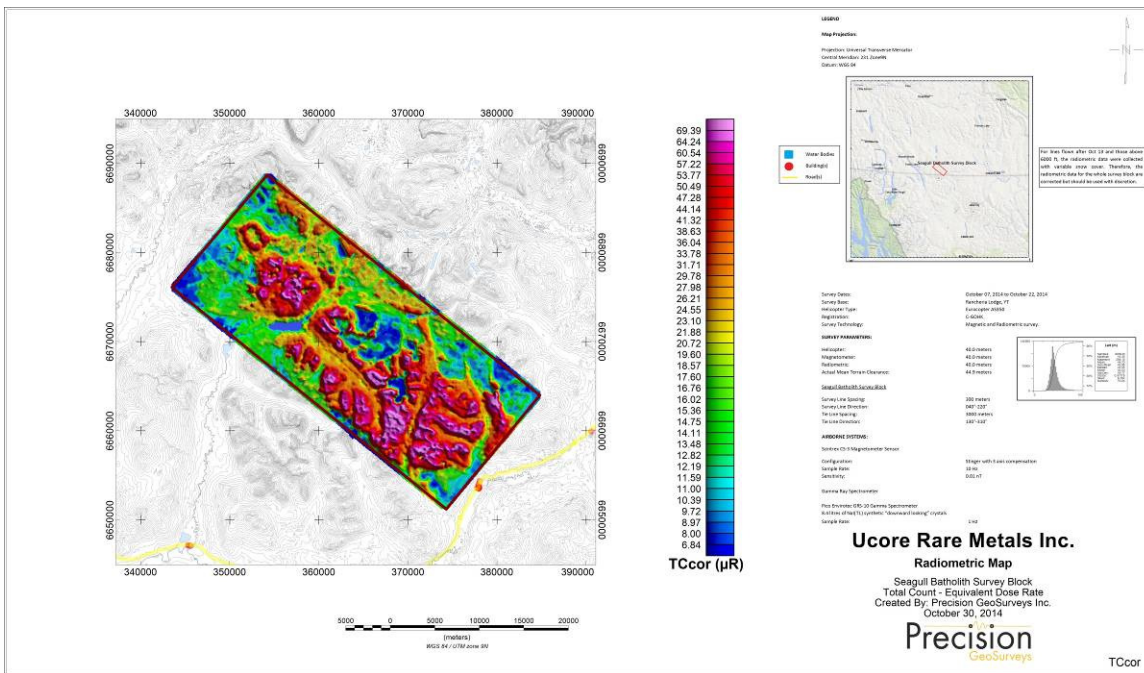
Map 7: Seagull Batholith survey block potassium – (percentage) equivalent concentration.



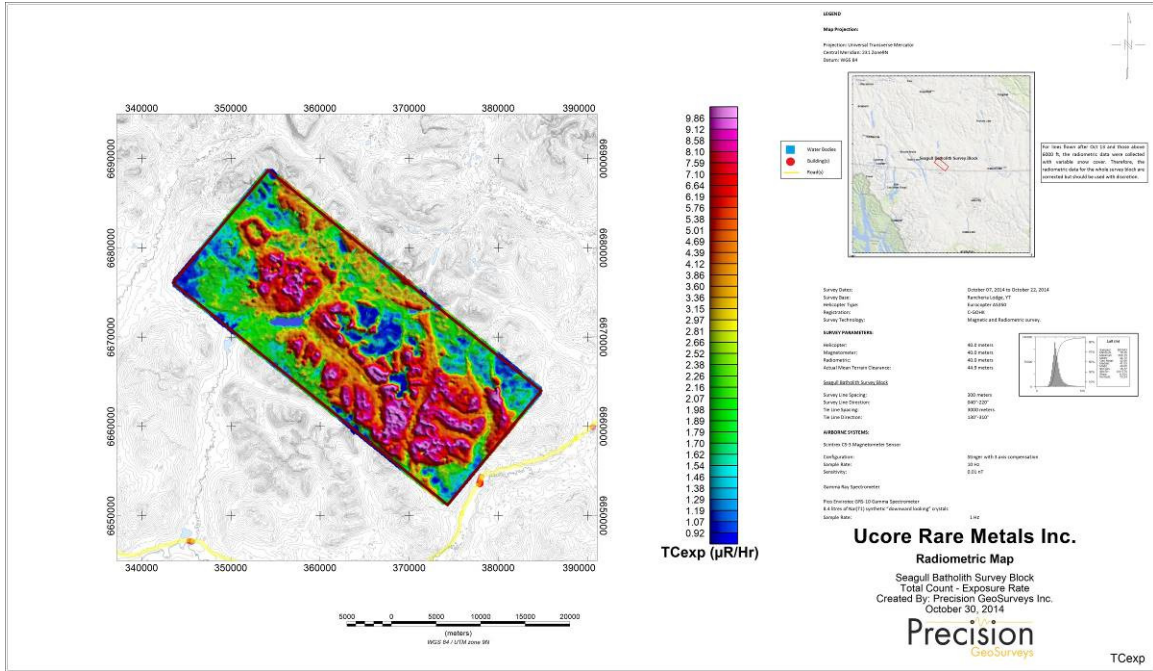
Map 8: Seagull Batholith survey block thorium – equivalent concentration.



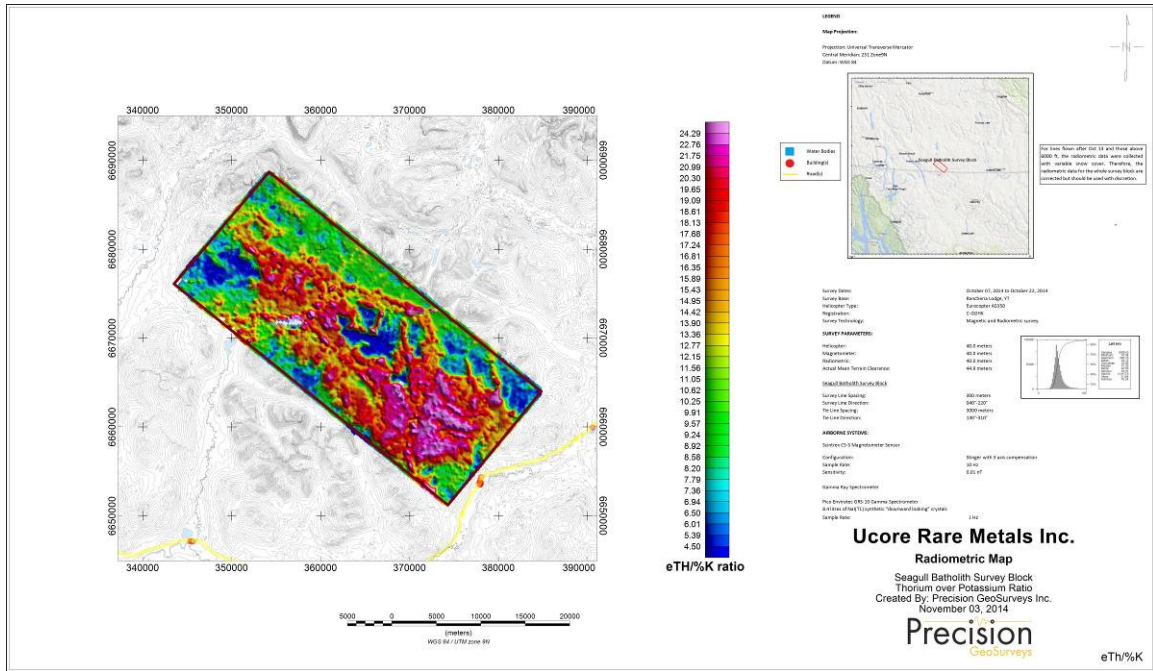
Map 9: Seagull Batholith survey block uranium – equivalent concentration.



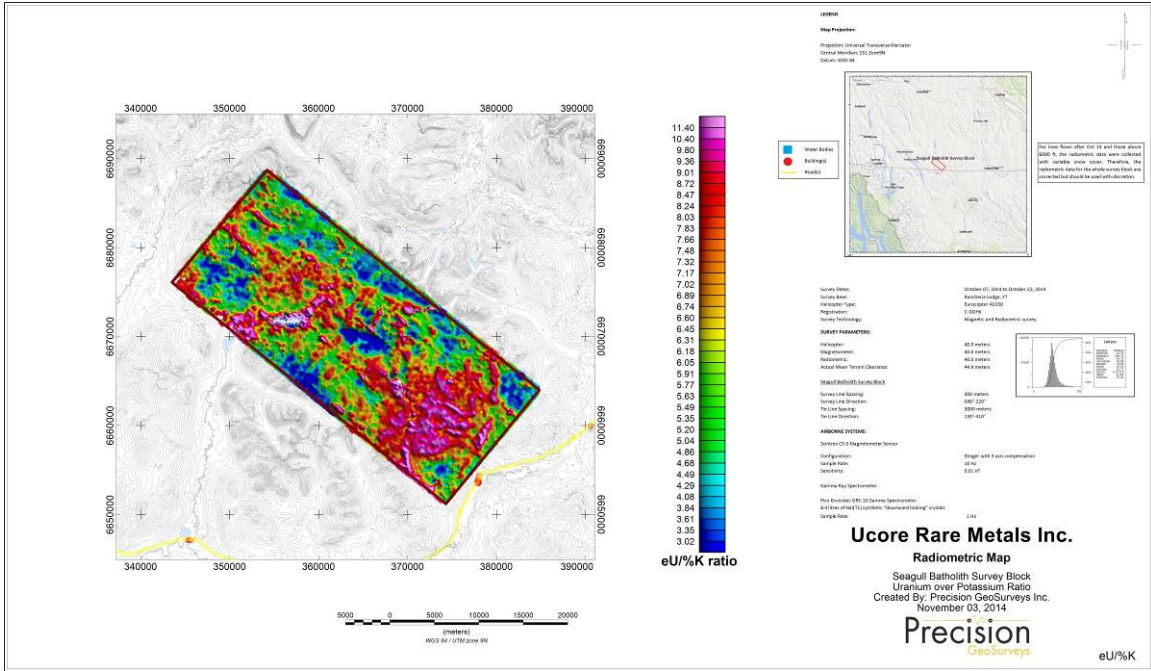
Map 10: Seagull Batholith survey block total count – equivalent dose rate.



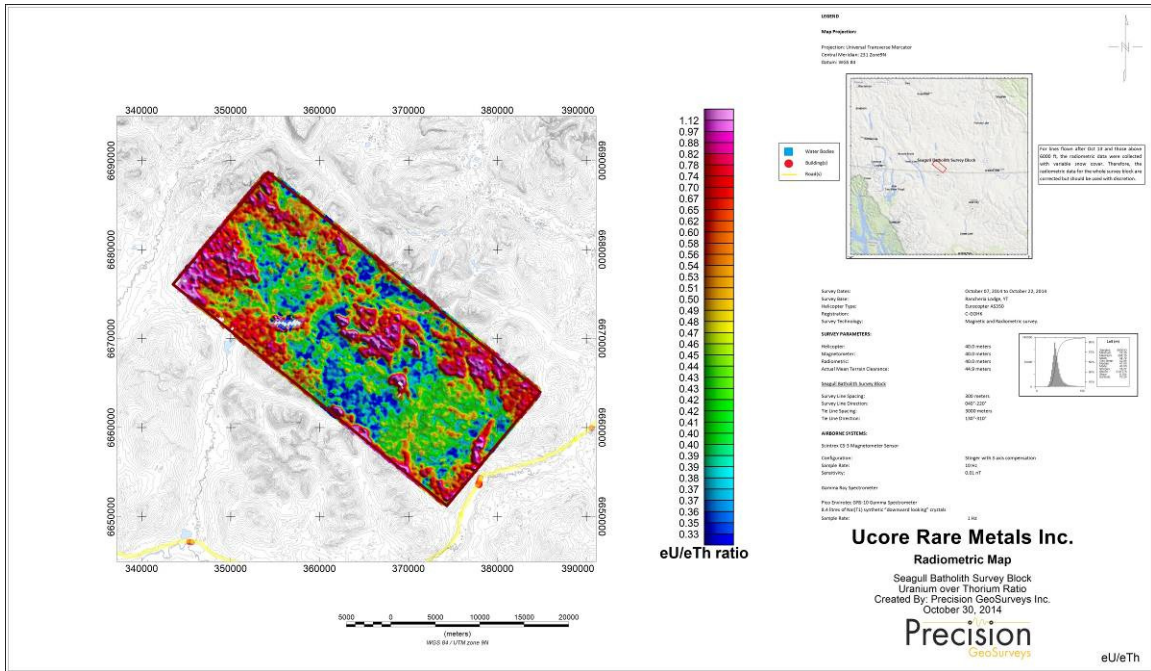
Map 11: Seagull Batholith survey block total count –exposure rate.



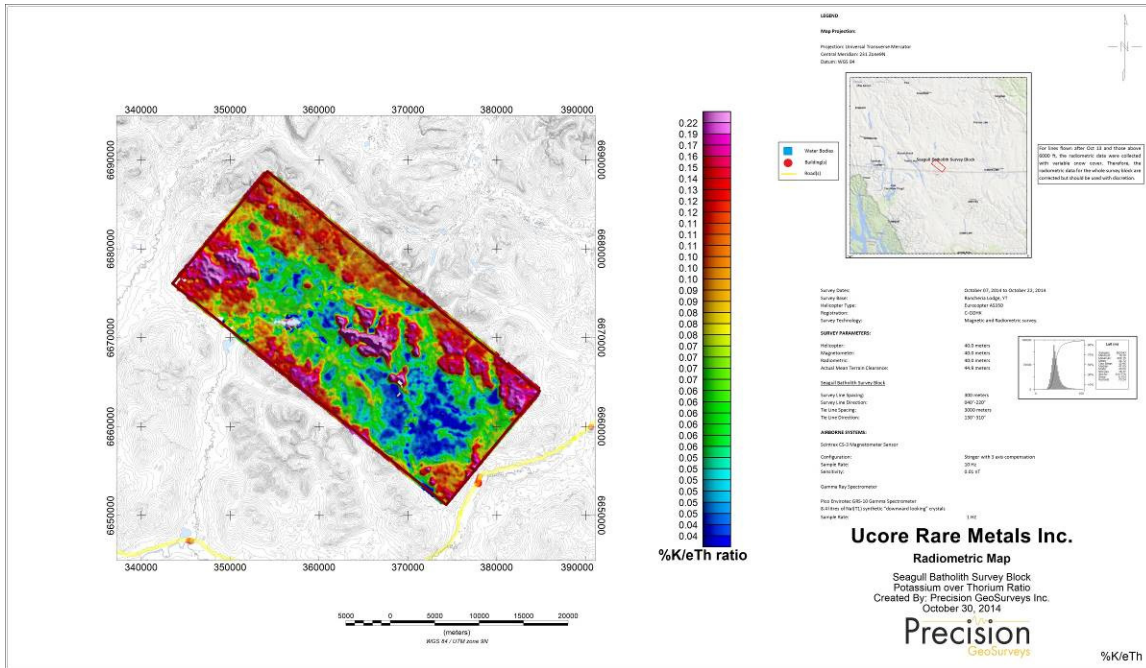
Map 12: Seagull Batholith survey block thorium over potassium ratio.



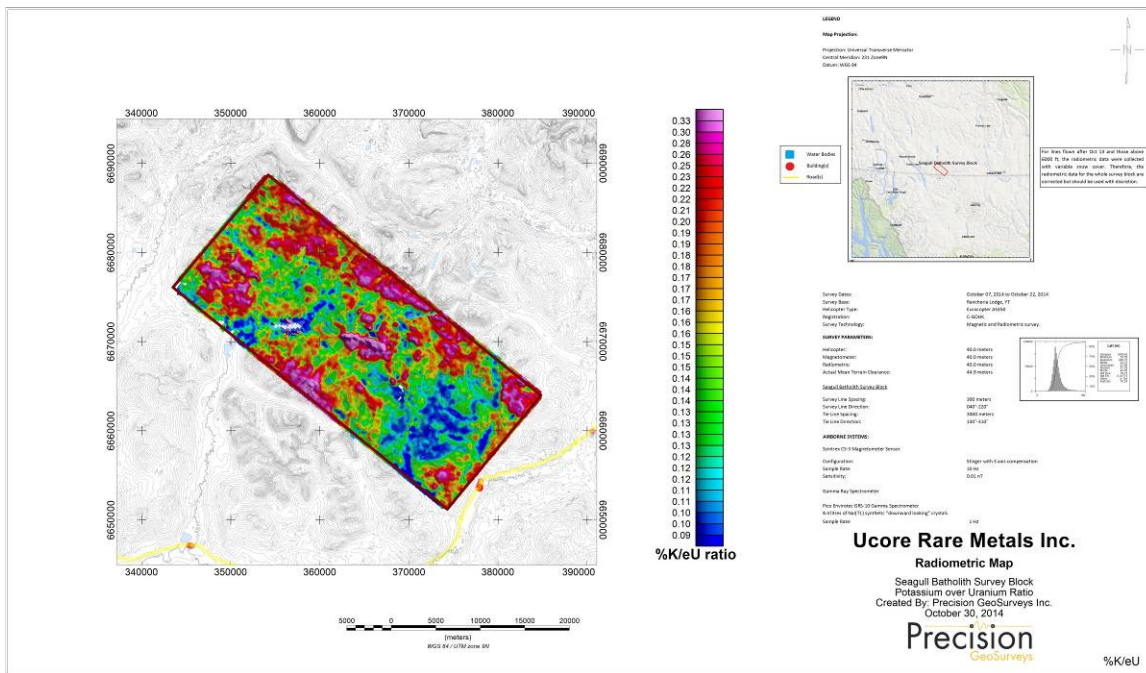
Map 13: Seagull Batholith survey block uranium over potassium ratio.



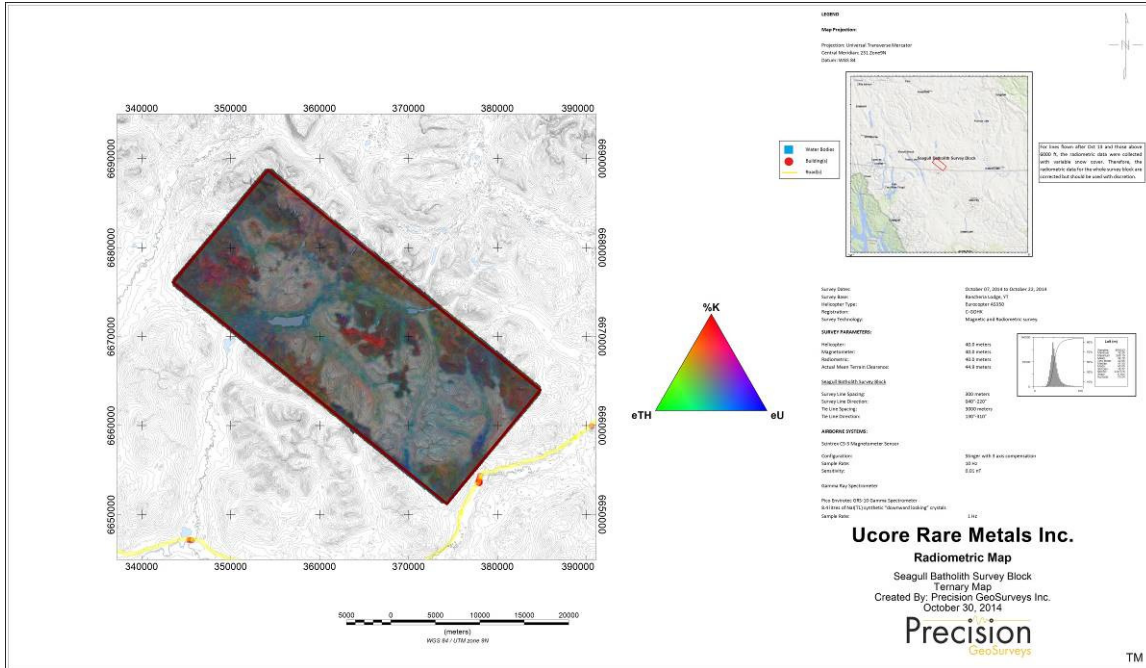
Map 14: Seagull Batholith survey block uranium over thorium ratio.



Map 15: Seagull Batholith survey block potassium over thorium ratio.



Map 16: Seagull Batholith survey block potassium over uranium ratio.



Map 17: Seagull Batholith survey block ternary map.

**Appendix V**

**Rock and Soil Sample Descriptions**

---

See Data Folder for  
Sample  
Descriptions

**Appendix VI**

**Assay Certificates**

---

See Data Folder for Assay Certificates